TRANSIENT NON-THERMAL MOBILITY IN SURFACE SUBSURFACE HETROGENEOUS CATALYTIC REACTION: COMPUTER SIMULATION

ABAID ULLAH QAISRANI

DEPARTMENT OF PHYSICS

GOMAL UNIVERSITY DERA ISMAIL KHAN

PAKISTAN, 2007

TRANSIENT NON-THERMAL MOBILITY IN SURFACE SUBSURFACE HETROGENEOUS CATALYTIC REACTION: COMPUTER SIMULATION

A Dissertation
Presented to the Department of Physics,
Gomal University, Dera Ismail Khan,
Pakistan

For the Degree of
Doctor of Philosophy in Physics

By
Abaid Ullah Qaisrani
2007

Certificate

Certified that **Mr. Abaid Ullah Qaisrani** has completed the work contained in this thesis under my supervision.

(Dr. M. Khalid)

Supervisor
Department of Physics
Gomal University
Dera Ismail Khan, Pakistan.

To

My Late Father

ACKNOWLEDGEMENTS

I would like to thank and pray for Dr.K.M.Khan (late) for introducing me in the field of simulation. He was the first person who gave me the opportunity to learn how to be a research worker.

I would like to thank to Dr. M.Khalid for all of the support and guidance that he has offered me throughout the research work here at Gomal University. His sympathetic attitude and encouraging discussions enabled me in broadening and improving my capabilities not only in computer programming, but also in other fields of life. He always helped me in every aspects of life. Without his guidance, I would not have had the desire to extend my education beyond my M.Phil.

I must thank Dr. N.A.Din Khattak for helping me and sharing his expertise in research work. I am grateful to the Chairman, Department of Physics, for providing me research facilities and moral support. I would also like to thank my friend Dr. Matiullah CSO, PIEAS, Islamabad for his constant encouragement and help throughout my period of study and research work.

I wish to express my thanks and appreciation to my daughter, Samina Naz, student of M.S at FAST, Islamabad for her encouragement during the research work. I also extend my thanks to my daughter Rubina Naz and my son M. Hasnain for taking keen interest in their study during the tough time of my work about simulation. Thanks also go to my children, Junaid, Shoaib, and Aqsa for the sacrifices and hardships they observed during this research work.

I wish to record my deepest obligations to my wife and especially to my mother for their love and patience.

Finally, I am humbly obliged to my late father (whom I miss on this great occasion) for their countless prayers.

LIST OF PUBLICATIONS

This thesis is based on the following publications.

Paper I Eley-Rideal Model for Monomer-Dimer Surface Catalytic reaction: Study of Subsurface Effects.
A.U. Qaisrani and M.Khalid, The Nucleus, **39** (3-4), 127 (2002).

Paper II Effect of Ballitic-Type Hot Atom Adsorption Mechanism on the Phase Digram of Monomer-Dimer CO-O_2 Surface catalytic Reaction: A Monte- Carlo Simulation.
M. Khalid, K.M. Khan, A.U. Qaisrani, Q.N. Malik, Chin. Phys. Lett.**21**, 1171 (2004).

Paper III Phase-Diagram of Catalytic Oxidation of CO on the Surface-Subsurface of a Body-Centred Cubic Structure with Eley-Rideal Process: A Monte Carlo Simulation.
A.U. Qaisrani, M.Khalid, Musa Kaleem Baloch, Chin. Phys. Lett.**21**, 1838 (2004).

Paper IV Effect of Eley-Rideal Process on the Phase Diagram of a Monomer-Dimer Catalytic Reaction on (001) Surface and Subsurface of a Simple Cubic Structure.
A.U. Qaisrani, K.M. Khan, M. Khalid, Int. J. Mod. Phys. C **15,** 1215 (2004).

Paper V Non-Thermal Effects on CO-NO Surface Catalytic Reaction on Square Surface: Monte Carlo Study.
M. Khalid, A.U. Qaisrani, W. Ahmad, Chin. Phys. Lett.**22,** 1533 (2005).

Paper VI CO-NO Catalytic Surface Reaction on Body-Centered Cubic Structure: Monte Carlo Study.
M. Khalid, A.U. Qaisrani, M. K. Khan, Int. J. Mod. Phys. C **16,** 1279 (2005).

Paper VII Effect of Precursor Mechanism on CO-NO Catalytic Reaction on Body-Centred Cubic Structure: Monte Carlo Simulation.
A.U. Qaisrani, M. Khalid, M. K. Khan, Chin. Phys. Lett.**22**, 2422 (2005).

Paper VIII Effect of Experimentally Observed Hot Atom Adsorption Mechanism on the Phase Diagram of Monomer-Dimer Catalytic reaction on Pt(111): Monte-Carlo Simulation Study.
M. Khalid, Q.N. Malik, A.U. Qaisrani, M. K. Khan, Brazillian J. Phys. **36**,164 (2006).

ABSTRACT

To study the effect of transient non-thermal mobility in surface-subsurface heterogeneous catalytic reaction, simulation work has been done for CO-O_2 and CO-NO catalytic reaction on different surfaces. One class of transient non-thermal mobility of species includes Ely-Rideal (ER) mechanism. The first simple lattice gas model was introduced by Ziff, Gulari and Barshad, as a computer simulation model and is known as the ZGB model, which was used to study CO- O_2 reaction system. It has been found through simulation that ER mechanism generates features in the ZGB model that brings it closer to the real system. The Consideration of ER mechanism annihilates second order phase transition of the ZGB model and the reaction rate begins to increase as soon as feed concentration CO departs from zero, which is consistent with the experimental results.

The other class of transient non-thermal mobility is precursor mechanism. This mechanism adds some additional features in the phase diagram of a particular catalytic reaction, which could not be observed by considering the Langmuir-Hinshelwood mechanism. In the precursor mechanism, three different ranges of the surface environment have been investigated. Each environment consists of specific pattern for set of sites around the striking site. It is observed that the reactive window depends on the mobility of the precursors. It is also observed that when the probability of the precursor is increased, the production rates increases.

Furthermore, the simulation is also performed to investigate the effect of diffusion of CO on the ZGB model. It has been found that the effect of diffusion of CO on the ZGB model is to increase the mobility of CO on the surface and hence the reaction rate increases with the result that the transition point y_2 shifts towards higher concentration of CO. However, the effect of diffusion of CO has no effect on the second order phase transition point y_1. The effect of diffusion of CO and N (atom) for CO-NO catalytic reaction has also been studied on BCC lattice. The effect of diffusion of CO and N on the production rates is found in the high concentration of CO. This mechanism is found responsible for slight increase in the window width where the concentration of CO is high. Through these models some experimental results have been reproduced of the real system.

TABLE OF CONTENTS

Dedication iv

Acknowledgements v

List of publication vi

Abstract vii

Table of contents viii

List of figures xi

List of tables xvii

Chapter 1: Introduction **1**

1.1 Role of computer simulation 1

1.2 Importance of heterogeneous catalytic reaction (HCR) 2

1.3 History of the project 4

1.4 Aim of the project 12

1.5 References 13

Chapter 2: Monte Carlo simulation and Catalytic Surface Reactions **15**

2.1 Introduction 15

2.2 The Monte Carlo simulation method 15

2.2.1 The constant coverage ensemble 17

2.2.2 Finite-size scaling approach 17

2.2.3 The epidemic method (EM) and dynamical scaling 18

2.2.4 The standard ensemble 20

2.3 References 21

Chapter 3: Surface Catalytic Reactions (SCR) **23**

3.1 Introduction 23

3.2 Elementary steps in surface reaction 23

3.2.1 Adsorption mechanism 24

3.3 Catalytic Reaction mechanisms 25
3.3.1 Langmuir- Hinshelwood mechanism 25
3.3.2 Precursor mechanism 27
3.3.3 Hot atom mechanism 28
3.3.4 Eley-Rideal mechanism 30
3.4 Basic Modelling of SCR 31
3.4.1 Ziff, Gulari and Barshad (ZGB) Model 32
3.5 Variants of ZGB Model 36
3.5.1 Desorption mechanism 36
3.5.2 Diffusion mechanism 36
3.6 References 37

Chapter 4: Simulation of CO-O_2 Reaction 39

4.1 Introduction 39
4.2 Simulation on simple cubic lattice (SCL) with ER 40
4.2.1 Model and simulation 40
4.2.2 Results and discussion 42
4.3 Simulation on BCC with ER 50
4.3.1 Model and simulation 50
4.3.2 Results and discussion 52
4.4 Simulation on SCL with Ballistic-Type Hot Atom 56
4.4.1 Model and simulation 57
4.4.2 Results and discussion 58
4.5 References 61

Chapter 5: Simulation of CO-NO Reaction 63

5.1 Introduction 63
5.2 Simulation on square surface with Precursor mechanism 64
5.2.1 Model and simulation 64
5.2.2 Results and discussion 66
5.3 Simulation on square surface with Precursor and diffusion mechanism 74
5.3.1 Model and simulation 74
5.3.2 Results and discussion 75

5.4 Simulation on BCC for CO-N0 with Precursor mechanism 79

5.4.1 Model and simulation 79

5.4.2 Results and discussion 81

5.5 Simulation on BCC with Eley Rideal and diffusion mechanism 96

5.5.1 Model and simulation 96

5.5.2 Results and discussion 98

5.6 References 107

Chapter 6: Results and Conclusion 109

6.1 Conclusion 109

6.2 Future Research Work 111

LIST OF FIGURES

1.1 Schematic view of the relationship between theory, experiment, and computer simulation. 2

1.2 Experimental Phase diagram of CO-O_2 catalytic reaction on Pt (210) at T = 500 K 7

2.1 Phase diagram of the ZGB model using standard ensemble, showing the dependence of the surface coverage with CO and oxygen (O) and the production rate of CO_2 on the partial pressure of CO (CO concentration) in the gas phase. 21

3. 1 Schematic description of the relevant steps involved in a surface catalyzed reaction within the reactive regime. 24

3.2 A schematic of the adsorption of CO and O_2 on the Pt surface. Carbon monoxide takes up one lattice site while oxygen takes up two. 27

3.3 Pattern of 1st, 2nd and 3rd environment on the square surface. 29

3.4 Phase diagram of the ZGB model. 35

4.1 A plot of surface oxygen coverage (solid circle), subsurface oxygen coverage (open circle), CO coverage (open square) and CO_2 production rate (solid square) versus CO partial pressure for model A, when the probability of ER step is taken to be 0.01. 43

4.2 Same as in Fig.4.1 for model A, when the probability of ER step is taken to be 0.6. 44

4.3 Same as in Fig.4.1 for model A, when the probability of ER step is taken to be 1.0 44

4.4(a) Same as in Fig.4.1 for model A, when the probability of ER step is taken to be 0.0 (LH mechanism only). 45

4.4(b) A plot of maximum production rate of CO_2 versus ER step probability for model A. A line of fit of the data is also shown. 45

4.5 Same as in Fig.4.1 for model B, when the probability of ER step is taken to be 0.01 46

4.6 Same as in Fig.4.1 for model B, when the probability of ER step is taken to be 0.1 47

4.7 Same as in Fig.4.1 for model B, when the probability of ER step is taken to be 0.06 48

4.8 Same as in Fig.4.1 for model B, when the probability of ER step is taken to be 1.0. 48

4.9 A plot of maximum production rate of CO_2 versus ER step probability for model B. A line of fit of the data is also shown. 49

4.10 Surface and sub-surface layers of a body centred cubic structure when extended into the z-direction. The sites marked by 1,2,3 and 4 are the sub-surface nearest neighbour and sites marked by 5,6,7 and 8 are the surface second nearest neighbours of a randomly selected site S. 51

4.11 A plot of surface oxygen coverage (open square), subsurface oxygen coverage (solid circle), CO coverage (open circle) and CO_2 production rate (solid square) versus CO partial pressure for first case (for reaction steps: 7-10). 52

4.12 A plot of surface oxygen coverage (open square), subsurface oxygen coverage (solid circle), CO coverage (open circle) and CO_2 production rate (solid square) versus CO partial pressure when the probability of ER step is taken to be 0.01 (top) and 1.0 (bottom) respectively for second case. 53

4.13 A plot of maximum production rate versus ER step probability for second case 54

4.14 A plot of surface oxygen coverage (open square), subsurface oxygen coverage (solid circle), CO coverage (open circle) and CO_2 production rate (solid square) versus CO partial pressure in the third case. 54

4.15 A plot of surface oxygen coverage (open square), subsurface oxygen coverage (solid circle), CO coverage (open circle) and CO_2 production rate (solid square) versus CO partial pressure with ER when the probability of ER step is taken to be 0.01 (top) and 1.0 (bottom) respectively for fourth case. 55

4.16 A plot of maximum production rate versus ER step probability for fourth case. 56

4.17 Coverages of O (open square), CO (open circle) and the production rate of CO_2 (solid square) versus CO partial pressure for case *a*. 58

4.18 Coverages of O (open square), CO (open circle) and the production rate of CO_2 (solid square) versus CO partial pressure for case *b*. 59

4.19 Coverages of O (open square), CO (open circle) and the production rate of CO_2 (solid square) versus CO partial pressure for case *c*. 59

4.20 Coverages of O (open square), CO (open circle) and the production rate of CO_2 (solid square) versus CO partial pressure for case *d*. 60

4.21 Snapshot on yCO = 0.14 (1 for oxygen, 2 for CO and 0 for vacant site). 61

5.1 Lattice snap shot illustrating the Model A for y_{co} = 0.15 (1 for oxygen, 3 for N). 66

5.2(a) Phase diagram from MC according to precursor mechanism for Model A with coverages of surface O (open square), CO (closed circle), and N (open circle) for 100% probability of precursor. 67

5.2(b) Production rate of CO_2 (open square) and N_2 (closed square) 67

5.3 Coverages of surface O (open square), CO (closed circle), and N (open circle); for Model B: with 20% precursor. 68

5.4 Coverages of surface O (open square), CO (closed circle), and N (open circle); for Model B: with 100% precursor. 69

5.5 Production rates of CO_2 (open square) and N_2 (closed circle) versus CO concentration for Model B with: (a) 20% precursor; (b) with 100% precursor (bottom). 70

5.6 Coverages of surface O (open square), CO (closed circle), and N (open circle); for Model C: with 20% precursor. 71

5.7 Coverages of surface O (open square), CO (closed circle), and N (open circle); for Model C: with 100% precursor. 71

5.8 The same as in Fig.5.5 for Model C with 20% precursor (top) and with 100% precursor (bottom). 72

5.9(a) Plots of y_1 (open square) and y_2 (closed circle) versus precursor probability for Model B. 73

5.9(b) Plots of y_1 (open square) and y_2 (closed circle) versus precursor probability for Model C. 73

5.10 Maximum production rates (MPR) versus environment first (closed square), environment second (open circle) and third (closed circle). 74

5.11 Snap shot on y_{co} = 0.14 (+ for oxygen, and * for N) for Model A. 76

5.12 Coverages of surface O (closed squares), CO (closed circles), and N (open circles) for Model A. 77

5.13 Production rate N_2(g) (closed circle)) and CO_2(g) (open square) for Model A. 77

5.14 Coverages of surface O (closed squares), CO (closed circles), and N (circle open) for Model B. 78

5.15 Production rate N_2(g) (closed circle)) and CO_2(g) (open square) for Model B 78

5.16(a) A plot of surface oxygen coverage (open circles), subsurface oxygen coverage (solid squares), CO coverage (open triangles), surface nitrogen coverage (solid triangle), CO2 production rate (open squares) and N2 production rate (solid circles) versus CO concentration for model A (LH Mech.) 82

5.16(b) A plot of CO_2 production rate (open squares) and N_2 production rate (solid circles) versus CO concentration for model A (LH Mech.) 82

5.17(a) The same as in Fig.5.16(a) with 20% precursor probability for the first environment of model B. 83

5.17(b) CO_2 production rate (open squares) and N_2 production rate (solid circles) versus CO concentration with 20% precursor probability for the first environment of model B. 83

5.18(a) The same as in Fig. 5.17(a) with 60% precursor probability for the first environment of model B. 84

5.18(b) The same as in Fig. 5.17(b) with 60% precursor probability for the first environment of model B. 84

5.19(a) The same as in Fig. 5.17(a) with 80% precursor probability for the first environment of model B. 85

5.19(b) The same as in Fig. 5.17(b) with 80% precursor probability for the first environment of model B. 85

5.20(a) Surface oxygen coverage (open circles), subsurface oxygen coverage (solid squares), CO coverage (open triangles), surface nitrogen coverage (solid triangle), CO_2 production rate (open squares) and N_2 production rate (solid circles) versus CO concentration; with 100% precursor probability for the first environment of model B. 86

5.20(b) CO_2 production rate (open squares) and N_2 production rate (solid circles) versus CO concentration with 100% precursor probability for the first environment for model B. 86

5.21(a) The same as in Fig. 5.20(a) with 20% precursor probability for the second environment of model C. 88

5.21(b) CO_2 production rate (open squares) and N_2 production rate (solid circles) versus CO concentration with 20% precursor probability for the second environment of model C. 89

5.22(a) The same as in Fig. 5.20(a) with 60% precursor probability for the second environment of model C. 89

5.22(b) CO_2 production rate (open squares) and N_2 production rate (solid circles) versus CO concentration with 60% precursor probability for the second environment of model C. 90

5.23(a) The same as in Fig. 5.20(a) with 80% precursor probability for the second environment of model C. 90

5.23(b) Production rate of CO_2 and N_2 versus CO concentration with 80% precursor probability for the second environment of model C. 91

5.24(a) The same as in Fig. 5.20(a) with 100% precursor probability for the second environment of model C. 91

5.24(b) Production rate of CO_2 and N_2 versus CO concentration with 100% precursor probability for the second environment of model C. 92

5.25(a) Surface oxygen coverage (open circles), subsurface oxygen coverage (solid squares), CO coverage (open triangles), surface nitrogen coverage (solid triangle), CO_2 production rate (open squares) and N_2 production rate (solid circles) versus CO concentration; with 20% precursor probability for the second environment of model D. 93

5.25(b) Production rate of CO_2 and N_2 versus CO concentration with 20% precursor probability for the second environment of model D. 94

5.26(a) The same as in Fig. 5.25(a) with 100% precursor probability for the second environment of model D. 94

5.26(b) Production rate of CO_2 and N_2 versus CO concentration with 100% precursor probability for the second environment of model D. 95

5.27 Maximum production rate of first environment (solid squares), second environment (open circles) and third environment (solid circles) versus precursor probability. 95

5.28(a) Coverages of surface O (circle open), sub-surface oxygen (square open), CO (triangle open), and N (square solid) for Model A. 101

5.28(b) Production rate of CO_2 and N_2 versus CO concentration of model A 101

5.29 Snap shot on y_{co} = 0.14 (1 for oxygen, 3 for N). 101

5.30(a) Coverages of surface O (circle open), sub-surface oxygen (square open), CO (triangle up open), and N (square solid) for model B. 102

5.30(b) The production rate of CO_2 (circle solid) and N_2 (triangle solid) versus CO partial pressure for model B. 102

5.30(c) Production rate vs ER step probability for Model B. 103

5.31(a) Coverages of surface O (circle open), sub-surface oxygen (square open), CO (triangle up open), and N (square solid) versus CO partial pressure for Model C. 103

5.31(b) The production rate of CO_2 (circle solid) and N_2 (triangle solid) versus CO partial pressure for Model C. 104

5.32(a) Coverages of surface O (circle open), sub-surface oxygen (square open), CO (triangle up open), and N (square solid) versus CO partial pressure for Model D. 104

5.32(b) The production rate of CO_2 (circle solid) and N_2 (triangle solid) versus CO partial pressure for Model D. 105

5.33(a) The same as in Fig. 5.32(a) for Model E. 105

5.33(b) The production rate of CO_2 (circle solid) and N_2 (triangle solid) versus CO partial pressure for Model E. 106

5.34(a) Coverages of surface O (circle open), sub-surface oxygen (square open), CO (triangle up open), and N (square solid) versus CO partial pressure for Model F. 106

5.34(b) The production rate of CO_2 (circle solid) and N_2 (triangle solid) versus CO partial pressure for Model F. 107

LIST OF TABLES

5.1 Effect of precursor on the first environment (model B) for the reaction of the CO-NO on BCC lattice. 87

5.2 Effect of precursor on the second environment (model C) for the reaction of the CO-NO on BCC lattice. 88

5.3 Effect of precursor on the third environment for the reaction of CO-NO on BCC lattice. 93

Chapter-1

INTRODUCTION

1.1 Role of Computer Simulation

The use of computer in science is becoming increasingly important. There is hardly any modern experiment thinkable where computers do not play an essential role one-way or other. An essential role of science is to develop models of nature. To know whether a model is consistent with observation, we have to understand the behaviour of model and its prediction. One way to do so is to implement the model on a computer. We call such an implementation a computer simulation or simulation for short. The simulation of physical phenomenon is the realm of Computational physics. The investigation of phenomena of computer simulation is now an established and rapidly growing practice in science and engineering. The most obvious examples are in the physical sciences where computer models are used to study the irreversible reaction systems, the stability of hot gas plasmas in fusion machines, turbulence in fluids, and the flow of electrons in a semiconductor device. The study of the irreversible reaction systems has also attracted great attention during the last decades due to, on the one hand, the rich and complex underlying physics, and, on the other, their relevance to numerous technological applications in heterogeneous catalysis, corrosions and coating, the development of microelectronic devices, etc. This is why the computer simulation methods have become established as a research tool in physics and other branches of sciences.

We can divide the type of computer experiments roughly into three categories:

- Simulation of complex systems where many parameters need to be studied before construction can take place. Examples come from engineering: car-crashing worthiness simulation, aircraft wing design, and general complex safety systems.
- Simulation of phenomenon with extreme temporal or spatial scale that cannot be studied in a laboratory. For instance: Astrophysical systems, mesoscopic systems, molecular design etc.
- Theoretical experiments, where the behaviour of isolated sub domains of complex systems is investigated to guide the theoretical physicist through

the development of new theories. Typical research fields are: non-linear system, plasma and quantum physics, light scattering from complex particles, nonequilibrium phenomenon in surface physics, etc.

It is evident that for understanding any physical phenomena, one has to go through simulation, theory and experiment. We therefore view the relationship between theory, experiment, and simulation to be similar to those of the vertices of a triangle, as shown in Fig. 1.1:

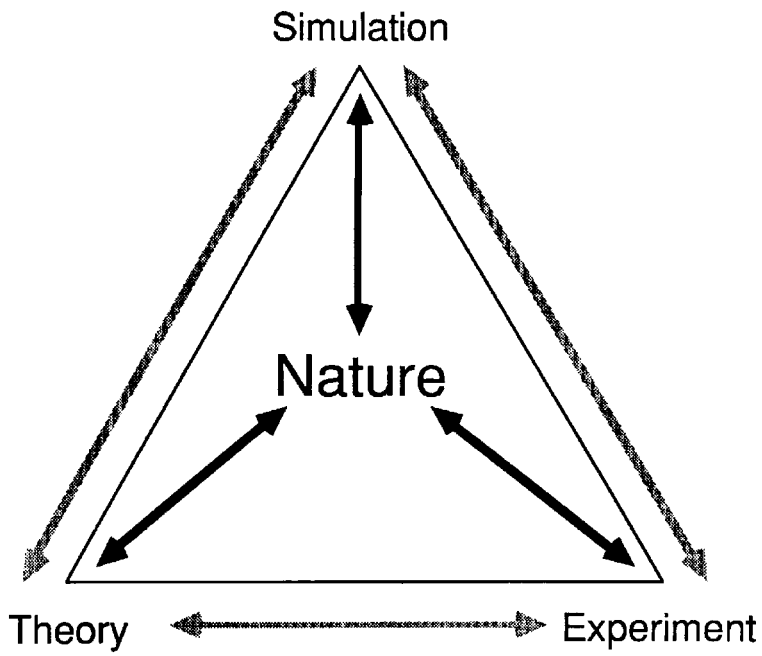

Fig.1.1 Schematic view of the relationship between theory, experiment, and computer simulation.

It is undeniable fact that catalytically activated heterogeneous reactions play an important role in various processes in chemistry, physics, and biology. Such reactions are involved in many industrial and technological processes. In the next section the importance of heterogeneous catalytic reaction (HCR) is discussed.

1.2 Importance of Heterogeneous Catalytic Reaction (HCR)

The functioning of industrial nations is based on a constantly growing economy. This economic growth has resulted in a constant increase in energy consumption over the last century. The main energy resource still consists of crude oil, which is converted into

gasoline or fuel oil. The catalytic conversion and modification of crude oil is essential for both providing an environmentally reconcilable consumption of this resource and for the performance of combustion engines or furnaces. Practically all these process involve heterogeneous catalysis. For the sake of a clean combustion, crude oil is separated into fractions by distillation, which are subsequently processed and purified. For example, the purification processes remove undesired content like sulphur and nitrogen because their oxidation products emerging during combustion lead to polluting products. For instance, NO_x contributes to ozone layer depletion and SO_x causes acid rain. Nitrogen and Sulphur are chemically extracted through heterogeneous catalyst.

The primary objective of these catalysts is to enhance the reaction rate and to yield the desired products at a high selectivity. To do so, the catalyst has to reduce the activation energy of the rate-limiting step. Consequently, reactions that would usually take an unimaginably long time, can proceed on a short time scale. Although surface reactions have been intensively investigated in the last decades, surprisingly little is known about the elementary reaction steps, which take place on the atomic length scale of these reactions. The $CO + O_2$ and the $CO + NO$ reaction system are by far the best explored ones both on low index single crystal and polycrystalline surfaces, but experimental investigations using new spectroscopic methods are very demanding to carry out and frequently cannot resolve the individual reaction steps.

The choice for a certain catalyst for a catalytic conversion is not only determined by the reaction itself but also by the industrial process. For example, heterogeneous catalysts are used for the production of bulk chemicals because the solid catalyst materials are unmixable with the products. This facilitates the separation of products and catalyst materials, especially if gaseous products are involved. Consequently, the reaction can be performed under continuous flow conditions, which permit the scaling up of production process to achieve high rates. This advantage of heterogeneous catalysis is of exceptional importance because it allows the production of gasoline, fuel oil and other bulk chemicals on a large scale, which is essential to provide sufficient bulk chemicals to satisfy the vast demands of the world market. Refining crude oil is just one example of a large-scale catalytic process; others include the synthesis of ammonia, methanol, polyethylene, ethane oxide and many more. As a consequence of the large-scale production of bulk chemicals, minor improvements of catalytic process have potentially large impacts on the profit margin of companies.

On the other hand, today's theoretical approaches do not master the complexity of most of the important reaction steps including correlations, fluctuations, formation of spatio-temporal pattern and energetic interactions both in the adsorbate layer and between the adsorbates and the surface. In this case computer simulation may be good tool to study details of these reactions. Certain aspects of the reaction can be simulated to examine the system behaviour as a function of these. The first simple lattice gas model was introduced by Ziff, Gulari and Barshad [1], as a computer simulation model and is known as the ZGB model.

1.3 History of the Project

The study and understanding of heterogeneously catalysed reactions is a field that contains an enormous wealth of still unclear, or even completely unexplained, phenomenon. This means it is an exciting and challenging domain for investigation and fundamental research. Furthermore, the occurrence of many complex and fascinating physical and chemical phenomenon has attracted the attention of many scientists.

In addition to the basic interest, heterogeneous catalysis is a field of central importance for numerous industrial (synthesis of ammonia, sulphuric and nitric acids, cracking and reforming processes of hydrocarbon, etc) and practical (catalytic control of environmental pollution such as the emission of CO, NO_x, SO_2, O_3, etc.) applications. Furthermore, the rapid advancement in the areas of information technology, heterogeneous catalysis, metallurgy, material science, environmental science, microelectronics, corrosion, energy conversion etc. is deeply linked to the physical and chemical properties of surface and interfaces. Within this context the understanding of surface chemical reactions is a challenge for researchers worldwide, which motivated both technical applications and scientific interest.

The recent development in experimental technique such as scanning tunneling microscopy (STM), low energy electron diffraction (LEED), high resolution electron energy loss spectroscopy (HREELS) and photoelectron emission microscopy (PEEM) allows the scientists to gather detailed information about surfaces, adsorbates and reaction products. Also surface reaction system is certainly a challenging scientific field for the development and application of analytical methods and theories, including recent advances in the area of non-linear dynamics. Complementing very well established approaches for the study of a scientific field, namely experiments and analytical theory,

recently computer simulation has become a powerful tool for the study of great variety processes occurring in nature in general, as well as surface chemical reactions in particular [2,3].

Despite the fact that heterogeneous reactions are irreversible and show complicated behaviour, these are of great practical interest because of their common use in industry and in controlling the toxic emission into the environment. Due to presence of microscopic fluctuations and correlations in the concentrations of reactants, it is very difficult to understand theoretically the mechanism behind these processes taking place on the surface of the catalysis. Therefore a microscopic understanding of the fundamental catalytic reaction is still lacking. Experimentally, it is difficult to probe the state of the reactant during reaction. Traditionally, information is only available before or after the event. In experiments difficult conditions are involved. Under these conditions computer simulation is another tool, which may be helpful for understanding certain aspects of the behaviour of such systems. The study of such processes is of great interest in surface science.

Lattice models have been used successfully to predict a wide range of experimental observations in catalysis. The first simple lattice gas model was introduced by Ziff, Gulari and Barshad [1], as a computer simulation model and is known as the ZGB model, which was used to study CO-O_2 reaction system. In this model, a square lattice models the surface. A reservoir containing CO and O_2 in a given proportion is in contact with the surface. It is assumed that the supply of the gas is inexhaustible. A monomer (CO) on the striking the surface adsorbs onto a single vacant site, while dimer (O_2) adsorbs onto two adjacent vacant sites. Whenever an oxygen atom finds itself sitting next to CO, the reaction takes place with the formation of CO_2 that desorbs from the surface leaving behind two vacant sites. It is worth mentioning here that the ZGB model is based on Langmuir-Hinschelwood (LH) mechanism. In LH mechanism, both the reactants are initially adsorbed on the surface and are in thermal equilibrium with the surface. Therefore, LH mechanism is also called thermal mechanism. The reaction rate is proportional to the probability that the reactants occupy adjacent sites. This ZGB model was used to study the catalytic oxidation of CO. The results of ZGB model exhibit two-phase transitions between active and non-active states. The only parameter in this model is the feed concentration of y of CO. This single parameter y, which represents the probability that the next molecule arriving at the surface is CO, called some time $y = y_{CO}$, which is proportional to the partial pressure of CO**.** The model shows two kinetic phase

transitions, a continuous one at $y = y_1$ and a discontinuous one at $y = y_2$; where $y_1 < y_2$. When $y_1 < y_2$; all the sites become occupied by oxygen, the so called oxygen-poisoned state. Real systems donot possess an oxygen-poisoned state because oxygen does not obstruct the adsorption of CO. If $y_1 > y_2$, all the sites become occupied by CO molecules, the so called CO- poisoned state. The results of the simulation of the ZGB model for square lattice; show that when the probability of a feed concentration of CO ($y = y_{CO}$) less than y_1, the surface is poisoned by oxygen atoms. As y_{CO} is increased above a critical value of y_1 ($y_1 = 0.389 \pm 0.005$), the nature of steady state changes. In this reactive steady state regime, the surface contains O, CO, and empty sites. Under these conditions, reaction can continue indefinitely and production of CO_2 starts. For large values of y_{CO} ($y_{CO} > y_2$) ($y_2 = 0.525 \pm 0.001$), the surface becomes completely covered by CO and no further reaction can occur (the surface is poisoned by CO). Only in the range $y_1 < y_{CO} < y_2$, the system exhibits a steady reactive state (SRS). Here y_1 is the critical concentration of CO at which SRS starts, while y_2 is the critical concentration of CO where SRS stops. The range (y_2-y_1) is called as window width. The widow width of CO-O_2 reaction on square lattice for the ZGB model is 0.136. The transition at y_1 is continuous, as at y_1 the densities of O and CO change continuously, while at y_2 the same densities change abruptly indicating a first order transition. Therefore, the transition at $y_1 \approx 0.389$ is of second order while the transition at $y_2 \approx 0.525$ is of first order. However, the second order phase transition (SOPT) has never been observed experimentally in the CO oxidation. The experiments show that production of CO_2 starts as soon as CO concentration departs from zero [4-8]. However, this simple model shows some physical properties, which are observed in real systems such as the poisoning with CO of the catalyst. This model (ZGB) has been extensively studied for different aspects of CO-O_2 reaction on different types of geometrical surfaces with different types of parameters [9-15].

Meakin and Scalapino [11] investigated the effect of the lattice type on the reactive window of the ZGB model. They found that by increasing the coordinate number of the lattice, a hexagonal lattice (each site having six nearest neighbouring sites) yields a wider reactive window in size as compared to the usual square lattice with $y_1 = 0.360 \pm 0.005$ and $y_2 = 0.561 \pm 0.001$. The widow width of CO-O_2 reaction on hexagonal lattice for the ZGB model was found to be 0.201.

Dickman [16] developed a mean-field theory for the ZGB model. This model gives results that are in good qualitative agreement with the simulation results described above.

The model leads to a value of 0.52410 for y_2 in good agreement with the simulation results [y_2 = 0.525 ± 0.001 (Ref 1)]. However, the mean field theory leads to a value of y_1 = 0.2497 that is substantially smaller than that obtained from simulations [0.389 ± 0.005 (Ref 1)].

Experimental results as can be seen from the experimental graph (Fig.1.2) corresponding to the catalytic oxidation of carbon monoxide on Pt(210) and Pt(111) [17,18] and these results are in qualitative agreement with simulation results of the ZGB model. One remarkable agreement is between the (almost) linear increase in the reaction rate observed when the CO pressure is raised and the abrupt drop of the reactivity when a certain 'critical' pressure is reached. In spite of the similarities observed, two essential differences are worth discussing: (i) the oxygen-poisoned phase shown by the ZGB model within the CO low-pressure regime is not observed experimentally. Therefore, one lacks experimental evidence of a second-order irreversible phase transition (IPT). (ii) The CO-rich phase showing low reactivity, found experimentally, resembles the CO-poisoned state predicted by the ZGB model. Of course, these and other disagreements are not surprising since the lattice gas reaction model, with a single parameter, is a simplified approach to the actual catalytic reaction, which is far more complex.

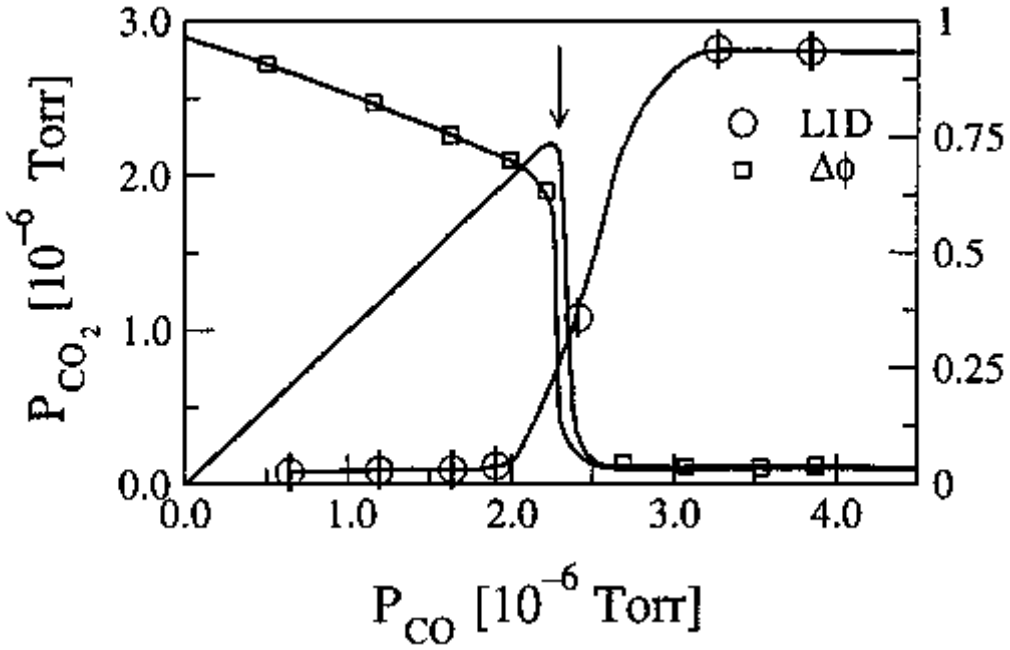

Fig.1.2 Experimental Phase diagram of CO-O_2 catalytic reaction on Pt (210) at T = 500 K.(From Ref. 17,18)

Following the introduction of ZGB model; several attempts have been made in order to give more realistic description of the ZGB model and its variants. It has been emphasized by many research groups that non-thermal processes are also important to understand the catalytic reactions. One of such processes includes the "Eley-Rideal" mechanism. In ER mechanism, the reaction occurs between gas-phase and chemisorbed particles. The chemisorbed particle is thermalized to the surface, while the second particle in gas-phase collides with the first particle (chemisorbed particle) without first thermalizing to the surface, forming a molecule that desorbs from the surface. This class of reactions (ER), halfway between the gas phase type and LH type, is of interest in surface science. Meakin [19] explored the effects of the ER process on the simple ZGB model for the catalytic oxidation of CO by oxygen. The ER process results in the formation of new regime in which a continuous reaction can be sustained. The main effect of adding the Eley-Rideal process is to remove the "continuous" transition at $y_{CO} = y_1$ and shift the "discontinuous" transition at $y_{CO} = y_2$.

The other class of transient non-thermal mobility is precursor mechanism. Harris and Kasemo [20] have given a detailed discussion on precursor mechanism. This mechanism involves direct collisions between chemisorbed species and molecules or atoms that are trapped in the neighbourhood of the surface but have not thermalized.

The effects of diffusion and desorption of CO on the ZGB model has been studied by various authors [10,17,21-24]. These two mechanisms (diffusion and desorption) are observed to have no effect on the second-order phase transition point y_1. The diffusion of CO increases the reaction rate, while, as a result, a clear-cut shift of the first order transition point y_2 towards higher values, thus increasing the window width of the reactive state. The desorption of CO slows and delays the saturation of the surface by CO, resulting in a smoothing and spread of the first-order transition.

Together with the great importance of studies of the CO oxidation reaction, there has also been great interest in the reduction of NO by CO. Both reactions are important in automotive exhaust emission control. It was found that catalytic activity of Pt surfaces in the NO-CO reaction is correlated with their efficiency in dissociating NO, which varies between zero and 100% for different planes and different temperature range [25,26]. At a typical operating temperature for a catalytic converter (700 K) the adsorption of NO results in the liberation of N_2 gas and in the formation of a stable surface oxygen species. These surface oxygen species are then used by CO molecules to be oxidized into CO_2 gas.

Yaldram and Khan [27,28] applied the ZGB model to the NO- CO surface reaction on square and hexagonal lattices. They showed that the type of lattice and the dissociation rate of NO (R_{NO}) into N and O are important factors for this reaction system. For a square lattice, they observed a poisoned state for all values of R_{NO} and feed concentration of CO (y_{CO}). However, a steady production of N_2 and CO_2 is observed for a hexagonal lattice when $R_{NO} > 0.80$. For $R_{NO} < 0.80$, no reactive window is obtained even for a hexagonal lattice. A maximum window width (≈0.153) is obtained at $R_{NO} = 1.0$ (i.e. complete dissociation of NO). This reactive window is enclosed by second-order phase transition (SOPT) and first-order phase transition (FOPT). An SOPT is observed at $y_1 = 0.185$ whereas an FOPT is observed at $y_2 = 0.338$. They also showed that the surface oxygen from NO reacts somewhat less readily with CO than with the oxygen from dissociated O_2, and thus the experimental results previously obtained were confirmed. Khan *et al.* [29] introduced the diffusion of N atoms in the simple Langmuir-Hinshelwood (LH) mechanism for CO-NO reaction system on the square lattice. They have shown that the steady reactive state exists only when the diffusion of N atoms on the surface is allowed. For maximum diffusion probability (P = 1), they obtained a reactive window of the order of ≈0.10. Dickman *et al*. [30] have also shown theoretically that the surface diffusion of nitrogen can only lead to an active state on a square lattice for this reaction system.

A controversial feature of the ZGB model concerns the second-order phase transition, which has never been observed experimentally in the CO oxidation. Khan *et al* [31] tried to remove this discrepancy through (simulation) by involving the role of sub-surface in CO-O_2 reaction system on the (001) surface and subsurface of a simple cubic structure. In this structure, each surface site has four nearest neighbouring (nn) sites on the surface and one nn site in the subsurface. It was found that the presence of subsurface favours the enhancement of the steady reactive state by reducing appreciably the poisoning of the surface by the adsorbed dimer (O_2) atoms. With the introduction of subsurface, the usual second order phase transition in CO-O_2 reaction under certain condition is eliminated and the reaction rate begins to increase as soon as the y_{CO} value departs from zero. This elimination of second order phase transition closely resembles the experimental situation. It has been shown that the elimination of SOPT in the model is due to the adsorption mechanism. The presence of subsurface oxygen on Pt (100) and Rh (110) has been observed experimentally in these reactions [6-8, 32]

Bangoli *et al*. [5] have tried to show that one can eliminate SOPT within the ZGB model by involving very specific local interaction. Satulovsky and Albano [33] generalized the ZGB model in order to account for both attractive and repulsive interactions between the reactants. They found that in most cases, the first-order phase transition point became second order, and the critical points were shifted. Jensen and Fogedby [34] extended the ZGB model in order to include diffusion of the adsorbed particle. They showed that fast diffusion causes SOPT to disappear from the system. Cortes *et al*. [35] have performed a Monte Carlo simulation study of the sensitivity of the CO oxidation reaction to changes in the characteristics of the catalyst's surface on which type of oxygen adsorption mechanism is dependent. They have shown that, if linear adsorption is assumed, the structural insensitivity becomes apparent in the phase diagram. In the case of structural sensitivity, it is seen that surface heterogeneity leads to a change in the character of the phase transition curve.

Khan [36] studied the influence of the subsurface oxygen in monomer-dimer (CO-NO) surface reaction. The introduction of subsurface oxygen produced some very interesting results. When NO adsorbs on two sites, it is equally likely that one of the site is filled with an N and one by an O atom, and this simple fact leads inevitably to poisoning on square lattice by a process of 'chequerboarding' of N atoms [37]. However, on a hexagonal lattice this chequerboarding process cannot occur geometrically and therefore, a steady reactive state is observed on the surface [27,36]. Meng *et al*. [38] have broken this chequerboarding process by introducing a hypothetical reaction between CO and N. Khan *et al*. [29] have broken the chequerboarding process of N atoms by introducing diffusion of N atoms on the surface. Khan [36] introduced one subsurface site in the usual four surface sites of a square lattice to break the chequerboarding process. More recently, Khan *et al.* [39] have studied a simple ZGB-like lattice gas model for the reaction of CO and NO on a Na-modified square lattice. The Na-induced NO dissociation in the model also breaks the usual chequerboarding process of Na atoms on the square lattice.

The interpretation of the kinetics of the CO-NO reaction is still limited. The experience accumulated in this field indicates [40] that quantitative fitting of experimental data is possible only if one takes into account such complicating factors as adsorbate-adsorbate interactions. With presumably reasonable values of parameters, the models proposed describe some of the features of the steady-state reaction kinetics, but even in the best cases the agreement between experiment and calculations is not complete. One of

the reasons for this state of art might be that the available models ignore steps. The review presented by Zhdanov *et al*.[40], describes in detail the evolution of the ideas for the mechanism of the reaction and also presents the data for the elementary reaction steps. The MC simulation [41], treating CO oxidation on Pt, illustrated that the manifestation of steps in steady-state kinetics can easily be hidden even if reaction runs primarily on steps Experimentally, the role of steps in the CO-NO reaction on Rh or Pd has not been studied either. The relevant scanning tunneling microscopy (STM) data is available [42] only for decomposition of NO preadsorbed on Ru(0001) at 300 K. In parallel with experiments, the role of steps in HCR can be studied theoretically by using such approaches as density-functional theory (DFT) [43] and/or mean-field (MF) and Monte Carlo (MC) simulation. L. Olsson and Zhdaove [44] have given detailed discussion on the role of steps in CO-NO reaction on the (111) surface of noble metals.

One of the non-thermal processes corresponding to variants of the ZGB model involves the 'hot' atom mechanism. Jackson and Person [45] have studied the dynamics of the 'hot' hydrogen dimmer in the ER mechanism (direct reaction between a gas phase H atom and an adsorbed H atom) using a fully three-dimensional flat surface model for Cu(111). 'Hot' dimers are molecules, which after adsorption dissociate, and the remaining 'hot' atoms fly apart up to a maximum distance R from the original adsorption site. Brune *et al.* [46] have demonstrated (by means of scanning tunneling microscopy observations) that oxygen molecules striking the A1(111) surface not only dissociate upon adsorption but also dissipate part of their excess energy in degrees of freedom parallel to the surface. The resulting 'hot' oxygen atoms fly apart, on average, up to a distance of at least 80 Å from the original impingement site, before being accommodated on their respective adsorption sites. After this ballistic flight oxygen atoms remain practically immobile at 300 K. By taking into account this experimental fact, Pereyra and Albano [47] have studied the influence of the 'hot' dimmer adsorption mechanism on the kinetics of a monomer-dimer (CO-O_2) catalytic reaction. Due to this 'hot' dimmer mechanism, they observed a remarkable enhancement of the rate of production (of CO_2). The catalytic reaction of H_2 and O_2 on polycrystalline Pt was studied with quartz crystal micro-beam data in the early work of Harris *et al*. [48]. They have analysed the data by means of a mean field approach and have shown that this particular reaction system is an example of a precursor mechanism. Harris and Kasemo[49] have given a detailed discussion on the precursor mechanism of surface reactions. This mechanism involves direct collisions between chemisorbed species and molecules or atoms that are trapped in

the neighbourhood of the surface but have not thermalized. The precursor kinetics is generally different from those characteristics of LH or ER mechanism [45,48,50].

Lately, many modified ZGB models have been proposed in order to give a more realistic description of complex reaction systems. On the one hand, one might easily introduce the repulsive interactions between the adsorbed species of the O atom to forbid the O atom to occupy the neighbour site. Then the adsorbed O atoms occur at next-nearest-neighbour pairs, thereby leaving at least half of the surface available for CO. Therefore, the oxygen poisoned is easily ruled out [5,33]. Recently, HUA Da-Yin *et al.*[51] presented the idea of co-adsorption of CO and O_2 on the catalytic surface. He studied the effect of the co-adsorption of CO and O_2 on the ZGB surface catalytic reaction system by Monte Carlo simulation. It assumed that CO can adsorb on an oxygen-occupied site with probability *p* and the adsorbed CO can react with the oxygen atom located in the selected site with unit probability. Under this assumption, it is shown that the adsorption of the CO molecule, even co-adsorption on the O-occupied site, is a prerequisite condition to react with the adsorbed oxygen atom. Therefore, this model follows the LH mechanism and such an additional process is different from the ER mechanism in which the CO molecule in the gas phase can react with an adsorbed oxygen on the surface directly. The co-adsorption of both species adds an extra reaction step to the classical ZGB model and the second-order phase transition from the reactive to the O-poisoned state is eliminated, and the production of CO_2 increases linearly along the feed concentration y_{CO} of CO in gas phase when it is low, in an agreement with the experimental results. However, it is pointed out that the process of the co-adsorption of CO with the oxygen adatom is very complicated and more experimental studies are needed to understand.

1.4 Aim of the Project

The aim of the project in this thesis is as follows:

- Using Mote-Carlo simulation techniques, to develop surface-subsurface models for square lattice, simple cubic and body centered cubic lattices based on Eley-Rideal mechanisms, Precursor mechanism. These models will be applied to range of catalytic reactions such as CO-O_2, CO-NO and to study their phase diagram and production rates.

- Comparison of the results obtained by above-mentioned models with results of the models based upon Langmuir-Hinshelwood mechanism.
- To study the effect of diffusion on CO-NO on square lattice and body centered cubic lattice.
- To study the effect of Precursor mechanism in the 1st, 2nd and 3rd environment on square surface.
- To study the effect of Precursor mechanism on body-centered cubic lattice.
- To study the effect of Eley-Rideal and diffusion mechanism on body-centered cubic lattice.

1.5 References

[1] R.M.Ziff, E. Gulari, and Y.Barshad, Phys. Rev. Lett. 56 (1986) 2553.

[2] E. V. Albano, The Monte-Carlo simulation method: A powerful tool for the study of reaction processes. H. Vhem. Rev. **3** (1996) 389

[3] E. Loscar and E. V. Albano, Rep.Prog.Phys.**66** (2003) 1343.

[4] M. Dumont, P. Dufour, B. Sente, R. Dagonnier, J. Catal. **122** (1990) 95.

[5] F. Bangoli, B. Sente, M. Dumont R. Dagonnier J. Chem.Phys. **94** (1991) 777.

[6] V. Schmatloch, I. Jirka, S. Heinze, N. Kruse, Surf. Sci. **331** (1995) 23.

[7] H.H. Rotermund, J. Lauterbach, G. Haas, Appl. Phys. A **57** (1993) 507.

[8] S. Ladas, R. Imbihl, G. Ertl, Surf. Sci. **219** (1989) 88.

[9] M. Dumont, M. Poriaux, P. Dagonnier, Surf.Sci. **169** (1986) L307.

[10] E.V. Albano, J.Chem.Phys. **94** (1991) 1499.

[11] P. Meakin and D. J Scalapino, J. Phys. **87** (1987) 731.

[12] M.A. Khan and K. Yaldram, Surf.Sci. **269** (1992) 476.

[13] E.V. Albano, Phys.Rev. Lett. **69** (1992) 656.

[14] E.V.Albano, J.Phys. A **25** (1992) 2557.

[15] K. Yaldram, M.A. Khan, J. Phys A **26** (1993) 6135.

[16] R. Dickman, Phys.Rev. A **34** (1986) 4246.

[17] M. Ehasasi, M. Mathloch, O. Frank, J.H. Block, K. Christman, F.S. Rys, W. Hirschwald, J. Chem. Phys. **91** (1989) 4949.

[18] J.H Block, M. Ehasasi, V. Gorodetskii, prog. Surf. Sci. **42** (1993) 143.

[19] P. Meakin, J. Chem. Phys. **93** (1990) 2903.

[20] J. Harris and B. Kasemo, Surf. Sci. **105** (1981) L281.

[21] H.P. Kaukonen, R.P. Neiminen, J. Chem.Phys.**91** (1986) 4380.

[22] E.V. Albano, Appl. Phys. A **55** (1992) 256

[23] B.J Brosilow and R. M. Ziff, Phys. Rev. A **46** (1992) 4534.

[24] Hua Da-Yin and Y.Q.Ma, Phys.Rev. E **66** (2002) 066103.

[25] W.F. Banholzer, Y.O. Park, K.M. Makand, R.I. Masel, Surf.Sci **128** (1983) 176.

[26] M.F.H. Von. Tol, B.E. Nieuwenheys, Appl.Surf.Sci. **67** (1993) 188.

[27] K.Yaldram , M.A. Khan, J. Catal. **131**, (1991) 369.

[28] K.Yaldram , M.A. Khan, J. Catal. **136** (1992) 279.

[29] M. A. Khan, K. Yaldram, G. K. Khalil, K.M. Khan, Phys. Rev. E **50** (1994) 2156

[30] A.G. Dickman, B.C.S. Grandi, W.Figueiredo, R. Dickman, Phys. Rev. E **59** (1999).6361

[31] K.M.Khan, K. Yaldram, J. Khalifeh and M.A. Khan, J. Chem. Phys.**106** (1997).8890

[32] F. Yamamoto, H. Kasai, A. Okeh, J. Chem. Phys. Soc. Jpn **60** (1991) 982.

[33] J. Satulavsky, E.V. Albano, J. Chem.Phys. **97** (1992) 9490.

[34] I. Jensen, H.C. Fogedby, Phys. Rev. A **42** (1990) 1969.

[35] J. Cortes, E. Vliana, P. Araya, J. Chem. Phys. **109** (1998) 5607.

[36] K.M.Khan, Surf. Sci. **470** (2000) 155.

[37] B. J. Brosilow, R.M.Ziff, J. Catal. **136**, (1992) 275.

[38] B. Meng, W.H.Wienberg, J. W. Evan, Phys. Rev. E **48**, (1993) 3577.

[39] K.M.Khan, A. basit, E.V. Albano, J. Phys. A: Math. Gen. **35** (2002) 3855.

[40] V.P. Zhdanov, B. Kasemo, Surf.Sci.Rep. **29** (1997) 31.

[41] V.P. Zhdanov, B. Kasemo, Surf.Sci. **412** (1998) 527.

[42] T. Zambelli, J. Wintterlin, J. trost, J. Ertl, Science **273**, (1996) 1688.

[43] Q.F. Ge, R. Kose, D.A. King, Adv. Catal. **45**, (2000) 207.

[44] L. Ollon, V.P Zhdanov, B. Kasemo, Surf.Sci. **529** (2003) 338.

[45] B. Jakson, M. Person, J. Chem. Phys. **103** (1995) 6257.

[46] H. Brune, J. Wintterlin, R.J. Behm,G. Ertl, Phys.Rev.Lett. **68** (1992) 624.

[47] V.D. Pereyra, E.V.Albano, App.Phys.A **57** (1993) 291.

[48] J. Harris, B. Kasemo, E. Tornqvist, Surf.Sci. **105** (1981) L288.

[49] J. Harris, B. Kasemo, Surf.Sci. **105** (1981) L281.

[50] N.O. Wolf, D.R. Burgess, D.K. Hoffman, Surf.Sci. **100** (1980) 453.

[51] HUA Da-Yin, Y.Q.Ma, Chin.Phys.Lett, **19**, (2002) 534.

Chapter -2

MONTE CARLO SIMULATION AND CATALYTIC SURFACE REACTIONS

2.1 Introduction

Monte Carlo (MC) simulation is one of the popular means to solve complex real world problem when other methods are too difficult or too complex to solve. Monte Carlo (MC) simulation is a stochastic technique where random numbers and probability statistics are used to obtain an answer.

In Monte Carlo Simulation, the random selection process is repeated many times to create multiple scenarios. Each time a value is randomly selected, it forms one possible scenario and solution to the problem. Together, these scenarios give a range of possible solution, some of which are more probable and some are less probable. When repeated for many scenarios [10.000 or 30,000 or more], the average solution will give an approximate answer to the problem. Accuracy of this answer can be improved by simulating more scenarios.

2.2 The Monte Carlo Simulation Method

The range of different physical phenomena, which can be explored using Monte Carlo (MC) methods, are exceedingly broad. Monte Carlo methods are applied to a wide range of problem: simulation of surface chemical reaction, nuclear reactor design, stock market fore- casting, radiation transport in the earth's atmosphere and simulation of the esoteric sub-nuclear process in high energy physics experiments, etc. MC method also forms the largest and the most important class of numerical methods used for solving statistical physics problems.

The study of heterogeneous catalysis is a part of industrial and academic activities. In this regard a very little is known about the reaction on microscopic level. The macroscopic interpretation of surface catalysis is obtained from the study of kinetics. The method of kinetics in general tells about the observable quantities such as reactants and products. In order to analyze the connection between the microscopic reaction steps and observed macroscopic behaviour, simulations are conducted and this is generally

performed through Monte Carlo simulation. Therefore MC simulations of heterogeneously catalyzed reactions can be considered as the computational implementation of microscopic reaction mechanism. In fact, such mechanisms are the 'rules'of computer algorithm. Of course, the operation of the rules may lead to the development of correlations, while stochastic fluctuations are inherent in the method [1].

For the practical implementation of the MC method, the catalyst's surface is replaced by a lattice. Therefore, lattice gas reaction models are actually considered. For this reason, the method often faces limitations imposed by the size of the lattice used to simulate the catalyst surface. Therefore, the minimum lattice size L = 40 is used in our simulation. An increase in the lattice size changes slightly the critical value but the overall qualitative nature of the phase diagram is not affected [2]. However, in some particular cases, e.g. when studying second-order phase transition, this shortcoming can be overcome by using to the well-established finite-size-scaling theory. Also, very often one can develop extrapolation methods that give reliable results for infinite lattices.

Another limitation arises when the diffusion rate of the adsorbed species is very large. In this case, most of the computational time has to be devoted to the diffusion process while the quantity of interest, namely the number of reaction events, become negligible. This drawback may be overcome by implementing a mixed treatment: mean field (MF) description of the diffusion and MC simulation of the reaction [1,3]. We have not used this approach in our study. However, this approach may become an interesting and powerful tool in the near future.

MC simulations of dynamic and kinetic process are often hindered by the fact that the MC time, usually measured in MC time steps, is different to the actual time. So, direct comparison with experiments becomes difficult. However, very recently a more sophisticated implementation of the MC method has been envisioned: namely the dynamic MC (DMC) approach that incorporates the actual time dependence of the process allowing direct comparison with experiments [4, 5-7]. Different techniques have been used to study the irreversible phase transitions (IPTs).

Usually, a phase transition is reversible. For example, water freezes to ice and its reverse process is that ice melts to water. Therefore, freezing of water is reversible process. However, the catalytic reaction: $CO + O_2 \rightarrow CO_2$ is mono directional — CO_2 is produced by the oxidation, while the reverse is not true, i.e. as soon as CO_2 is produced, CO and O_2 is not produced in reverse order from CO_2. This is why the catalytic oxidation of CO is called irreversible reaction. In other word, in irreversible reaction,

the backward reaction is not possible. Hence the ZGB model is intrinsically irreversible because the molecules stick to the site that they hit (if there is no reaction) and remain stationary there until removed by the reaction.

The following subsections describe different MC approaches suitable for the study of irreversible phase transitions (IPTs) reaction system.

1. The constant coverage (CC) ensemble
2. The Finite-size-scaling approach to the second order irreversible phase transitions (IPTs).
3. The epidemic method (EM) and dynamic scaling.
4. The standard ensemble.

2.2.1 The Constant Coverage (CC) ensemble

MC simulations using CC ensemble, as proposed by Ziff and Brosilow [8], are probably the most powerful method available for the study of first-order irreversible phase transitions (IPTs).. In order to implement the CC method, it is convenient first to achieve a stationary configuration of the system using the standard ensemble algorithm, and will be described in section 2.2.4. For this purpose, one selects a value of the parameter close to the coexistence point but within the reactive regime. After achieving the stationary state, the simulation is actually switched to the CC method. Then one has to maintain the coverage, with the majority species of the corresponding absorptive state as constant as possible around a prefixed value. This goal is achieved by regulating the number of adsorption events of competing species. The ratio between the number of attempts made trying to adsorb a given species and the total number of attempts is the measure of the corresponding effective partial pressure. In this way, in the CC ensemble, the coverage assumes the role of the control parameter[1].

2.2.2 Finite-Size-Scaling Approach to the Second Order irreversible phase transitions (IPTs)

For the practical implementation of Monte Carlo Simulation (in the ZGB model), the catalytic surface is replaced with suitable lattice size. For this reason, the method often faces limitations imposed by the size of the lattice used to simulate the catalyst surface. Therefore, the minimum lattice size L = 40 is used in our simulation. An increase in the lattice size slightly changes the critical value of y_2 and y_2 but the qualitative nature of the phase diagram is not affected. Hence there is a flaw in the ZGB to simulate an

infinite lattice. This shortcoming can be overcome by using the well-established finite-size-scaling theory; in some particular cases, e.g. when studying second-order phase transition, Also, very often one can develop extrapolation methods that give reliable results for infinite lattices. Since true phase transitions only occur on the thermodynamic limit, i.e. infinite lattice and computer simulations are always restricted to finite samples, numerical data are influenced by rounding and shifting effects around pseudo-critical points [9,10]. Within this context, the finite-size scaling theory [11, 12] has become a powerful tool for the analysis of numerical results, allowing the determination of critical points and the evaluation of critical exponents. The experience gained in the study of reversible critical phenomena under equilibrium conditions can be employed in the field of second-order irreversible phase transitions (IPTs). Examples of the applications of finite –size scaling to various reaction systems can be found in the literature [1,13-16]. Finite-size scaling theory, though originally developed for equilibrium systems, is also applicable to non- equilibrium second-order phase transition.

2.2.3 The Epidemic Method (EM) and Dynamic Scaling

One of the theoretical methods, which we term "epidemic analysis" has also been successfully applied to study the kinetics near the second order catalytic poisoning transition. In order to obtain accurate values of the critical point and the critical exponents using the standard ensemble and applying finite-size scaling, it is necessary to perform MC simulations very close to the critical point. However, at criticality and close to it, due to the large fluctuations always present in second-order phase transitions, any finite system will ultimately become irreversibly trapped by the absorbing state. So, the measurements are actually performed within metastable states facing two competing constraints: on the one hand, the measurement time has to be long enough in order to allow the system to develop the corresponding correlations and, on the other hand, such time must be short enough to prevent poisoning of the sample. This shortcoming can to an extent be crude by taking averages over many samples and disregarding those that have been trapped by the absorbing state. However, it is difficult to avoid those samples that are just evolving to such an absorbing state, unless the fluctuations are suppressed by comparing two different samples evolving through the phase space following very close trajectories [17]. In view of these shortcoming, experience indicates that the best approach to the second-order irreversible phase

transitions (IPTs). is to compliment finite-size scaling of stationary quantities, as obtained with the standard ensemble, with epidemic simulations.

The application of the EM to the study of IPTs has become a useful tool for the evaluation of critical points, dynamic critical exponents and eventually for the identification of universality classes [18,19]. The idea behind the EM is to initialize the simulation using a configuration very close to the absorbing state. Such a configuration can be achieved by generating the absorbing state using the standard ensemble and, subsequently, removing some species from the center of the sample where a small patch of empty site is left. In the case of ZGB model, this can be done by filling the whole lattice with CO, except for a small patch.

After the generation of the starting configuration, the time evolution of the system is followed using the standard ensemble that will be described in section 2.2.4 (the standard ensemble). During this dynamic process, the following quantities are recorded: (i) the average number of empty sites (N (t)); (ii) the survival probability P(t), which is the probability that the epidemic is still alive at time t; and (iii) the average mean square distance, $R^2(t)$, over which the empty sites have spread. Of course, each single epidemic stops if the sample is trapped in the poisoned state with N(t) = 0 and, since these events may happen after very short times (depending on the patch size), results have to be averaged over many different epidemics. It should be noted that N(t) ($R^2(t)$) is averaged over all (surviving) epidemics.

It is expected that at the critical point, these quantities would follow the power law behaviour namely:

$$N(t) \alpha t^{\eta}$$

$$P(t) \alpha t^{-\delta}$$

and

$$R^2 (t) \alpha t^{z}$$

Where η, δ and z are dynamic critical exponents. Thus, at the critical point log-log plots of N(t), P(t) and R^2 (t) will asymptotically show a straight line behaviour, while off-critical points will exhibit curvature. This behaviour allows the determination of the critical point and from the slopes of the plots the critical exponents can also be evaluated accurately [1].

2.2.4 The Standard Ensemble

In this ensemble, the catalyst is assumed to be in contact with an infinitely large reservoir containing the reactant in the gas phase. Adsorption events are treated stochastically, neglecting energetic interactions. The reaction between reactants takes place on the surface of the catalyst, i.e. the so called Langmuir-Hinshelwood mechanism.. After the reaction, the product is removed from the surface and its partial pressure in the gas phase is neglected, so that re-adsorption of the product is not considered. The main theme of this thesis is focused on the use of MC by standard ensemble approach.

In order to further illustrate the practical implementation of the standard ensemble, the simulation method of the lattice gas reaction version of the catalytic oxidation of CO (equations (1.1)-(1.3)) according to the ZGB model [20] in a two-dimensional square lattice is described.

$$CO(g) \rightarrow CO\ (a) \qquad (1.1)$$

$$O_2\ (g) \rightarrow 2O\ (a) \qquad (1.2)$$

$$CO\ (a) + O\ (a) \rightarrow CO_2\ (g) \qquad (1.3)$$

The MC algorithm is as follow:

1. CO or O_2 molecules are selected at random with reactive probabilities P_{CO} and P_O, respectively. These probabilities are the relative impingement rates of both species, which are proportional to their partial pressures in the gas phase in contact with the catalyst. Due to the normalization, $P_{CO} + P_O = 1$, the model has a single parameter, i.e. P_{CO}. If the selected species is CO, one surface site is selected at random, and if that site is vacant, CO is adsorbed on it according to equation (1.1). Otherwise, if that site is occupied, the trial ends and a new molecule is selected. If the selected species is O_2, a pair of nearest-neighbour (NN) site is selected at random and the molecule is adsorbed on them only if they are both vacant, as required by equation (1.2).
2. After each adsorption event, NNs of the added molecule are examined in order to account for the reaction given by equation (1.3). If more than [CO(a), O(a) pair is identified, a single one is selected at random and removed from the surface [1].

The Phase diagram of the ZGB model which is obtained using the standard ensemble is shown in the following Fig. 2.1 and will be further discussed in section 3.4.1. It is worth mentioning here that for our research work, the standard ensemble method is adopted.

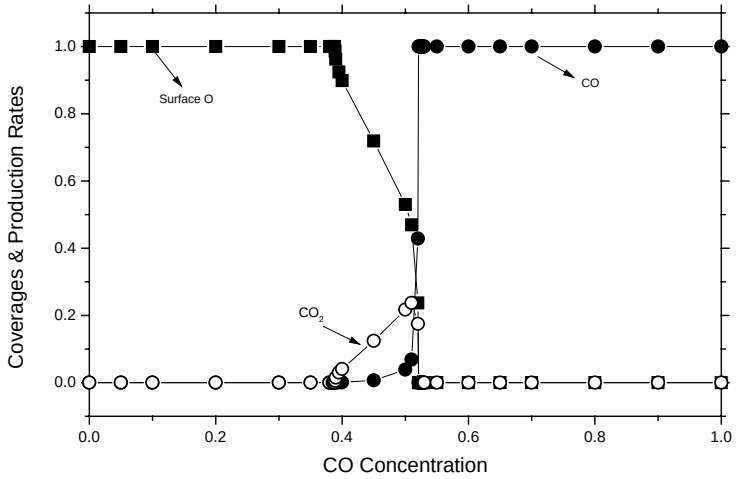

Fig. 2.1 Phase diagram of the ZGB model obtained using the standard ensemble, showing the dependence of the surface coverage with CO and oxygen (O) and the production rate of CO_2 on the partial pressure of CO (CO concentration) in the gas phase.

2.3 References

[1] E. Loscar and E. V. Albano, Rep.Prog.Phys.**66**, (2003) 1343.

[2] K. M Khan, K. Yaldram, N. Ahmad, Qamar-ul-Haque,Physica A **268**, (1999) 89.

[3] M. Silverberg, A. Ben-Shaul, J.Chem. Phys. **87** (1987) 3178.

[4] R.J. Gelten, A.P.J. Jansen, R.A. van Santen, J. Chem. Phys. **108** (1998) 5921.

[5] K.A. Fichthorn, W.H. Weinberg, J.Chem. Phys. **95** (1991) 1090.

[6] B. Meng, W.H. Weinberg, J.Chem. Phys. **100** (1994) 5280.

[7] A.P.J. Jansen, Comp. Phys. Commun, **86** (1995) 1.

[8] R.M.Ziff, B. J. Brosilow, Phys. Rev. A **46** (1992) 4630.

[9] K.Binder, Rep. Prog. Phys, **60** (1997) 487.

[10] K.Binder and D Heermann, Monte Carlo Simulation in Statistical Physics. An Introduction 4th edn (Berlin: Springer, 2002).

[11] J Cardy, Scaling and Renormalization in Statistical Physics ed P Goddard and J.M Yeomas (Cambridge: Cambridge University Press, 1997).

[12] M.N Barber, Phase Transitions and Critical Phenomena vol II, ed C Domb and J.L Lewobitz (London: Academic, 1983) p 146.

[13] E.V. Albano, Phys. Rev. B **42** (1990) R10818.

[14] T. Aukrust, D.A. Browne, I. Webman, Phys. Rev. A **41** (1990) 5294.

[15] I. Jensen and R. Dickman, Phys. Rev. E **48** (1993) 1710.

[16] I. Jensen, Phys. Rev. E **50** (1994) 3623.

[17] E.V. Albano, Phys. Rev. E **49** (1994) 1738.

[18] I. Jensen, H. Fogedby, R.Dickman, Phys. Rev. A **41** (1990) R3411.

[19] P. Grassberger, J. Phys. A: Math.Gen. **22** (1989) 3673.

[20] R.M.Ziff, E. Gulari, and Y.Barshad, Phys. Rev. Lett. **56** (1986) 2553.

Chapter-3

SURFACE CATALYTIC REACTIONS

3.1 Introduction

Catalyst is a substance that increases the rate at which a chemical system approaches equilibrium, without being consumed in the process. Catalysis is the phenomenon of a catalyst in action. Now-a-days catalysis is a part of many industrial activities. Because of its application in industrial activities, catalysis plays a prominent role in our society. The majority of all chemicals and fuels produced in the chemical industry have been in contact with one or more catalysts. Catalysis becomes also progressively more important in environmental pollution control. Particularly heterogeneous catalysis is very important in oil refinery, organic synthesis, depollution and many other fields. In short, catalysis is vitally important for our economics now and it will be even more important in the future. The general textbooks on the physics and chemistry about the surfaces and introductory textbooks on the theory of catalysis are listed in the references [1-10].

3.2 Elementary Steps in Surface Chemical Reactions Processes

In most cases surface reactions proceed according to well- established elementary steps, as schematised in Fig.3.1.

The first one comprises trapping, sticking, and adsorption. The adsorption of the reacting species on the active phase of the catalyst takes place mostly on the metal particles. There on the metal surfaces, intra-molecular bonds are broken or weakened. Subsequently the adsorbed species react with each other or with gas phase species. This generally occurs in consecutive steps until the desired product is reached which desorbs afterwards. The role of the catalyst is to reduce the activation energy of the rate limiting reaction step. Particularly important, from the catalytic point of view, is that molecules frequently undergo dissociation; e.g.; N_2, O_2, H_2, etc,. Sticking and adsorption are processes dependent on surface structure (both geometric and electronic). In some cases

chemisorptions of small atoms and molecules may induce the reconstruction of the surface.

After adsorption, species may diffuse on the surface, eventually, become absorbed in the bulk. Due to collision between adsorbed species of different kinds the actual reaction step can occur. The result of the reaction step is the formation of a product molecule. This product can be either an intermediate of a reaction or its final output.

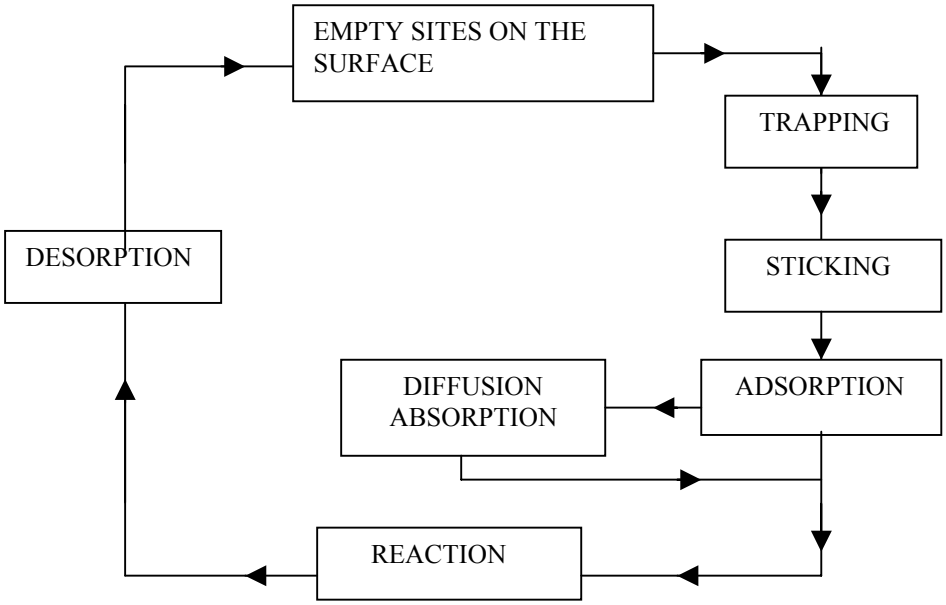

Fig.3.1 Schematic description of the relevant steps involved in a surface catalyzed reaction within the reactive regime. The cycle starts with the empty sites of the surface (top) and is followed by interactions between reactants and the surface (right branch). Such interaction finally leads to the reaction (bottom) and desorption of the products (left branch), a process which generates new empty sites [4].

The final step of the whole reaction process is the desorption of the products. This step is essential not only for the practical purpose of collecting and storing the desired output, but also for the regeneration of the catalytic active sites of the surface. The role of a good solid-state catalyst is to obtain an acceptable output rate of the products. Reactions occurring in this way are commonly known as heterogeneously catalysed [4].

3.2.1 Adsorption Mechanism

Two types of adsorption phenomena have been recognized in principles for many years: physical adsorption and chemical adsorption, or chemisorption.

(i) Physical adsorption (Physisorption) is the relatively weak bond between adsorbates with a closed valance electronic shell (e.g. rare gas atom) and solid surface. Two interaction mechanisms contribute to the physisorption potential: The attractive van der Waals and the Pauli repulsion. The van der Waals is caused by secondary attractive forces such as dipole-dipole interaction and induced dipoles and is similar in character to condensation of vapour molecules onto a liquid of the same composition. This dipole-dipole attraction is long-ranged and dominates the physisorption potential at large distances from the surfaces. The short-ranged Pauli repulsion dominates the physisorption potential close to the surface.

(ii) Chemisorption involves chemical bonding, is similar in character to a chemical reaction, and involves transfer of electrons between adsorbent and adsorbate. Therefore, when a molecule or atom is brought in contact with surface, it may combine with the surface through the formation of a chemical bond (chemisorption). This type of chemisorption is a first step in surface catalysis. The forces involved in physical adsorption are much smaller than those involved in chemical bonding.

3.3 Catalytic Reaction Mechanisms

The study of catalytic reaction mechanism continues to be a topic of great interest. The following reaction mechanisms are studied through Monte Carlo simulation.

1. Langmuir-Hinshelwood mechanism.
2. Precursor mechanism.
3. Hot atom mechanism.
4. Eley Rideal mechanism

3.3.1 Langmuir-Hinshelwood Mechanism

The CO oxidation is one of the simplest catalytic reactions to investigate the heterogeneous catalysis. The possible reaction paths for the oxidation of CO to take place at platinum metals were expressed nearly 60 years ago by Langmuir as follows. “There are two possibilities. A carbon monoxide molecule can condense on a surface of platinum and an oxygen atom can condense by the side of it, and then the two can interact. Or you can have an oxygen atom adsorbed on the surface and the carbon monoxide molecule can

combine with it during collision". The first type of elementary process is now called the Langmuir-Hinshelwood mechanism (thermal) and it turns out that CO oxidation actually proceeds along this path, whereas the second mechanism is named after Eley and Rideal (non-thermal). The assumptions made by Langmuir-Hinshelwood (LH) mechanism are:

1. The adsorbed species are held onto definite points of attachment on the surface. Each site can accommodate only one adsorbed species.
2. The surface is completely uniform so that there is the same probability of adsorption on all sites. Attractive or repulsive forces between adjacent adsorbed molecules are taken to be negligible.

The Langmuir- Hinshelwood mechanism LH [11,12] forms an important class of reactions. Generally speaking, in the LH mechanism both particles involved in the reaction are initially adsorbed on the surface of the catalyst and are thermalized to it. Subsequently, these particles move across the surface by tunneling or by diffusion. The energy released will be partly absorbed by the surface and partly taken away by the product molecule.

Briefly we now write that the LH mechanism consists of the following types of steps:

- Adsorption from the gas-phase
- Desorption to the gas-phase
- Dissociation of molecules at the surface
- Reaction between adsorbed molecule

As an example, the formation of CO_2, through catalytic oxidation of CO for LH mechanism, the reaction may proceeds as:

$$CO(g) + S \longrightarrow CO(a) \qquad (1)$$

$$O_2(g) + 2S \longrightarrow 2O(a) \qquad (2)$$

$$CO(a) + O(a) \longrightarrow CO_2(g) + 2S \qquad (3)$$

Here S is an empty site on the surface, while (a) and (g) refer to the adsorbed and gas phases, respectively. Moreover, it is known that under suitable temperature and pressure conditions, CO molecule may diffuse on the surface. Furthermore, there is a small probability of CO desorption that increases as the temperature is raised.

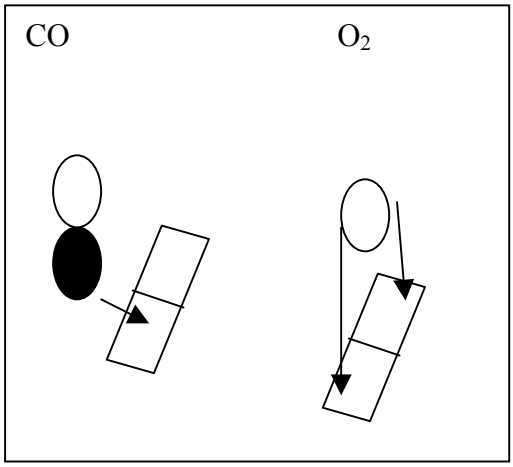

Fig. 3.2: Schematic of the adsorption of CO and O_2 on the Pt surface. Carbon monoxide takes up one lattice site while oxygen takes up two.

Therefore, in the above reaction as an example, CO is first chemisorbed and has an appreciable surface lifetime during which it may react. The CO_2 yield should be highest if the surface concentrations of CO*(a)* and O*(a)* are about equal. In LH mechanism, the mechanism of adsorption of each species is different, since their interaction with the surface is different. The schematic representation of this (LH mechanism for CO oxidation) is shown in figure 3.2: If a CO molecule strikes the surface, only one vacant site is needed for the molecule to stick to the surface. If the striking molecule is O_2, then two pair of adjacent sites is chosen at random for the adsorption of O_2 molecule.

The algorithm of reaction treated is as follows:

> After an adsorption has taken place, each resulting occupied site must have its four nearest neighbour sites checked for reactants of the opposite type. If there are any, then one pair is randomly selected to react. If the reaction is successful, then both sites become empty.

3.3.2 Precursor Mechanism

When an atom or molecule strikes a surface, it may be trapped or be scattered back into the gas phase. A trapped molecule, however, will not "chemisorb" instantaneously. In general, a period of time, T_{th}, will elapse between the initial collision of a molecule with a surface and the attaining of chemisorbed state. During this time, the ad-particle is not in

thermal equilibrium with the surface. Its motion may take one of several forms, perhaps involving parallel transport along the surface, depending on the nature of the surface-ad-particle interaction. We will refer to trapped particles not in thermal equilibrium with the surface as "precursors" and note that this is a more general usage of the word than is usually found in the literature. A precursor mechanism involves such consideration of non-thermal adsorption and reaction of the reacting species. Wolf et al. [13] have pointed out the existence of "precursors" in the adsorption of N_2 on W(100) surface. If the precursor collides with a chemisorbed atom a direct reaction may take place followed by immediate desorption of the product. The central idea that a molecule striking a surface does not immediately come to thermal equilibrium with the surface but remains for some period of time in "precursor motion" A collision of this "precursor" with a chemisorbed species may lead to direct reaction followed by desorption of the product, in which case the mechanism is no-thermal and the products can be in states of high translational or internal excitation [14].

The approach of precursor mechanism for CO-NO reaction and CO- O_2 reaction has been applied and results of simulation work are presented in forthcoming chapters of this thesis.

3.3.3 Hot Atom Mechanism

The existence of transient mobility of adsorbed particles on solid surface is still in a state of turmoil. It concerns the question whether the chemical energy, which is released during adsorption is directly dissipated to the heat bath of the solid, or may, at least in part, be transformed into kinetic energy, causing non-thermal motion of the adsorbed particles across the surface, or even inducing chemical reaction [14]. Recent experiments by scanning tunneling microscopy (STM) on the dissociative adsorption of oxygen molecules on an Al (111) surface [15,16] pointed to a "hot atom" mechanism according to which the two oxygen atoms are propelled apart upon dissociation, by distances exceeding 80 Å in a ballistic type of motion before equilibrating with the substrate. Molecular dynamics simulation [17] concluded however, that, with realistic assumptions about the initial kinetic energy, hyper-thermal motion could lead only to separations between the O atoms of less than 16 Å. All these effects are important for the general understanding of energy dissipation during adsorption.

The two "hot" oxygen atoms created, react with adsorbed CO molecule or can stimulate desorption of other co- adsorbed particles [16,18-19]. Wintterlin *et al.* [18]

showed existence of a hot atom mechanism for the dissociation of O_2 on Pt (111) surface through variable temperature. Pt (111) surface can be approximated to a two dimensional hexagonal lattice where first nearest neighboring (nn) sites have a distance of one atomic spacing. The second and third sites have distances of 1.73 and 2 lattice constants respectively. It was found by Wintterlin *et al*. [18] that two oxygen atoms created by the dissociation, appeared in pairs, with average distance of two lattice constants. Moreover it was also found that the appearance of two oxygen atoms in pair, having one atomic spacing distance, has very small probability [18].

Recently [20], we have taken the idea of "hot atom" that whenever an O_2 molecule hits a randomly vacant selected site, the molecule breaks up into atomic form and then executes a ballistic flight. The path of oxygen atoms are taken exactly to be opposite to each other, i.e. anti-parallel and the ranges of the atoms are taken to be equal. For example, for square lattice, these hot atoms may fly up to 1 or √2 or of 2 of the atomic spacing from the site of impact. The pattern of each environment is shown in the following figure 3.3.

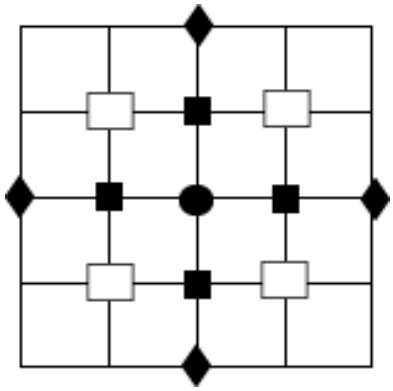

Fig.3.3. Pattern of 1st, 2nd and 3rd environment on the square surface. Solid circle for the site of impact, solid squares for 1st environment, open squares for 2nd environment and solid diamonds for 3rd environment.

Simulation of this idea of ballistic flight on square surface is applied on the ZGB model [21]. Then through the simulation, the effect of transient mobility of hot atoms on the phase diagram reveals that the production of CO_2 starts as soon as CO partial pressure departs from zero, which clearly verifies the experimental observation. These results are also presented and discussed in the next chapters of the thesis.

3.3.4 Eley Rideal Mechanism

One class of non-thermal processes is the transient non-thermal mobility of one species based on Eley-Rideal (ER) mechanism. In ER mechanism only one particle is adsorbed on the catalytic surface and thermalized to it. The second particle collides with the first particle without first being thermalized to the surface, forming a molecule that desorbs from the surface. Therefore, the possible steps involved in ER Mechanism are shown in the following steps:

1. An atom adsorbs onto the surface
2. Another atom passes by, which interacts with the one on the surface
3. A molecule is formed which desorbs from the surface

In ER mechanism more excess energy will be available to the product, because only one bond with surface has to be broken. The possible elementary steps involved in CO_2 formation can be formulated as:

$$O_2(g) + 2S \rightarrow 2O(a) \quad (3.1)$$

$$CO(g) + S \rightarrow CO(a) \quad (3.2)$$

$$CO(a) + O(a) \rightarrow CO_2(g) + 2S \quad (3.3)$$

$$CO + O(a) \rightarrow CO_2(g) + S \quad (3.4)$$

In the above reaction mechanism, the reaction step (3.3) proceeds via L-H mechanism, where as the reaction step (3.4) proceed via ER mechanism. The reaction- step (3.4) is a reaction path for the formation of CO_2 through catalytic oxidation in which an oxygen atom can condense on the site and the carbon monoxide can combine with it during collision. Since the collision time of CO molecule striking the surface as well as the surface lifetime of a physisorbed CO species is immeasurably short, the time of lag between the impact of CO molecule on an O_{ad} layer and the formation of CO_2 would also be immeasurably short in the case of the ER mechanism. The reaction rate (at constant CO flux) should be highest when the O_{ad} coverage is highest. However, the so far ER mechanisms have only been observed experimentally for somewhat artificial reaction triggered by a beam of atomic hydrogen (or deuterium) [22-25].

This class of reaction (ER) is halfway between the gas phase and the LH type. Jackson and Persson [26] have studied the dynamics of a 'hot' hydrogen dimer in ER

process (the direct reaction between a gas phase H atom and an adsorbed H atom) using a fully three-dimensional flat surface model for Cu (111). Meakin [27] have explored the effects of the ER process on the simple ZGB model for the catalytic oxidation of CO by oxygen. The ER process results in the formation of a new regime in which a continuous reaction can be sustained and a continuous production of CO_2 starts as soon as the CO partial pressure departs from zero.

Briefly, an Eley Rideal reaction involves the direct impingement of an atom or molecule on a chemisorbed species resulting an immediate formation of product and desorption to the gas phase. For example a direct reaction between a gas phase H atom and an H atom adsorbed on Cu is an exothermic ER reaction.

Generally, for the vast majority of surface catalytic reactions, it has been accepted that LH mechanism is preferred, while few reactions proceed via Eley-Rideal mechanism [22,23,28]. Baxter [29], has investigated the catalytic CO oxidation on Pt(111) and has compared the LH mechanism and ER mechanism on the basis of reaction barrier. For example reaction barriers in CO oxidation via ER was calculated to be 0.72 eV, while reaction barrier on the exact same system via LH mechanism was determined to be 0.80. A comparison between the reaction barriers for these two mechanisms (LH & ER) yields a surprising result: The reaction barrier from the Eley-Rideal (ER) mechanism is, in fact lower than that of Langmuir-Hinshelwood (LH). It is generally thought that a reaction usually follows a mechanism or a pathway with a lower barrier, implying that the ER mechanism should be followed due to having a lower reaction barrier. However, experimental evidence shows that LH mechanism is favoured for the catalytic CO oxidation on Pt (111). Baxter [29] has explained as to why it is more probable for the reaction to proceed via LH mechanism, despite the LH mechanism possesses a higher reaction barrier than that of ER mechanism.

In this thesis the approach of ER mechanism has been applied to CO-O_2 and CO-NO reaction. The modelling and simulation work in this regard is presented in the next chapters.

3.4 Basic Modelling of SCR

Because of technological importance and its simplicity, the oxidation of carbon monoxide to form carbon dioxide is one of the most extensively studied heterogeneous catalytic reactions. The macroscopic interpretation of such reaction is obtained from the study of

kinetics, which is simply the observation of the bulk concentration of all species in the system over that time, whereas the understanding about the fundamental catalytic reaction steps in heterogeneous catalysis, the use of Monte Carlo simulation is examined in simulating the monomer-dimer catalytic reaction of the type:

$$CO + (½)\ O_2 \rightarrow CO_2$$

Monte Carlo method is the basic tool for the study of surface catalytic reaction. In a Monte Carlo simulation, random numbers are used to generate microscopic scale events, which give rise to the appropriate macroscopic behaviour. The first assumption in modelling the reaction is that the surface of the catalyst be represented by two-dimensional lattice with periodic boundary conditions. For the reaction to take place a gas mixture composed of CO and O_2 molecules with fixed molecular concentration of y_{CO} and $1\text{-}y_{CO}$ respectively, is brought in contact with a surface. At any given time, a lattice site can either be vacant, occupied by a CO molecule, or occupied by an O atom. In the following section the technique of the Monte Carlo simulation is applied to a monomer-dimer catalytic reaction through the ZGB model.

3.4.1 Ziff, Gulari And Barshad (*ZGB*) Model

Computer simulation have been used extensively to explore adsorption, desorption, phase transition, reaction kinetics, phase separation, and other aspects of surface chemistry and physics. In particular, interest is growing in the use of simple models to develop a better understanding of heterogeneous catalysis. A simple model for the catalytic oxidation of carbon monoxide by oxygen was introduced by Ziff, Gulari and Barshad (ZGB) in 1986 as a computer simulation [21]. It is usually referred as the ZGB model. The ZGB model is based on Langmuir-Hinshelwood (LH) mechanism. According to this mechanism the reaction takes between “chemisorbed” reactants i.e. all reactants are adsorbed on the surface and attain thermal equilibrium with the surface before reaction. Therefore LH mechanism is also called a thermal mechanism. The ZGB model is based upon some of the known steps of the CO-O_2 reaction on a single-crystal catalyst surface. The basic steps in heterogeneous catalysis of a chemical reactions are:

(i) The adsorption of the reacting species on the surface

(ii) Their reaction

(iii) The desorption of the product CO_2

The ZGB model deals with the monomer-dimmer reaction. The reaction occurs by the following three steps:

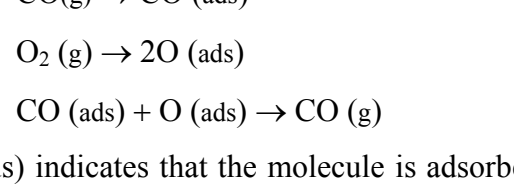

$CO(g) \rightarrow CO\ (ads)$

$O_2\ (g) \rightarrow 2O\ (ads)$

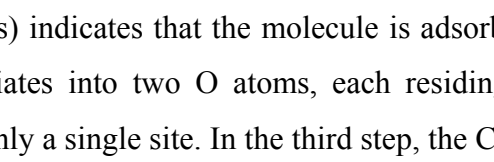

$CO\ (ads) + O\ (ads) \rightarrow CO\ (g)$

where (ads) indicates that the molecule is adsorbed on the surface. Upon adsorption, the O_2 dissociates into two O atoms, each residing on a separate surface site, while CO requires only a single site. In the third step, the CO_2 desorbs after it is produced. The ZGB model uses square lattice to present the catalyst surface. In this model it is assumed that when gas-phase molecules of CO or O_2 collide with blank sites, they absorb immediately, and when the O and CO occupy adjacent (nearest neighbour) site, they react immediately. The CO_2 that is produced desorbs instantly and does not interact further with the system. The composition in the gas phase is not changed by the reaction; the gas volume is assumed to be very large. The other mechanisms, such as finite reaction rates, diffusions of the species about the surface, reassociation and desorption of the O atoms, desorption of unreacted CO molecules are not considered in the simplest ZGB model.

The relative impingement of CO and O_2 species, which are proportional to their partial pressures, are normalized ($y_{CO} + y_{O_2} = 1$), so the model has a single parameter, i.e.; y_{CO}. The ZGB model is an idealized model and there are no energy parameters. In this regard it is analogous to a hard-particle gas, and the only independent variable is the gas-phase composition i.e.; the relative amounts of O_2 and CO.

This model is intrinsically irreversible because the molecules stick to the site that they hit and remain stationary until removed by a reaction. Thus it is assumed that surface impingement rate is much greater than the surface diffusion rate. In the simulation of ZGB model, a trial begins with the random collision of a gas molecule on a square lattice, which represents the surface. Carbon monoxide or oxygen molecules are selected randomly with relative probability y_{CO} and ($1-y_{CO}$), and an attempt is made to add the selected molecule to the surface. If the selected molecule is CO, the following happens:

(a) A site on the lattice is randomly selected. If that site is already occupied, then the trial ends (the CO bounces of the surface); otherwise, CO adsorbs. After a CO molecule has been added to the surface, its four nearest neighbours (nn) are checked randomly. If an O is found in any of the nn sites, reaction takes place with the formation

of CO_2 that desorbs from the surface leaving behind two vacant sites. If the selected molecule is an O_2, the following happens:

(b) The two adjacent sites are selected randomly on the surface. If either site is occupied, the trial ends; otherwise the O_2 disassociates and adsorbs on two adjacent sites. All the six nn (nearest neighbour) sites are checked randomly. If any of the six nn sites has a CO, it is reacted with the adjacent O atom, with the formation of CO_2 and the two sites are vacated.

The above *algorithm* can be summarized as follows:

(1) Select a molecule CO with probability Y_{CO} and O_2 with probability 1- Y_{CO}.

(2) If the molecule is CO then

- (a) Select a site randomly.
- (b) If the site is unoccupied then CO adsorbs, Else CO is back scattered.
- (c) The adsorbed CO, checks randomly the adjacent sites. If O is found, it reacts, CO_2 is produced and is desorbed from the surface.

(3) Else the molecule is O_2

- (a) Select the adjacent sites randomly.
- (b) If either site is occupied, the trial ends, Else O_2 dissociates and adsorbs
- (c) All six neighbours are checked randomly for the presence of CO
- (d) If a CO-O pair is found, CO_2 is produced with the creation of two vacant sites.

The algorithm of the ZGB model is applied on catalytic surface, to reproduce literature results for the specific case of $CO + ½ O_2 \rightarrow CO_2$. Although similar effects can be demonstrated using ODE's of the mean field type, while the ZGB model has less parameter and give much more detailed microscopic description of the system than is possible with the former. Both the qualitative and quantitative results of the present simulation by the ZGB model are discussed. The results of simulation based on ZGB model are illustrated in the following figure 3.4.

All the results of simulation in this thesis are based on the programming language used as C++.

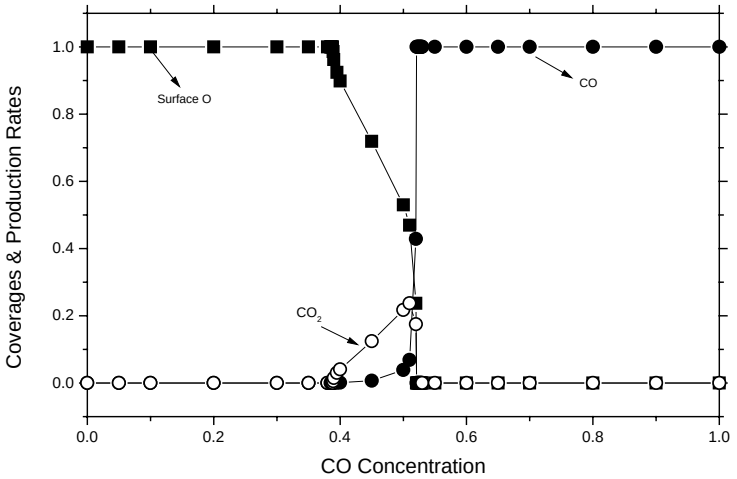

Fig. 3.4. Phase diagram of the ZGB model obtained using the standard ensemble, showing the dependence of the surface coverage with CO and oxygen (O) and the production rate of CO_2 on the partial pressure of CO (CO concentration) in the gas phase.

It is noted that in the limit of large y_{CO} (when $y_{CO} \approx 0.525$), the surface is totally covered by CO and reaction stops. Similarly in the limit of small y_{CO} (when $y_{CO} \leq 0.389$), the surface is saturated by O_2 species. In fact, the surface of the catalyst fully covered by a single type of species, where further adsorption of the other species is no longer possible, corresponds to an inactive state of the system. This state is known as 'poisoned', in the sense that adsorbed species on the surface of the catalyst are the poison that causes the reaction to stop. Physicist used to call such a state (or configuration) 'absorbing' because a system can be trapped by it forever, with no possibility of escape.

The ZGB model, in spite of its simplification, describes qualitatively the main characteristics of a large number of experiments carried out with the CO- O_2 reaction over various catalysts. For example, the reaction mechanism exhibits two phase transitions y_1 and y_2. At a feed concentration of CO less than y_1, the surface is completely covered with oxygen. Above a second value y_2 the lattice is filled with CO. Only in the range $y_1 < y_{co} < y_2$, the system shows a steady reactive state (SRS). The transition at y_1 (=0.389) is continuous, whereas at y_2 (=0.525), the system has a discontinuous phase transition. A second-order phase transition (SPOT) at y_1 (=0.389) separates an oxygen-poisoned state from a steady reactive state (SRS) while a first-order phase transition (FOPT) at y_2 (=0.525) separates a CO poisoned state from SRS. However, a controversial feature of the

ZGB model concerns the second-order phase transition, which has never been observed experimentally in the oxidation of CO. (**see the experimental Fig. 1.2 Chapter 1).**

3.5 Variants of The ZGB Model

In the ZGB model the reaction occurs via Langmuir-Hinshelwood (LH) mechanism, in which both reactants are initially adsorbed on the surface and are in thermal equilibrium with the surface prior to reaction to form the product. In the ZGB model the effect of desorption and diffusion of species were ignored. Inclusion of these processes also extends the applicability of the algorithm to other chemical systems as in the case of CO-NO reaction. The other class of variants of ZGB model is the inclusion of non-thermal processes. These processes include Precursor, Eley-Rideal (ER) mechanism and hot atom mechanism.

3.5.1 Desorption Mechanism

This is the process in which both CO and O_2 can remove themselves from the surface and return to the gas phase. The probability that this will occur generally depends on the temperature of the catalyst surface but in terms of the Monte Carlo simulation, it is best represented by a probability of desorption. For the carbon monoxide oxidation reaction on Pt, only the CO desorption, is important for temperatures below ≈ 500 K. Oxygen is less likely to desorb since the atoms must recombine before leaving the surface, a highly endothermic process. Thus, the step which is added to the ZBG algorithm is to include CO desorption to see the effect of temperature on the surface of the catalyst.

3.5.2 Diffusion Mechanism

Diffusion is a transport property of a system, which describes the flow of mass across a concentration gradient. In the case of the Monte Carlo simulation, this translates to the possibility that once on the surface, reactants can move to another empty lattice site. Like desorption, this is dependent on the temperature of the surface and it represented by the probability of diffusion. For the reaction of carbon monoxide and oxygen on Pt, only the CO phase is very mobile. In the case of CO-NO reaction the diffusion of NO is taken in to consideration. The simulation work based on the diffusion work has been presented in the next forthcoming chapters.

3.6 References

[1] G.A. Somorjai, Chemistry in Two Dimensions: Surface, Cornell University Press,1981.

[2] A. Zangwill, Physics at Surfaces, Cambridge University Press, 1988.

[3] M.Prutton, Surfaces Physics, Oxford University Press, 1983.

[4] E.V.Albano, in: M Borowko (Ed.), Computational Methods in Surface and Colloid Science,. Marcel Dekker, New York, 2000, p.387. .

[5] T.N. Rodin and G.Ertl, The Nature of the Surface Chemical Bond, North Holland, Amsterdam, 1979.

[6] R.A. van Santen, Theoretical Heterogeneous Catalysis, World Scientific, Singapore, 1991.

[7] J.M.Thomas and W.J. Thomas, Introduction to Heterogeneous Catalysis, Academic Press, 1967.

[8] B.C. Gates, J.R. Katzer and G.C.A. Schuit, Chemistry of Catalytic Process, McGraw Hill, New York, 1979.

[9] G.A. Somorjai, Chemistry in Two Dimensions: Surface, Cornell University Press,1980.

[10] I.M. Campbell, Catalysis at surfaces, Chapman and Hall, London, 1988.

[11] Engle T and Ertl G, J. Chem. Phy.**69** (1978) 1267

[12] Engle T, J. Chem. Phy.**69** (1978) 373.

[13] N.O. Wolf, D.R. Burgess, D.King. Hoffman, Surf. Sci.**100** (1980) 453.

[14] J. Harris and B. Kasemo, Surf. Sci. **105** (1981) L281.

[15] H. Brune, J. Winterlin, R. J. Behm, G. Ertl, Phys. Rev. Lett. **68** (1992) 624.

[16] H. Brune, J. Winterlin, J. Trost, G. Ertl, J. Wiechers, R. J. Behm, J. Chem. Phys. **99**, (1993) 2128.

[17] C. Engdahl, G. Wahnstrom, Surf. Sci, **312** (1994) 429.

[18] J. Winterlin, R. Schuster, G. Ertl, Phys. Rev. Lett.**77** (1996) 123.

[19] A.N. Artsyukhovich, I. Harrison, Surf. Sci. **350** (1996) 1199.

[20] M. Khalid, A.U. Qaisrani, K. M. Khan, Q.N. Malik, Chin. Phys. Lett.**21** (2004) 1171.

[21] R.M.Ziff, E. Gulari, and Y.Barshad, Phys. Rev. Lett. **56** (1986) 2553.

[22] E.W. Kuipers, A. Vardi, A. Danon, A. Amirav, Phys. Rev. Lett. **66** (1991) 116.

[23] C. T. Rettner, Phys. Rev. Lett. **69** (1992) 383.

[24] C. T. Rettner, D. J. Auerbach, Phys. Rev. Lett. **74** (1995) 4551.

[25] C. T. Rettner, Chem. Phys. **101** (1994) 1529.

[26] B. Jackson, M. Persson, J. Chem. Phys.**103** (1995) 6257.

[27] P. Meakin, J. Chem. Phys.**93** (1990) 2903.

[28] C.Stampfl, M. Scheffler, Phys.Rev.Lett. **78** (1997) 1500.

[29] R.J. Baxter, P.HU, J. Chem. Phys. **116** (2000) 4379

Chapter-4

SIMULATION OF CO-O_2 REACTION

4.1 Introduction

The detailed understanding of catalytic reactions is very important in applied research but such an understanding has rarely been achieved either from the experiment or from theory. Computer simulation is another tool that may be helpful for the understanding of certain aspects of kinetics involved in the catalytic process. For this purpose, the catalytic oxidation of carbon monoxide, namely:

$$2CO + O_2 \rightarrow 2CO_2,$$

which is one of the simplest and most studied heterogeneous catalytic reaction, has been selected. In 1986, Ziff, Gulari and Barshad (ZGB) [1] introduced a simple model as a computer simulation to describe the surface catalysis of the chemical reaction:
$CO + O \rightarrow CO_2$. The results of ZGB model reveal that for small values of y_{CO} ($y_{CO} < y_1$), the surface is poisoned by oxygen atoms. As y_{CO} is increased above a critical value of y_1, steady production of CO_2 starts. For large values of y_{CO} ($y_{CO} > y_2$), the surface becomes poisoned by CO and no further reaction takes place.The transition at $y_1 \approx 0.389$ is of second order while the transition at $y_2 \approx 0.525$ is of first order. However, the second order phase transition (SOPT), has never been observed experimentally in the CO oxidation. The experiments show that production of CO_2 starts as soon as CO concentration departs from zero [2-4].

In heterogeneous catalysis, generally three main reaction mechanisms have been proposed, namely, Precursor mechanism, Langmuir- Hinshelwood mechanism and the Eley-Rideal mechanism. Haris and Kasemo [5] have given a detailed discussion on the precursor mechanism. In the Eley-Rideal mechanism [6] only one species is adsorbed on the surface and thermalized to it; whereas the second species reacts directly from the gas phase, with the chemisorbed species without being thermalized to the surface, forming a molecule that desorbs from the surface.

The original ZGB model assumes that the reaction between CO and O_2 on the square surface proceeds according to the L-H process. However it excludes the non-thermal process i.e ER and Precursor mechanism. Now in this chapter we want to

investigate that how ER mechanism affects the mode of reaction on simple cubic and body centered cubic lattice.

4.2 Simulation on Simple Cubic Lattice (SCL) With ER

Many research groups have given evidence that non-thermal processes are also important to understand the catalytic reactions [5, 7- 12]. The Ely-Rideal (ER) process is one of these processes. In this current study (simulation), the effects of the ER process on the phase diagram of the LH type monomer-dimer (CO-O_2) catalytic reaction on surface and subsurface of a simple cubic structure has been investigated. With the consideration of a new pathway in which oxygen molecule (dimer) is adsorbed in such a way that it takes one surface site whereas second site may be from surface or from subsurface.

4.2.1 Model and Simulation

The usual simple LH surface-subsurface model of the system can be written in the form of the following equations.

$$CO\,(g) + S \rightarrow CO^{S} \tag{4.1}$$

$$O_2\,(g) + S + SS \rightarrow O^{S} + O^{SS} \tag{4.2}$$

$$O_2\,(g) + 2S \rightarrow 2O^{S} \tag{4.3}$$

$$CO^{S} + O^{S} \rightarrow CO_2\,(g) + 2S \tag{4.4}$$

$$CO^{S} + O^{SS} \rightarrow CO_2\,(g) + S + SS \tag{4.5}$$

With the introduction of Eley-Rideal process, one has to add the following equation:

$$CO\,(g) + O^{S} \rightarrow CO_2\,(g) + S \tag{4.6}$$

Here (g), S and SS indicate gas phase, active surface and subsurface sites respectively while X^{S} and X^{SS} represent X adatom on the surface and subsurface respectively. There appears to be considerable uncertainty concerning the relative importance of LH and ER reaction steps given by equations (4.4) and (4.6) respectively [13, 14]. It is worthwhile to mention that the relative frequency of LH reaction step and the ER reaction step depends upon oxygen coverage. If the initial oxygen coverage on the surface is higher (small y_{CO} values), then ER reaction step becomes dominant otherwise LH reaction step becomes important [15]**.** We have investigated the addition of reaction step (4.6) to the usual simple LH surface-subsurface model of the reaction system. Here in this model a simple cubic structure is considered. Two layers of square lattices are exercised so that each surface site (upper layer site) has a subsurface site (lower layer site) just below it. This is

exactly the (001) surface and subsurface of a simple cubic structure. For each surface, periodic boundary conditions are employed to avoid the boundary effects. According to this model scheme, each surface site S has five first nearest neighbours (nn); four on the surface and one in the subsurface just below S. In the present work, the simulation starts with a clean surface and a clean subsurface. The equilibrium coverages are measured as a function of y_{CO}. In order to locate the critical points ten independent runs each up to 50,000 Monte Carlo (MC) cycles were carried out. If all the ten runs proceed up to 50,000 MC cycles without the lattice being poisoned (fully occupied), the particular point is considered to be within steady reactive state (SRS). The poisoning of even a single run is a sufficient criterion for considering the point to belong to the poisoned state. If the run does not end up in a poisoned state, then in order to get the coverages corresponding to the SRS, the initial 10,000 MC cycles are disregarded and averages are taken over the subsequent 40,000 MC cycles. The values of coverages (production rate) are obtained after 10 MC cycles, so that the final coverage (production rate) is an average taken over 4000 configurations.

The steps involved in the simulation are as follows: a surface site S is selected at random.

(a) If CO happens to be selected, then one of the following events may occur:

(i) If the randomly selected site is vacant then CO is adsorbed on it (CO^S) via step (4.1). Five nn sites (four on the surface and one in the subsurface) of the adsorbed CO molecule are scanned randomly for the presence of O^S or O^{SS}. If any of the nn sites are occupied by O^S then the reaction step (4.4) takes place otherwise the presence of O^{SS} leads to the reaction step (4.5) and the trial ends. In the first case two surface sites are vacated whereas in the second case one site each from surface and subsurface are vacated**.** It should be noted that the reaction step (4.4) has precedence over the reaction step (4.5). Experiments reveal that CO utilizes from the subsurface only when there is no oxygen available on the surface [16]. That is why the reaction step (4.4) is preferred over the reaction step (4.5). In this way the catalytic activity is mostly over the surface and the subsurface acts only as a reservoir for oxygen. The generation of vacant sites on the surface is necessary to maintain catalytic activity in an efficient way.

(ii) If the randomly selected site S is occupied by an O^S atom then the CO (g) molecule in gas phase directly reacts with it with some probability P_E in order to

complete the ER step (4.6) and the trial ends. In this case if the reaction takes place then the site occupied by O^S will be vacated.

(b) If O_2 happens to be selected and if the randomly selected site S is occupied, then the trial ends. In case the randomly selected site S is vacant, then another vacant site is required to adsorb the O_2 molecule in atomic form. For this purpose we have considered two cases.

(i) The second vacant site is always taken from subsurface (Model A). If the subsurface nn site of the site S is occupied, then the trial ends and a new molecule is selected. If a subsurface nn site is vacant, then the O_2 molecule dissociates into O^S and O^{SS}. The four-nn sites of O^S are then scanned randomly for the presence of CO^S in order to complete reaction steps (4.4).

(ii) The second vacant site is picked randomly from five nn sites of S (Model B). If the second vacant site is on the surface, then O_2 adsorbs in atomic form on these two surface sites (reaction step (4.3)). The surface nn sites of these two atoms (O^S) are scanned for the presence of CO^S to complete the reaction step (4.4). If the second vacant site is in the subsurface, then one O atom is adsorbed on the surface (O^S) and the other atom is adsorbed in the subsurface (O^{SS}). Surface nn sites of O^S are scanned for the presence of CO^S to complete the reaction step (4.4) (here it may be noted that CO^S can only be found on the surface). However, the surface nn of O^{SS} cannot contain CO^S, therefore it is not scanned for the possibility of reaction step (4.5). This O^{SS} atom remains in the subsurface reservoir.

4.2.2 Results and Discussion

MODEL A Steps (4.1), (4.2), (4.4), (4.5) and (4.6)

In model A, the adsorption of oxygen molecule in the atomic form is taken in such a way that one oxygen atom is always adsorbed on the surface and the other on the subsurface. In this model the reaction steps (4.1), (4.2), (4.4), (4.5) and (4.6) are considered with the assumption that reaction step (4.4) has precedence over reaction step (4.5). In this situation, an interesting situation is observed. For $y_{CO} = 0$, the surface as well as the subsurface are totally covered by oxygen but the moment $y_{CO} \neq 0$, a continuous formation of CO_2 takes place and it keeps on increasing until $y_{CO} = 0.4$ Then it starts decreasing quite rapidly until $y_{CO} = 0.48$ where it stops and the surface is completely covered by CO^S while the subsurface becomes totally empty. This trend of CO_2 production is consistent

with the experimental situation. It is observed in experiments that the surface coverage with oxygen decreases slowly with increase in y_{CO} [17]. The term coverage of a species means the number of sites covered by that species divided by the total number of the available sites on a given surface. Figures 4.1, 4.2 and 4.3 show the situation when the probability of ER step is taken to be 0.01, 0.6 and 1.0 respectively. The situation is qualitatively same as seen in surface-subsurface model of Khan *et al.* [18]**.** However in this case when $y_{CO} \neq 0$, the coverage of surface oxygen sharply drops from 1.0 to 0.15, which shows a rather worse situation as seen in Khan *et al.*[18]. This means that the introduction of ER step has no significant effect on the LH phase diagram of the system. This is because O_2 molecule has already been adsorbed as a pseudo monomer and the moment $y_{CO} \neq 0$, the surface oxygen O^S reacts readily as a result of the reaction step (4.4). However with increase in ER step probability, the maximum production rate (MPR) slightly increases. Figure 4.1 shows the behaviour of MPR versus ER step probability for model A. Figure 4.1 shows that with the increase in ER step probability, the maximum production rate (R_{max}) slightly increases

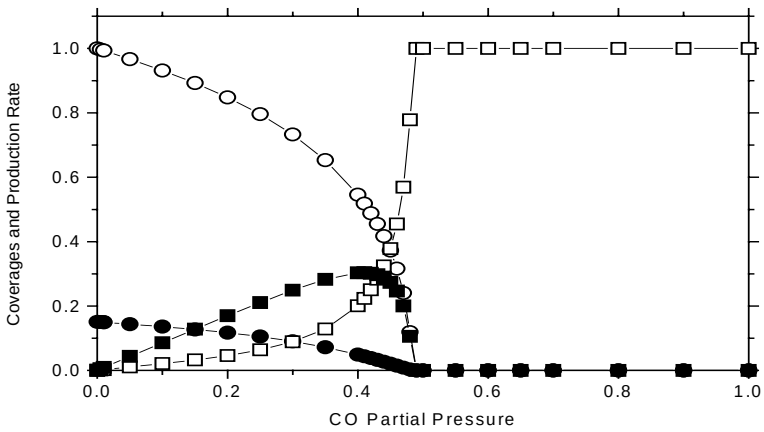

Fig. 4.1 A plot of surface oxygen coverage (solid circle), subsurface oxygen coverage (open circle), CO coverage (open square) and CO_2 production rate (solid square) versus CO partial pressure for model A, when the probability of ER step is taken to be 0.01.

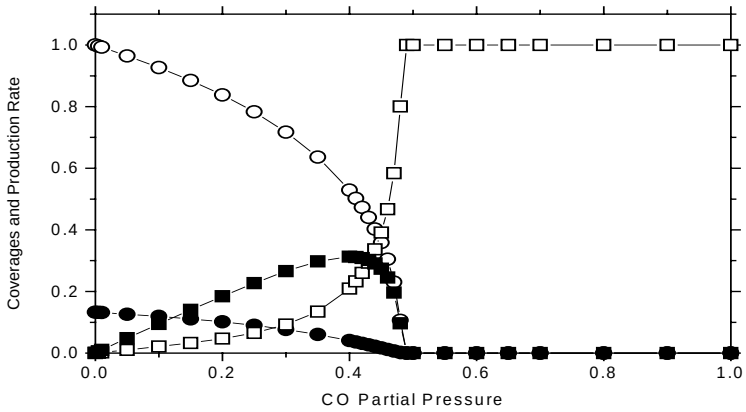

Fig. 4.2. Same as in Fig.4.1 for model A, when the probability of ER step is taken to be 0.6.

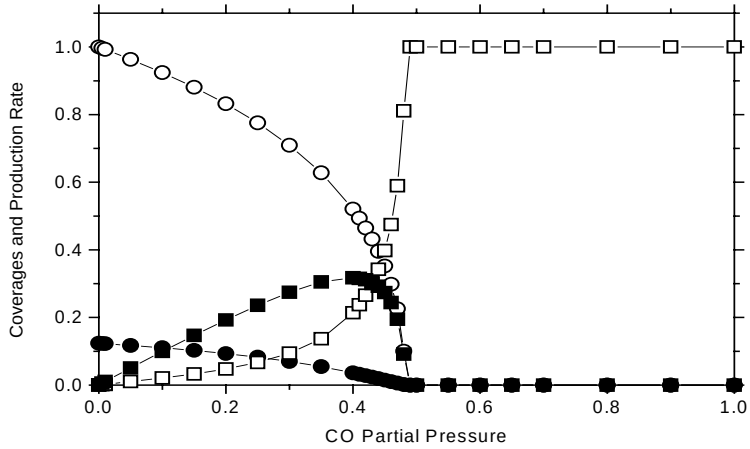

Fig. 4.3. A plot of surface oxygen coverage (solid circle), subsurface oxygen coverage (open circle), CO coverage (open square) and CO_2 production rate (solid square) versus CO partial pressure for model A, when the probability of ER step is taken to be 1.0

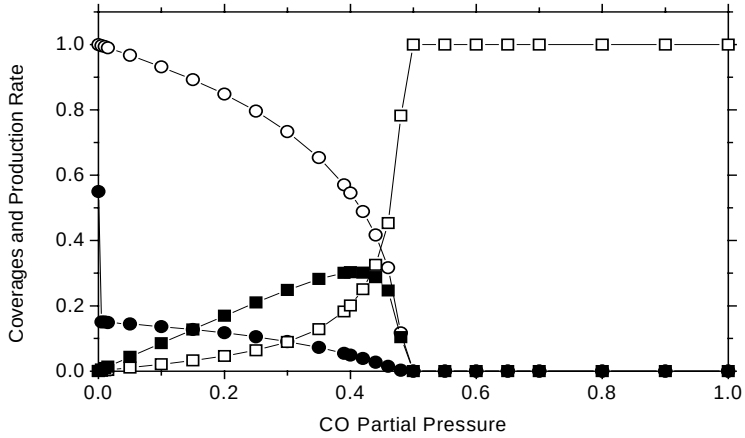

Fig. 4.4 (a). A plot of surface oxygen coverage (solid circle), subsurface oxygen coverage (open circle), CO coverage (open square) and CO_2 production rate (solid square) versus CO partial pressure for model A, when the probability of ER step is taken to be 0.0 (LH mechanism only)

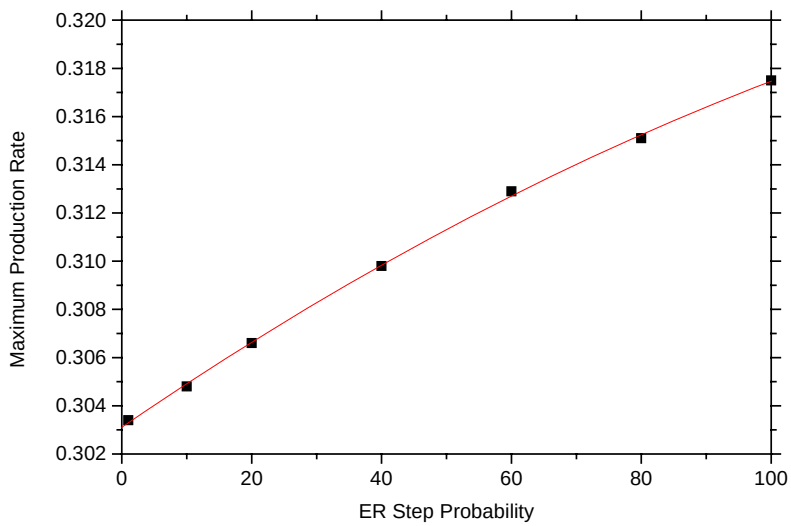

Fig. 4.4(b). A plot of maximum production rate of CO_2 versus ER step probability for model A. A line of fit of the data is also shown.

Model B. Steps (4.1), (4.2), (4.3), (4.4), (4.5) and (4.6)

In model B, the oxygen molecule is adsorbed in such a way that it takes one surface site whereas the second site may be from surface or from subsurface. In this model the reaction steps (4.1), (4.2), (4.3), (4.4), (4.5) and (4.6) are considered with the assumption that reaction step (4.4) has precedence over reaction step (4.5). A fairly remarkable situation is observed in this situation. The following figures 4.5, 4.6, 4.7 and 4.8 show the situation when the probability of ER steps is taken to be 0.01, 0.1, 0.6 and 1.0 respectively.

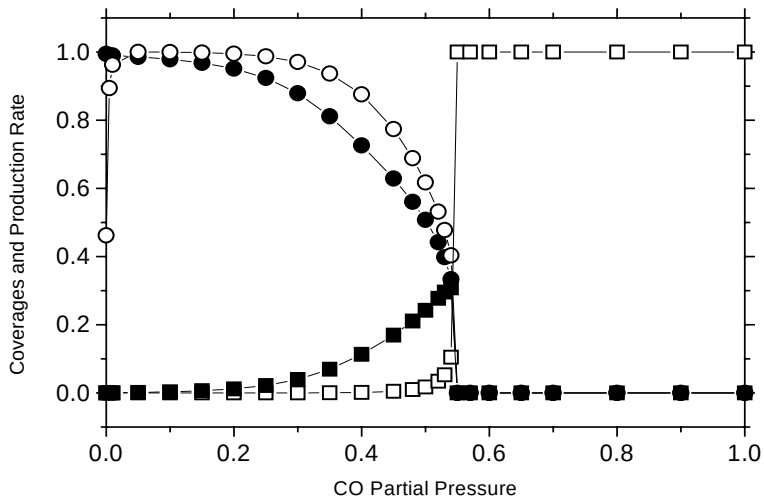

Fig. 4.5. A plot of surface oxygen coverage (solid circle), subsurface oxygen coverage (open circle), CO coverage (open square) and CO_2 production rate (solid square) versus CO partial pressure for model B, when the probability of ER step is taken to be 0.01.

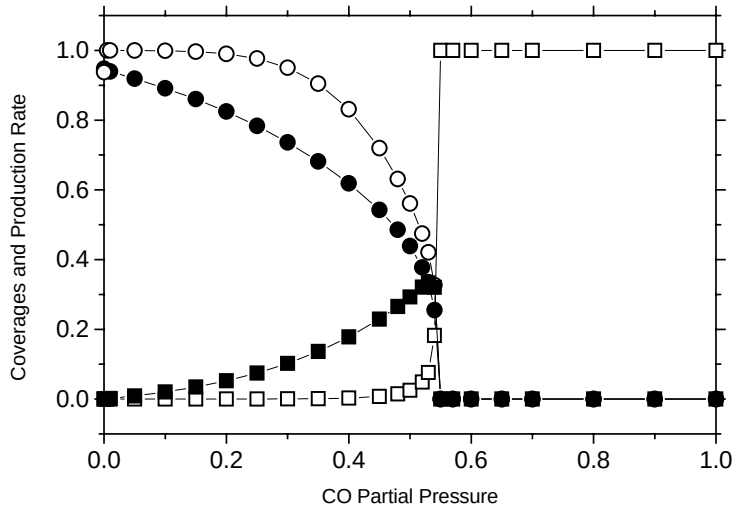

Fig. 4.6. A plot of surface oxygen coverage (solid circle), subsurface oxygen coverage (open circle), CO coverage (open square) and CO_2 production rate (solid square) versus CO partial pressure for model B, when the probability of ER step is taken to be 0.1.

In the first case (when $P_E = 0.01$), for $y_1 < y_{CO} < 0.1$, the surface as well as subsurface are almost covered by oxygen but the moment $y_{CO} = 0.1$, a continuous production of CO_2 takes place and it keeps on increasing until $y_{CO} = 0.54$ and the surface is completely covered by CO^S while the subsurface is totally empty. In the second case (when $P_E = 0.1$, Fig. 4.6), the surface oxygen decreases more rapidly than the subsurface oxygen. This means that even a very small value of P_E has a significant effect on the LH phase diagram of the system. It increases the reactive region as observed by Khan *et al.*[18] without ER step. Since Khan et al. [18] found the width of SRS (without ER step) $W = y_2 - y_1 = 0.13$. Here in this case it has been found that with ER step, the width of SRS window, $W = y_2 - y_1 = 0.44$. With further increase in P_E the value of y_2 almost remains unchanged whereas the value of y_1 shifts towards a lower value of y_{CO}.

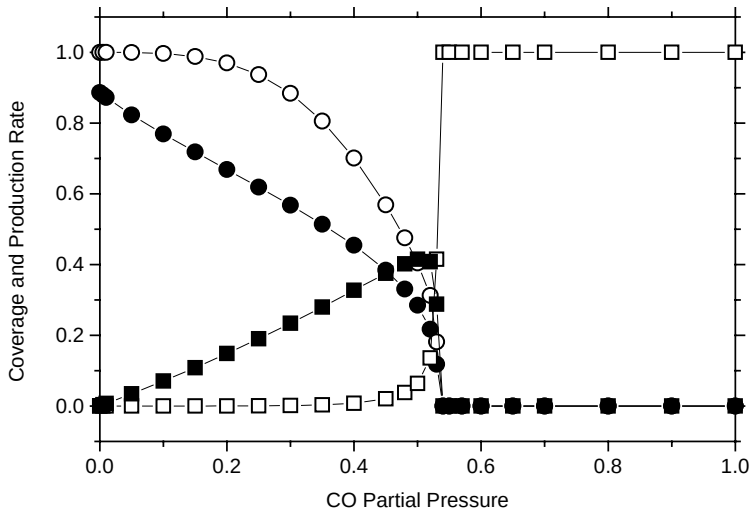

Fig. 4.7. A plot of surface oxygen coverage (solid circle), subsurface oxygen coverage (open circle), CO coverage (open square) and CO_2 production rate (solid square) versus CO partial pressure for model B, when the probability of ER step is taken to be 0.6.

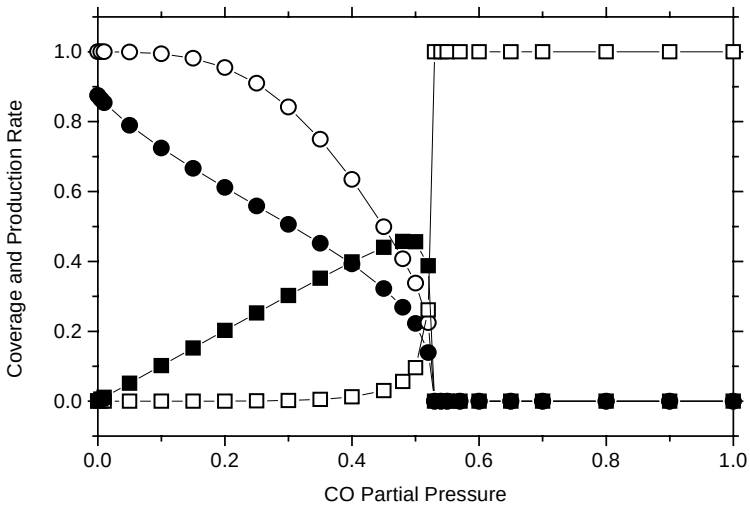

Fig. 4.8. A plot of surface oxygen coverage (solid circle), subsurface oxygen coverage (open circle), CO coverage (open square) and CO_2 production rate (solid square) versus CO partial pressure for model B, when the probability of ER step is taken to be 1.0.

When the probability of ER step is taken to be = 0.10, we get a situation where the production of CO_2 starts the moment y_{CO} departs from zero and it continues till the feed concentration, $y_{CO} = 0.54$. It is obvious that with the introduction of reaction step (4.6) the monomer CO^S starts to react surface species (O^S) more rapidly and thus vacancies are produced on the surface. Since the subsurface is still occupied, therefore, surface vacancies cannot be used for adsorption of O_2 (g) via step (4.2). However, CO can adsorb on these surface vacancies. When the CO concentration is further increased (for same ER step probability) then the reaction step (4.5) becomes more effective and hence the coverage of subsurface species (O^{SS}) decreases until all the subsurface species is reacted. With further increase in ER probability, more surface adatoms are picked by CO to form CO_2 (g) and hence the value of y_1 shifts towards lower y_{CO} value whereas the position of y_2 is unaffected. When ER probability becomes 0.10, y_1 is eliminated and the production of CO_2 (g) starts the moment the value of y_{CO} departs from zero (Fig. 4.6.). This is consistent with the findings of Gates [13] that the ER reaction step becomes dominant when the initial oxygen (dimer) coverage on the surface is higher (smaller y_{CO} values), otherwise the LH reaction step becomes important. On the other hand an increase in the P_E value also increases the value of maximum production rate (Fig. 4.7 & Fig. 4.8.). Figure 4.9 shows that with the increase in ER step probability, the maximum production rate (MPR) slightly increases.

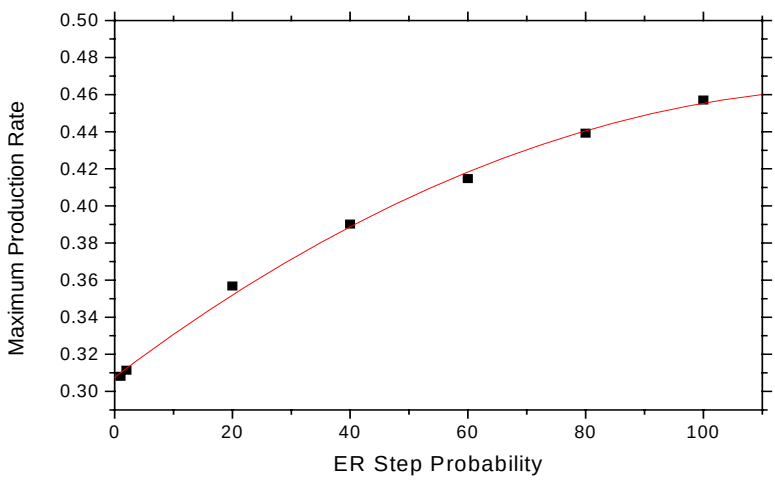

Fig. 4.9. A plot of maximum production rate of CO_2 versus ER step probability for model B. A line of fit of the data is also shown.

It is noted that starting from $y_{CO} = 0$, even for a small value of y_{CO} such as $y_{CO} = 0.001$, there is a sudden jump to the continuous reaction state. Thus, $y_{CO} \approx 0$ is a first-order transition point from poisoned to steady reactive state.

4.3 Simulation on BCC with ER

Following the extension of ZGB model by introducing the ER mechanism on the simple cubic lattice, the ER process on body centred cubic structure is also is presented in this section. There are certain situations where the subsurface plays a more important role as compared to the surface sites for a dimmer adsorption. One particular example may be (001) surface and subsurface of a body-centred cubic structure, which extends to only two layers in the z-direction. In this structure, each surface (upper layer) site has four nn sites in the subsurface (lower layer) and four second nn on the surface itself. Therefore, here, the subsurface layer may play a more dominant role in the catalytic reactions as compared to a simple cubic structure.

4.3.1 Model and Simulation

The usual simple LH surface-subsurface model of the system can be written in the form of the following equations:

$$CO\,(g) + S \rightarrow CO^{s} \qquad (4.7)$$

$$O_2\,(g) + S + SS \rightarrow O^{s} + O^{ss} \qquad (4.8)$$

$$CO^{s} + O^{s} \rightarrow CO_2\,(g) + 2S \qquad (4.9)$$

$$CO^{s} + O^{ss} \rightarrow CO_2\,(g) + S + SS \qquad (4.10)$$

With the introduction of Eley-Rideal process that involves a CO molecule in the gas phase directly reacting with an oxygen-adsorbed species, that is, one has to add the following equation:

$$CO\,(g) + O^{S} \rightarrow CO_2\,(g) + S \qquad (4.11)$$

Here (g), S and SS indicate gas phase, active surface and subsurface sites respectively while X^{S} and X^{SS} represent X adatom on the surface and subsurface respectively. We consider a body-centred cubic structure, which has been extended to only two layers in the z-direction. In this structure, each surface (upper layer) site has four nn sites in the subsurface (lower layer) and four second nn on the surface itself (Fig.4.10). Therefore, here the subsurface layer may play a more dominant role in the catalytic reactions as compared to a simple cubic structure.

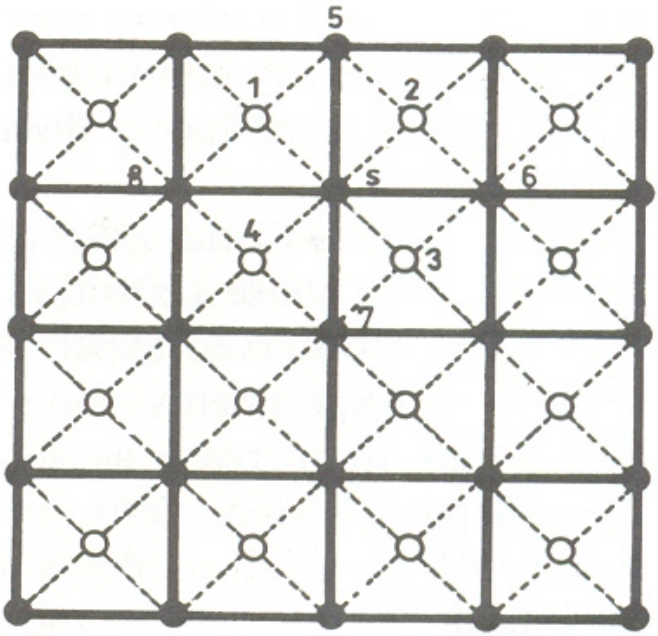

Fig. 4.10: Surface and sub-surface layers of a body centred cubic structure when extended into the z-direction. The sites marked by 1,2,3 and 4 are the sub-surface nearest neighbour and sites marked by 5,6,7 and 8 are the surface second nearest neighbours of a randomly selected site S.

In this fig, the subsurface nn are labelled 1, 2, 3, 4. The sites labelled 5, 6, 7 and 8 are the surface second nn of a randomly selected site S. The simulation starts with a clean surface and clean subsurface.

The steps involved in the simulation are as follows: a surface site S is selected at random. If CO happens to be selected, then one of the following events may occur: (i) if the randomly selected site is vacant then CO is adsorbed on it (CO^S) via step (4.7). Eight (4 first nn and 4 second nn) sites of the adsorbed CO molecule are scanned randomly for the presence of O^S or O^{SS}. If any of the nn sites are occupied by O^S, then the reaction step (4.9) takes place, otherwise the presence of O^{SS} leads to the reaction step (4.10) and the trial ends. In the first case, two surface sites are vacated, whereas in the second case one site each from surface and subsurface are vacated. (ii) If the randomly selected site S is occupied by an O^S atom, then the CO (g) molecule in gas phase directly reacts with it with some probability P_E in order to complete the ER step (4.11) and the trial ends. In this case if the reaction takes place, then the site occupied by O^S will be vacated. If O_2 happens to be selected and if the randomly selected site S is occupied, then the trial ends.

In case the randomly selected site S is vacant then another vacant site in the sub-surface is required to adsorb the O_2 molecule in atomic form via reaction step (4.8). The surface nn sites of these atoms (O^S) are scanned for the presence of CO^S to complete reaction step (4.9). The O^{SS} also scans on the surface for CO^S to complete reaction step (4.10).

4.3.2 Results and Discussion

In the first case steps (4.7), (4.8), (4.9) and (4.10) of surface-subsurface model are considered with reaction step (4.9) has precedence over reaction step (4.10). When y_{CO} = 0, the surface and subsurface are totally covered by oxygen, but the moment $y_{CO} \neq 0$, the surface oxygen coverage drops sharply, whereas subsurface is still almost filled with oxygen. The continuous formation of CO_2 takes place the moment $y_{CO} \neq 0$ which is consistent with the experiment [2,3] and continues to increase until y_{CO} = 0.6. Then it starts to decrease until y_{CO} = 0.65, at which point it stops, the surface is completely covered by CO, and the subsurface is totally empty (**Fig.4.11**). It is interesting to note that not only SOPT gets destroyed, but also the steady reactive window width is significantly large (of the order of 0.65).

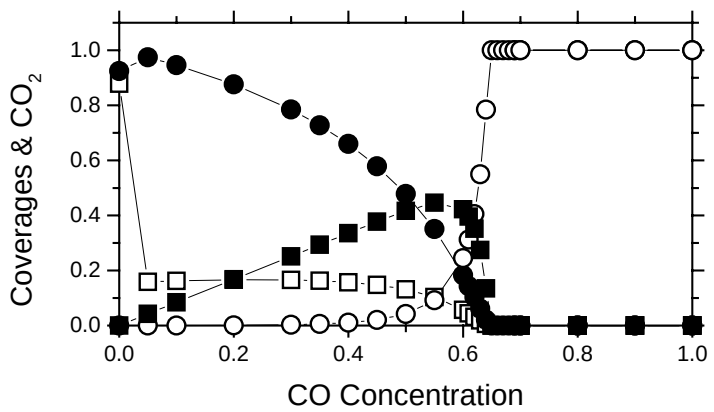

Fig. 4.11 A plot of surface oxygen coverage (open square), subsurface oxygen coverage (solid circle), CO coverage (open circle) and CO_2 production rate (solid square) versus CO partial pressure for first case (for reaction steps: 4.7- 4.10).

In the second case, steps (4.7)-(4.11) of surface-subsurface model are considered with reaction step (4.9) has precedence over reaction step (4.10). Almost same situation is observed in this case. However, when $y_{CO} \neq 0$, the coverage of surface oxygen drops sharply from 1.0 to 0.1, which is not seen in the experimental situation [19]. It is observed

in experiments that the coverage of surface oxygen decreases slowly with increase in y_{CO} [19].

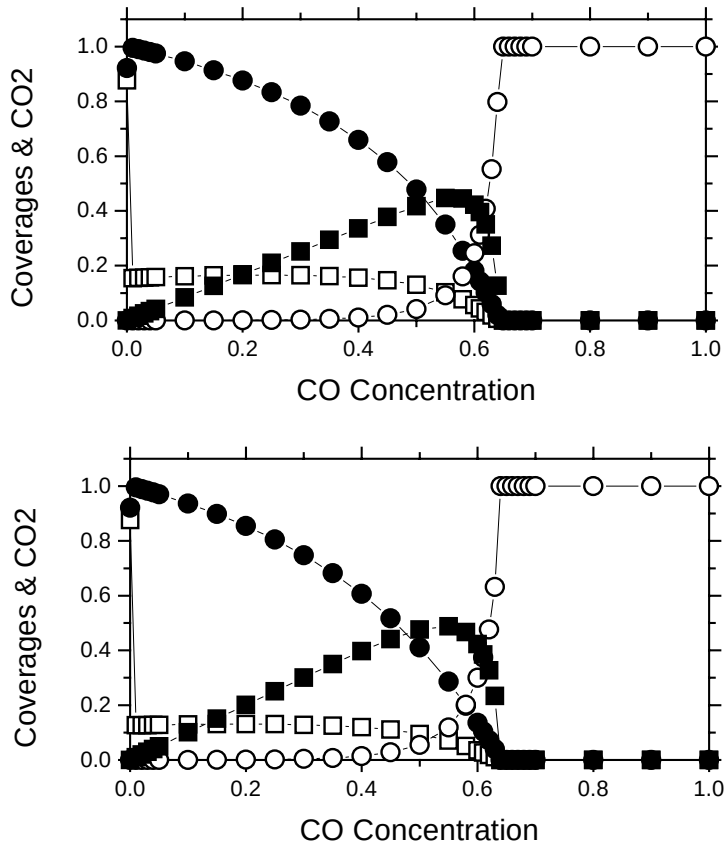

Fig. 4.12 A plot of surface oxygen coverage (open square), subsurface oxygen coverage (solid circle), CO coverage (open circle) and CO_2 production rate (solid square) versus CO partial pressure when the probability of ER step is taken to be 0.01 (top) and 1.0 (bottom) respectively for second case.

Figure 4.12 shows the situation when the probability of ER step is taken to be 0.01 (top) and 1.0 (bottom) respectively. It can be seen that the qualitative nature of figure 4.11 and 4.12 is the same (i.e. the position of the critical transition points y_1 and y_2). This means that the probability of ER step has no significant effect on the LH phase diagram of the system. This is because O_2 molecule has already been adsorbed as a pseudo monomer and the moment $y_{CO} \neq 0$ the surface oxygen reacts readily as a result of the reaction step (4.9). However, with increase in ER step probability, the maximum production rate (R_{max}) slightly increases. The other important factor of our study is that the production of CO_2 (R) can be written in the form of a mathematical relation. The behaviour of the type R =

0.44779 + 0.0426 (y_{CO}) (polynomial of degree 1) with standard deviation equal to 0.00146 when the data from the Fig. 4.13 (P_E = 1) is fitted.

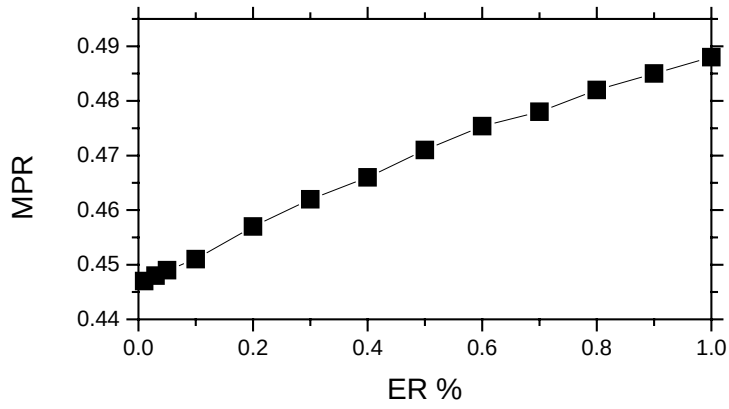

Fig. 4.13. A plot of maximum production rate versus ER step probability for second case.

In the third case steps (4.7)-(4.10) of surface-subsurface model are considered with reaction step (4.10) has precedence over reaction step (4.9); then situation is shown in Figure 4.14.

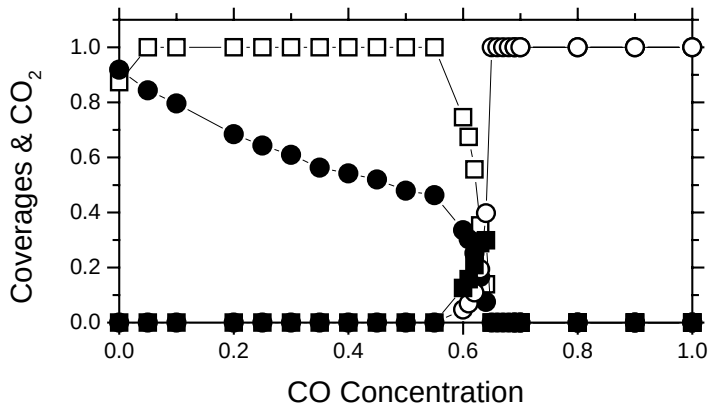

Fig. 4.14 A plot of surface oxygen coverage (open square), subsurface oxygen coverage (solid circle), CO coverage (open circle) and CO_2 production rate (solid square) versus CO partial pressure in the third case.

It appears that in the present situation O^S behaves as a pseudo-monomer and therefore the phase diagram shown resembles to that of usual monomer-monomer model, i.e. there is a single transition point at y_{CO} = 0.6, below (above) which surface gets poisoned with O^S

(CO^S) monomers. The result differs significantly from the first case in which reaction step (4.9) has precedence over reaction step (4.10). In this case, SOPT is not destroyed, and a situation that is qualitatively similar to ZGB model is observed.

In the fourth case steps (4.7)-(4.11) of surface-subsurface model are considered with reaction step (4.10) has precedence over reaction step (4.3) (**Fig. 4.15**).

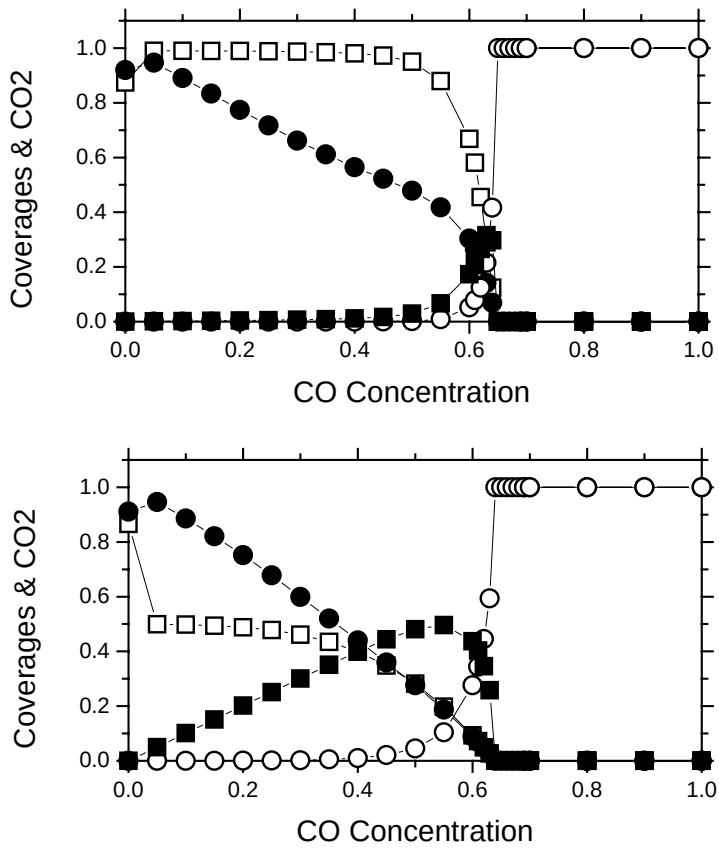

Fig. 4.15 A plot of surface oxygen coverage (open square), subsurface oxygen coverage (solid circle), CO coverage (open circle) and CO_2 production rate (solid square) versus CO partial pressure with ER when the probability of ER step is taken to be 0.01 (top) and 1.0 (bottom) respectively for fourth case.

The **Figure 4.15** shows the situation when the probability of ER step is taken to be 0.01 (top) and 0.1 (bottom) respectively. With the introduction of ER process i.e. step (4.11) drastic change in the situation is observed. The production rate of CO_2 starts as soon as y_{CO} departs from zero which is consistent with the experimental observation [2-3]. The surface oxygen coverage also seems to be more close to the experimental observation [19] i.e. the coverage of surface oxygen decreases slowly with increase in y_{CO}. The other

important factor of our study is that the production of CO_2 (R) can be written in the form of a mathematical relation. The behaviour of the type R = 0.3128 + 0.30477 (y_{CO}) - 0.12407 $(y_{CO})^2$ (polynomial of degree 2) with standard deviation of 0.0009358 when the data from the bottom of **Figure 4.16** (P_E = 1) is fitted.

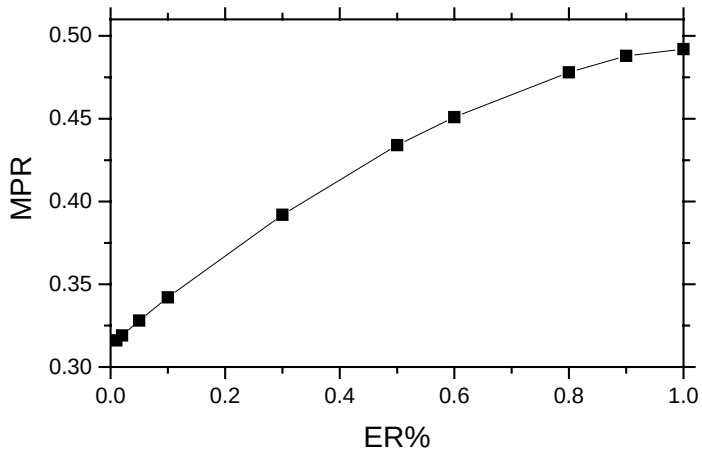

Fig. 4.16 A plot of maximum production rate versus ER step probability for fourth case.

4.4 Simulation on SCL with Ballistic-Type Hot Atom

Recent experiments by scanning tunneling microscopy on the dissociative adsorption of oxygen molecule on Al (111) [20] surface pointed to a 'hot atom' mechanism. According to this, two oxygen atoms are propelled apart upon dissociation by distances exceeding 80 Å before equilibrating with the surface. The hot oxygen atoms react with adsorbed CO molecules. Here in this section, we investigate the effect of the ballistic mechanism of the hot atom on the phase diagram using a square surface. While using this mechanism whenever an O_2 molecule hits a randomly vacant site, the molecule breaks up into atomic form and then executes a ballistic flight. The paths of the two oxygen atoms are taken exactly to the opposite to each other, i.e. anti-parallel, and the ranges of the atoms are taken to be equal, i.e. they may fly up to 1 or 1.414 or 2 of the atomic spacing from the site of impact.

To investigate the influence of ballistic-type mechanism, the CO-O_2 reaction on the square surface has been selected. On such a square surface, the first, second and third nearest neighbouring sites have distances of 1, 1.414 and 2 atomic spacing respectively.

4.4.1 Model and Simulation

The usual simple LH surface-subsurface model the system can be written in the form of the following equations:

$$CO\,(g) + S \rightarrow CO^S, \qquad 4.12$$

$$O_2\,(g) + S \rightarrow O^b + O^b + S, \qquad 4.13$$

$$O^b + S \rightarrow O^S, \qquad 4.14$$

$$CO^S + O^S \rightarrow CO_2\,(g) + 2S, \qquad 4.15$$

$$O^b + CO^S \rightarrow CO_2\,(g) + S, \qquad 4.16$$

Here g indicates the species in the gas phase and S represents a vacant surface site. O^b represents the oxygen atom executing ballistic motion and CO^S is the adsorbed state of CO on the surface. The simulation starts with a clean surface. The simulation proceeds as follows.

A surface site chosen randomly might be vacant or occupied. The trial will end if the selected site is occupied. If the site is vacant and the selected molecule is CO, then adsorption is carried out via reaction step 4.12. After adsorption, CO goes through reaction step 4.14.

If the selected molecule is O_2 and the selected site is vacant, then the O_2 molecule after colliding with the vacant site is dissociated into two hot atoms via reaction step 4.13. These two hot atoms executes a ballistic flight and fly in the opposite direction (anti-parallel) from the site of impact, and their range is taken to be equal, i.e. both atoms may fly up to the first nearest (1 atomic spacing from the site of impact) or second (1.414 atomic spacing from the site of impact) or third nearest neighbours (2 atomic spacing from the site of impact). Two hot atoms may take one of the following courses: (i) if the selected site (one or both) is occupied by oxygen, then the trial will end; (ii) if both the sites are vacant, then both the oxygen atoms will be adsorbed via reaction step 4.14 and then go through reaction step 4.15; (iii) if one site is vacant and CO occupies the other one, then one O^b atom is adsorbed via reaction step 4.14 and the reaction goes through step 4.15; the other O^b will directly react with CO^S via reaction step 4.16; (iv) if CO occupies both randomly selected sites, then both O^b atoms go through reaction step 4.16. Four cases have been studied on the basis of range of hot atoms of oxygen.

- In case *a*, two atoms may be adsorbed on any of the two sites from four first-nearest neighbours at a distance of 1 atomic spacing from the site of impact.

- In case *b*, two atoms may be adsorbed on any of the two sites from four second nearest neighbours at a distance 1.414 atomic spacing from the site of impact.
- In case *c*, two atoms may be adsorbed on any of the two sites from four third-nearest neighbours at a distance of 2 atomic spacing from the site of impact.
- In case *d*, two atoms may be adsorbed on any of the two sites from twelve nearest neighbours at a distance of 1, 1.414 and 2 atomic spacing from the site of impact.

4.4.2 Results and discussion

Figures 4.17- 4.20 show the coverages of the species and production of CO_2 plotted as a function of y_{CO} for cases *a*-*d*, respectively.

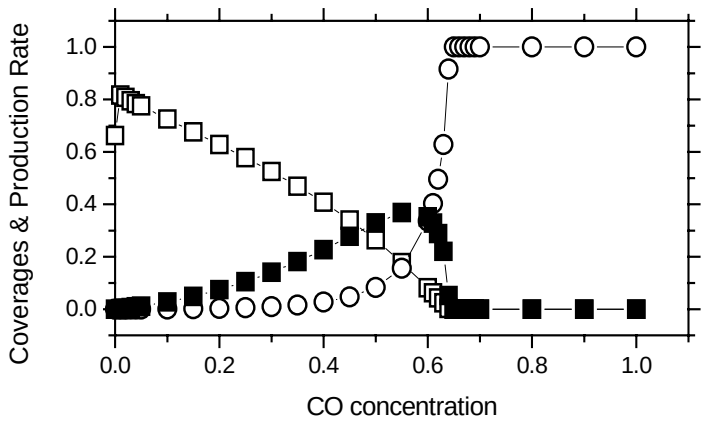

Fig.4.17. Coverages of O (open square), CO (open circle) and the production rate of CO_2 (solid square) versus CO partial pressure for case *a*.

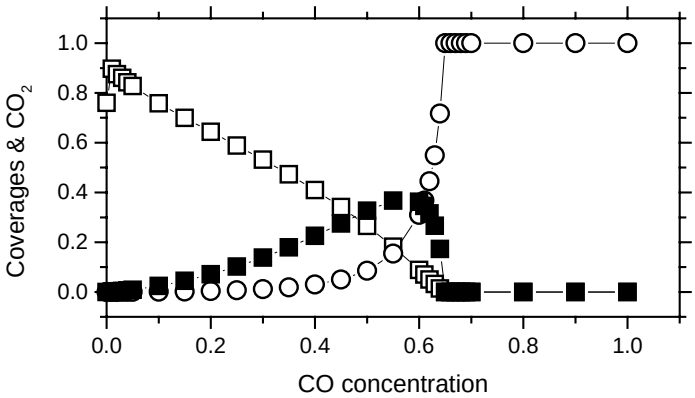

.

Fig. 4.18. Coverages of O (open square), CO (open circle) and the production rate of CO_2 (solid square) versus CO partial pressure for case *b*.

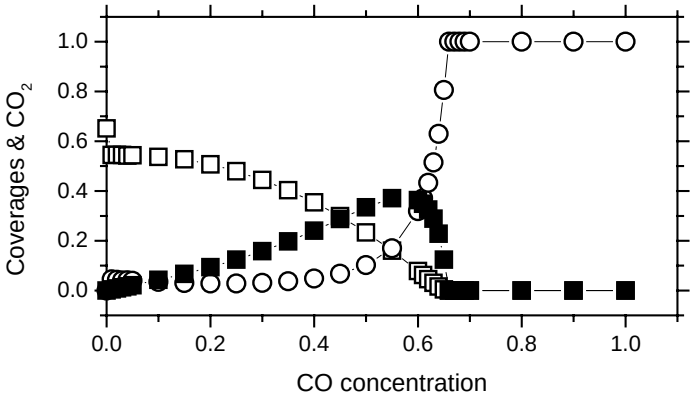

.

Fig. 4.19. Coverages of O (open square), CO (open circle) and the production rate of CO_2 (solid square) versus CO partial pressure for case *c*

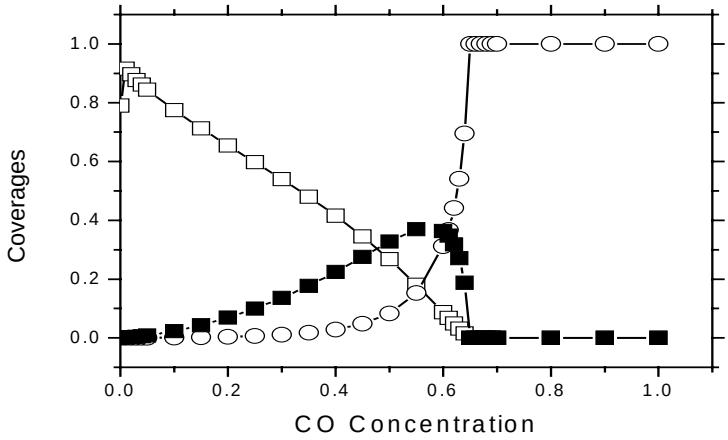

Fig. 4.20. Coverages of O (open square), CO (open circle) and the production rate of CO_2 (solid square) versus CO partial pressure for case *d.*

In the ZGB model a pair of vacancy in the first-nearest neighbourhood is required for impingement and consequent dissociation of the O_2 molecule. The trial will end (in the ZGB model) if a pair of vacancy is not available. On the other hand, in the present model only a simple site is required for impingement and consequent dissociation of O_2 molecule. However, the requirement of a single vacancy for the accommodation of O_2 molecule in contrast to the ZGB model plays an important role in the region where CO starts adsorbing on the surface. In the ZGB model, when the supply of oxygen is limited due to unavailability of pair of vacancy, CO starts occupying the single vacancies, whereas in the present model only a single vacancy is required to accommodate both the species (O_2 and CO) on the surface. Therefore, naturally in contrast to the ZGB model, the reaction will be sustained to a higher value of feed concentration, which results in the shift of y_2 from 0.525 (in ZGB) to 0.65 (in the present model). It is well known that at high partial pressures, oxygen forms large island (Fig. 4.21). In this situation, if a single vacancy is picked as a site of impact, there will be a small chance that the other vacancy at distance mentioned above can be obtained. Under these conditions, every trial of O_2 impingement will end unsuccessfully.

```
000000110010011100111020111000011100011 1
002011110000111110000100111001001110010 1
200111010001101111000110010111001011100 0
000111000001010111101011000110110011100 2
111100110011000111111111101111010111011 0
101000111100002011110000111001000100011 1
000111101101102000111110011101001110001 1
111111101101100001111100011111111110111 1
111000111020011000111100000011101101111 1
110101110001111100001110000100110011101 1
010001110001111110000111000011111011000 0
000001111110000111020111110010111001000 2
011110111110102011101000111102000111001 0
111100001011000101111100011110011111011 0
100011000011100001111022001111110101111 0
```

Fig. 4.21. Snapshot on y_{CO} = 0.14 (1 for oxygen, 2 for CO and 0 for vacant site).

However, in the same situation every trial of CO impingement will end in the reaction of oxygen. This means that indirectly, adsorption (supply) rate of O_2 is decreased whereas that of CO is increased. This fact will shift the value of y_1 towards lower feed concentration. That is why the value of y_1 in all the four cases has been shifted from 0.39 (in ZGB) to 0.005, which verifies the experimental results in the literature [4,16]. It is noted that the qualitative characteristics of the phase diagram are similar for cases *a-d*

However, the phase diagrams shown in Figs. 4.17- 4.20 closely resembles to that of experimental one [17], which is consistent with the observation of Wintterlin *et al*.[21] that the two hot oxygen atoms appear in pair.

4.5 References

[1] R.M.Ziff, E. Gulari, and Y.Barshad, Phys. Rev. Lett. **56** (1986) 2553.

[2] M . Dumont, P.Dufour , B.Sente , and R. Dagonnier, J. Catal **122** (1990) 95.

[3] F. Bagnoli, B. Sente , M. Dumont, R. Dagonnier, J. Chem. Phys. **94** (1991) 777.

[4] H. H Rotermund., J.Lauterbach., G.Haas , Appl. Phys. A **57** (1993) 507.

[5] J. Harris, B. Kasemo, E. Tornqvist, Surf. Sci **105** (1981) L 288.

[6] D. D Eley, E. K Rideal,. Nature **146** (1940) 401.

[7] N.O. Wolf , D.R. Burgess, D.K. Hoffman, Surf. Sci.**100** (1980) 453.

[8] S.P. Singh-Boparai, M. Bowker, D.A. King, Surf. Sci. **53** (1975) 55.

[9] G. Boato, P. Cantini, L. Mattera, J. Chem. Phys. **65** (1976) 544.

[10] G. Comsa, R. David, B.J. Schumacher, Surf. Sci. **95** (1980) L 210.

[11] B. Jackson, M. Persson, J. chem. Phys. **103** (1995) 6257.

[12] J. Harris, B. Kasemo, Surf. Sci **105** (1981) L 281

[13] B.C. Gates, Catalytic Chemistery eds. B.C. Gates ,New York:, Willy (1992) .359

[14] T. Engel and G. Ertl, Adv. Catal. **28** (1997) 1.

[15] K. M. Khan and E.V Albano, J. Phys, A **35** (2002) 1167.

[16] S. Ladas, R. Imbihl and G. Ertl, Surf.Sci..**219** (1989) 88.

[17] E.V.Albano, Computational Methods in Surface and Colloid Science, ed. M Borowko Marcel Dekker, Inc; 2000), p.387.

[18] K. M. Khan, J. Khalifeh, K. Yaldram and M. A. Khan J. Chem. Phys. **106** (1997) 8890.

[19] J.H Block, M. Ehasasi, V. Gorodetskii, prog. Surf. Sci. **42** (1993) 143.

[20] H. Brune, J. Wintterlin, J. Trost, G. Ertl, J Wiechers and R J Behm, J.Chem.Phys.**99** (1993) 2126.

[21] J. Wintterlin, R. Schuster and G. Ertl, Phys. Rev. Lett. **77** (1996) 123

Chapter-5

SIMULATION ON SQUARE SURFACE WITH PRECURSOR AND DIFFUSION MECHANISM

5.1 Introduction

The CO-NO catalytic reaction is a complicated reaction and this reaction has been studied in detail by many experimental methods on different catalytic surfaces [1-7]. It was found that catalytic activity of Pt surface depends on the rate of dissociation of NO [8,9]. Fink *et al.* [7] have shown that NO molecule adsorbs in its molecular form at room temperature while, after being adsorbed, the NO molecule dissociates upon heating above ≈ 380 K. The molecular desorption of NO also takes place with a maximum rate around 400 K when saturated surfaces are heated [9]. At a typical operating temperature for a catalytic converter (700 K), the adsorption of NO results in the liberation of N_2 gas and in the formation of stable surface oxygen species [2,3]. These surface oxygen species are then used by CO molecule to produce CO_2 gas.

Based on the ZGB model, other lattice models have been introduced to simulate different catalytic surface reactions. Yaldram and Khan [10,11] proposed a monomer-dimer (MD) reaction model for CO-NO reaction. This MD reaction in which NO reacts with CO is based on the Langmuir-Hinshelwood (LH) mechanism. With this simple LH mechanism they showed that the MD reaction model has no steady reactive state (SRS) on the square lattice. However, increasing the coordination number of the lattice, it was found that a hexagonal lattice shows an SRS. Latter Khan *et al*. [12] introduced the diffusion of N atoms in the simple LH mechanism on the square lattice. They have shown that the steady reactive state exists only when the diffusion of N atoms on the surface is allowed. Latter Khan [13] studied the role of sub-surface oxygen on the phase diagram for CO-NO on the simple cubic lattice and a steady reactive window of width of 0.105 was observed.

We have studied the effect of precursor mechanism for CO-NO reaction on the square surface and on bcc structure. The effect of ER and diffusion mechanism has also been studied on bcc structure in this chapter.

5.2 Simulation on Square Surface with Precursor Mechanism in the 1st, 2nd and 3rd Environment

Here, in this section, the kinetics of an irreversible monomer-dimer (CO-NO) reaction has been studied using a non-thermal mobility of CO molecule i.e. precursor mechanism on the square surface using Monte Carlo simulation. The three models have been studied. In the first, second and third model, the range of precursor molecule is extended up to first, second and third nearest neighbours respectively. The objective of this work is to explore the effect of the mobility of CO molecules (precursors) of CO-NO reaction system up to a maximum distance R having values d, $\sqrt{2}$ d and 2d respectively.

5.2.1 Model and Simulation

According to LH mechanism, it is assumed that the reaction occurs according to the following steps:

$$CO(g) + S \rightarrow CO^S \qquad (5.1)$$

$$NO(g) + 2S \rightarrow N^S + O^S \qquad (5.2)$$

$$N^S + N^S \rightarrow N_2(g) + 2S \qquad (5.3)$$

$$CO^S + O^S \rightarrow CO_2(g) + 2S \qquad (5.4)$$

Whenever Precursor mechanism is taken into the consideration then following step is simulated

$$CO(g) + S \rightarrow CO^p + S \qquad (5.5)$$

$$CO^p + O^S \rightarrow CO_2 + S \qquad (5.6)$$

Here (g), and S indicate gas phase and active surface sites respectively; while X^S, and X^p represent X adatom on the surface and the molecule executing precursor mechanism respectively. We have considered three different ranges of the surface environment. The simulation of these three environments is carried out separately. The square lattice is considered for which the first four nearest neighbours on the surface from site of impact are at a distance of d, the four second nn neighbours are at a distance of $\sqrt{2}$ d and four third nn neighbours at a distance of 2d. The simulation starts with clean surface. The following models are studied:

Model A

In Model A, steps 5.1-5.6 are considered. The simulation proceeds as follows: a surface site is chosen randomly and for this chosen site there are two possibilities, i.e. this site is either (i) occupied or (ii) empty. If the selected site happens to be occupied then trial ends. If the selected site is empty and CO happens to be the incoming molecule then adsorption and reaction is made via reaction step (5.1) or reaction step (5.5) & (5.6) with probability y_{CO}. The selection of steps (5.1) and (5.5) & (5.6) is made on the basis of percentage of probability of precursor. If the step (5.1) is selected then CO gets adsorbed via reaction step (5.1). Soon after the adsorption, CO goes through reaction step (5.4), with the production of CO_2 and leaving behind two vacant sites on the surface. On the other hand, if reaction step (5.5) & (5.6) is selected, which represents the precursor mechanism, then CO molecule goes for precursor mobility. During this mechanism, the CO molecule hits the randomly selected vacant site and is not thermalized with the substrate. This molecule executes precursor motion in the first nearest neighbours and if it finds oxygen there, it reacts with adsorbed oxygen atom via reaction step (5.6). The output of this reaction step is production of CO_2 and creation of one vacancy. If it does not find oxygen there, then it gets adsorbed on any of the five sites (one site of impact and four sites in the nearest neighbours) via reaction step (5.1) and then goes for usual reaction step as mentioned above. While for adsorption of NO the reaction step (5.2) is simulated. After adsorption, N atoms go for reaction step (5.3). In the first case N atom scans in its first nn another N atom. If it finds N atom there, then it reacts with it and N_2(g) with two vacancies are produced. In the second case adsorbed O atom reacts with CO^S molecule and produces CO_2(g) and two vacancies.

Model B

For Model B all the simulation steps remain the same as mentioned in model A but the only difference is in the range of precursor molecule. In this model CO molecule executes precursor motion up to second nn neighbours i.e. 4 first nn sites and 4 second nn sites.

Model C

For Model C all the simulation steps remain the same as mentioned in Model A but range of the mobility of CO molecule (precursor range) gets extended up to third nn neighbours i.e. 4 first, 4 second and 4 third nn sites.

5.2.2 Results and discussion

Earlier attempts [10,14] on the square lattice failed to obtain the SRS (without diffusion of N) for NO-CO reaction of all values of y_{CO}, while for hexagonal lattice it gets established. For low concentration of CO (high NO), the square surface gets poisoned and most of the adsorbed oxygen atoms, are trapped between nitrogen atoms and adsorbed nitrogen atoms between oxygen atoms (Figure 5.1).

```
113131311313113131311111313111131313 1
131311113111131313113113131111311131 1
111113111313113131131131131111111131 1
311131131131311311311111131313111131 1
131113111313131111113131113111131131 1
111311311111313113131113131131111311 3
311131111311111131111131313113111131 1
113113111111313113131111311111311111 1
111131111111111111131113113131131131 1
111311313111313131111131131311131131 1
311113111311113111311311111113131111 3
111111131111111311111131111111131113 1
131131113113111131311111131311311111 3
111113111131111311111311131111111111 1
131311111311313111311113131131131131 1
311111111111111313113111313131111113 1
113131111131131111111313111111111311 1
111111311111111131311111111111311113 1
113113111313111111311313113113111131 3
111131131111113131313113111113113111 1
113111111311111311131131111131111113 1
```

Fig.5.1 Lattice snap shot illustrating the Model A for y_{co} = 0.15 (1 for oxygen, 3 for N).

The poisoning and trapping of atoms stop the reactive state to be established. Any attempt capable of breaking the traps mentioned above can help in establishing the SRS. This is the reason behind this study. Figure 5.2(a) shows the coverages of the species and Figure 5.2(b) shows the production of CO_2(g) and N_2(g) plotted as a function of y_{CO} for model A. It is evident from these figures ((Fig. 5.2(a) & Fig. 5.2(b)) that introduction of precursor of CO molecule generates SRS on square lattice.

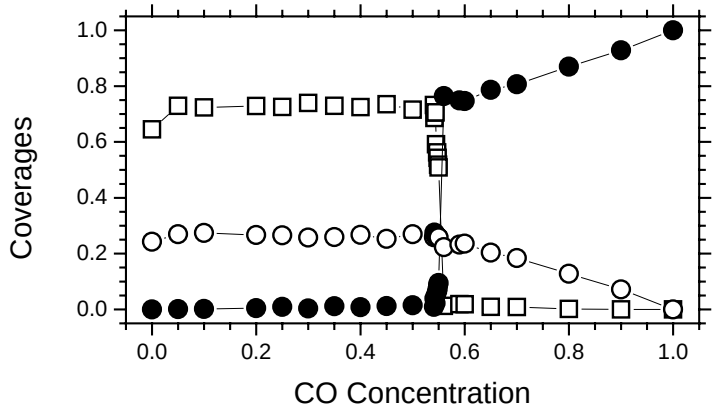

Fig.5.2(a) Phase diagram from MC according to precursor mechanism for Model A with coverages of surface O (open square), CO (closed circle), and N (open circle) for 100% probability of precursor.

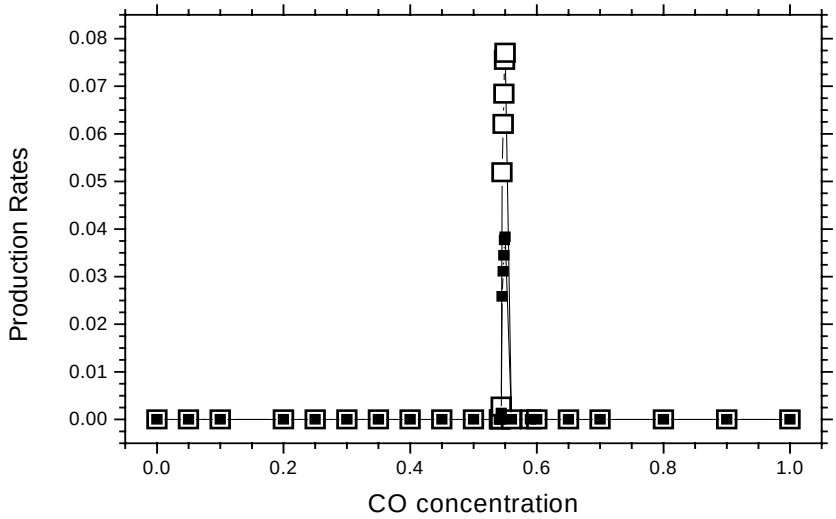

Fig. 5.2(b) Production rate of CO_2 (open square) and N_2 (closed square) versus CO partial pressure for Model A.

In this situation for model A, when the probability of precursor is made 100%, the first transition occurs at lower critical point y_1 =0.54, while the second transition occurs at y_2 = 0.55. The difference $y_2 - y_1$ = 0.01, called the window width for SRS, is separated by two-phase transitions. For CO oxidation quite different results are produced by Khan et al

[15] as trapping of oxygen atom by CO^S- CO^S pair and CO^S trapping between O^S- O^S pair, helps in production of CO_2. In our Model A, the maximum production rate of CO_2 and N_2 is found at y_{CO} =0.555, after which it falls abruptly to zero. For $y_{CO} < y_1$, the surface is mostly covered (poisoned) with combination of N^S and O^S, while for $y_{CO} > y_2$; the surface is poisoned with N^S and CO^S. At y_{CO} = 0.56, the coverage of CO on the surface increases suddenly and jumps to a large value (≈0.76) and the coverage of surface oxygen drops to a very small value (≈0.012). For $y_{CO}>y_1$, the coverage of N on the surface decreases slowly and drops to zero quite smoothly. The production rates of N_2 and CO_2 shows that the steady production starts at y_1 and keeps on increasing gradually until it gets a maximum, after which both (CO_2 and N_2) drop to zero abruptly. Moreover, it has been found that for a particular value of y_{CO}, the production of CO_2 is greater than that of N_2. In Figure 5.2, we present a situation when the mechanism of precursor is introduced to the first environment. The range of the precursor in this environment extends up to four first nearest neighbours. The coverages of reacting species on square lattice in the first environment of the precursor with probability 100% are plotted as a function y_{CO} (Figure 5.2(a)). If 100% probability of CO precursor is taken in the first environment, the values of of y_1 and y_2 are found to be 0.544 and 0.555 respectively. It is has been found in our simulation that with the introduction of Precursor mechanism of CO molecule in CO – NO reaction system, the steady reactive state is established.

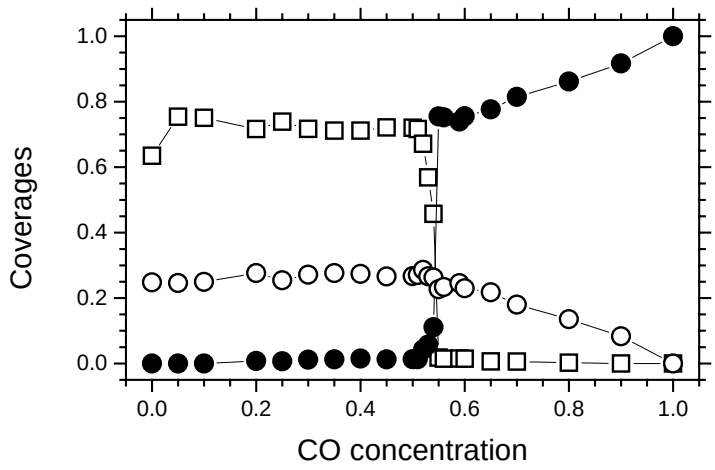

Fig. 5.3. Coverages of surface O (open square), CO (closed circle), and N (open circle); for Model B: with 20% precursor.

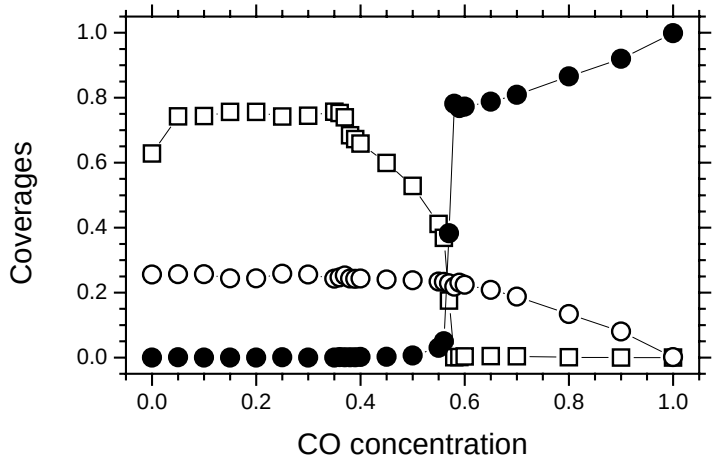

Fig.5.4. Coverages of surface O (open square), CO (closed circle), and N (open circle); for Model B: with 100% precursor.

The SRS of the order 0.01 is observed when the probability of CO precursor is 40% to 100%. The catalytic activity is very fast in this small steady reactive state. The reacting rate of oxygen is very high and at y_{CO} =0.555, CO consumes all the oxygen of surface. This observation is in contrast to the previous observation [10]. The reason for the establishment of SRS is that the mobility of CO helps in breaking the traps around N by producing CO_2 gas. As soon as the trap around the nitrogen breaks up, the so called trapped nitrogen atom gets the opportunity to react with another adsorbed nitrogen atom by producing N_2(g). This process in turn helps in breaking the poisoned state of Nitrogen and Oxygen atoms. This process creates vacancies for further adsorption of NO molecule and production of N_2 and CO_2. The figures 5.3 and 5.4 are with 20% and 100% precursor probability respectively for model B. It is observed that when the range of CO^P is extended to second neighbourhood, the position of y_1 and y_2 changes. The values of y_1 and y_2 are found to be 0.53 ± 0.01 and 0.54 ± 0.01, respectively when the probability of mobility of CO molecule is 20%. If 100% probability of CO precursor is taken), the values of of y_1 and y_2 are found to be 0.40 ± 0.01 and 0.57 ± 0.01, respectively. Figure 5.5 (a-b) shows the production rate for 20% and 100% precursor probability respectively for model B.

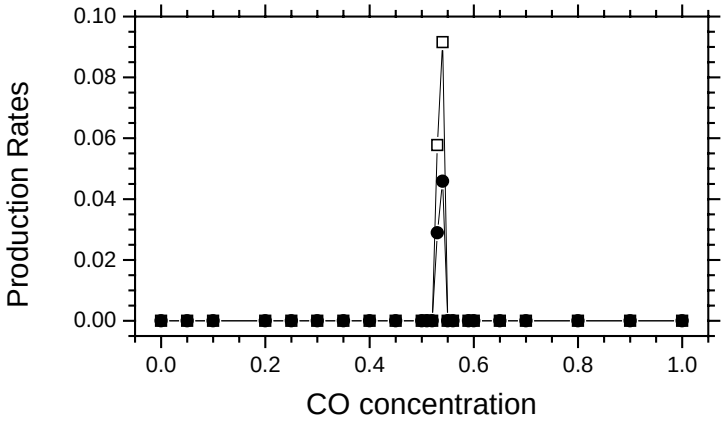

Fig.5.5(a)

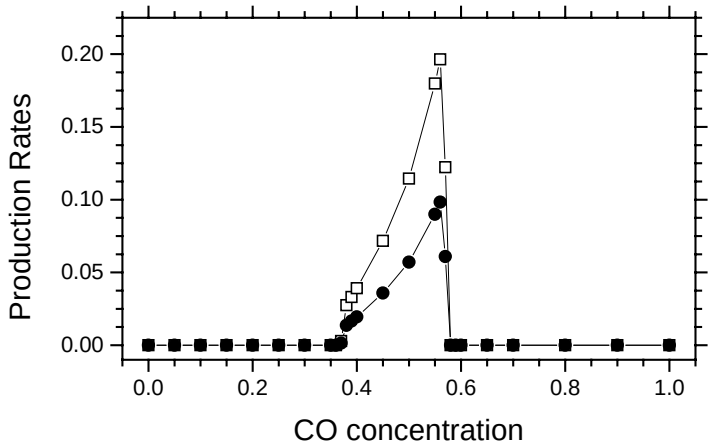

Fig. 5.5(b). Production rates of CO_2 (open square) and N_2 (closed circle) versus CO concentration for Model B with: (a) 20% precursor; (b) with 100% precursor (bottom).

Finally, the simulation was performed for the precursor of CO molecule to the third environment, i.e. up to all eight sites of the second environment and additional four third-nearest neighbouring sites. Figure 5.6 and 5.7 shows the phase diagram for the third environment when the probability of precursor is made 20% and 100% respectively. In figure 5.6, the values of y_1 and y_2 are found to be 0.52 ± 0.01 and 0.55 ± 0.01, respectively when the probability of mobility of CO molecule is 20%. If 100% probability of CO precursor is taken, the values of of y_1 and y_2 are found to be 0.05 ± 0.01 and 0.58 ± 0.01, respectively.

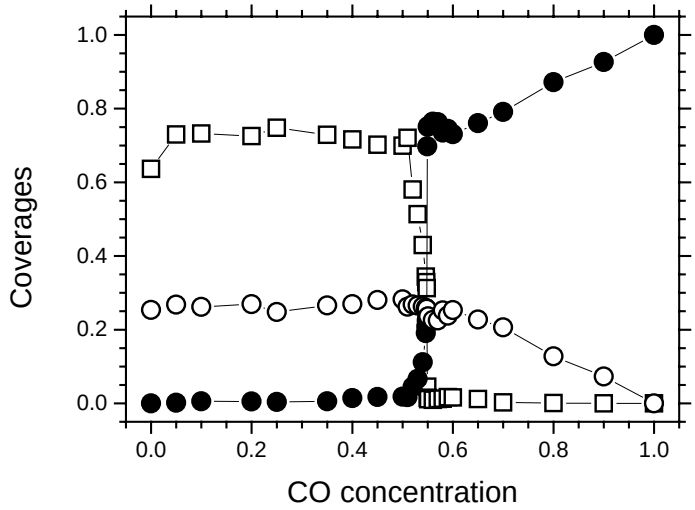

Fig. 5.6 Coverages of surface O (open square), CO (closed circle), and N (open circle); for Model C: with 20% precursor

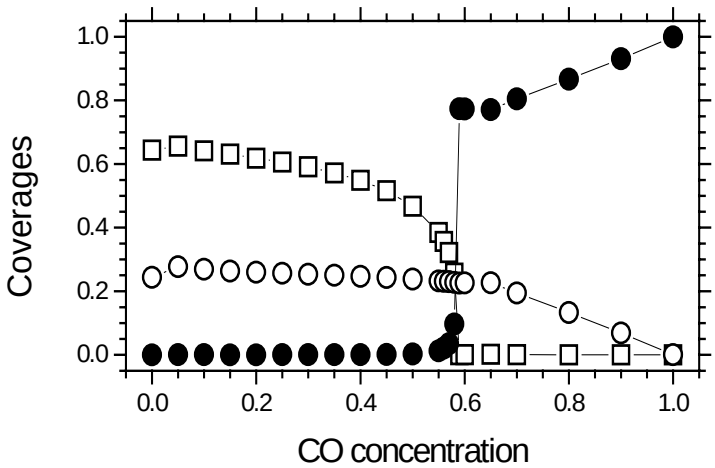

Fig. 5.7 Coverages of surface O (open square), CO (closed circle), and N (open circle); for Model C: with 100% precursor.

It is observed that if the range of the environment of CO^P is extended to second and third neighbourhood, then y_1 is shifted towards a lower value of y_{CO}. In fact, for low pressure of CO, the hopping of CO^P molecules into the second and third environment reacts with more oxygen and creates more single vacant sites. Therefore in other words, indirect supply of CO gas is increased and hence y_1 is shifted towards lower value of y_{CO}.

On the other hand, for high pressure of CO ($y_{CO} > y_2$) and in the higher environment, fewer CO^P precursors end their life as CO^S as compared with the first environment and hence NO molecule can find more vacant pairs for adsorption; therefore, y_2 shifts towards higher values of y_{CO}.

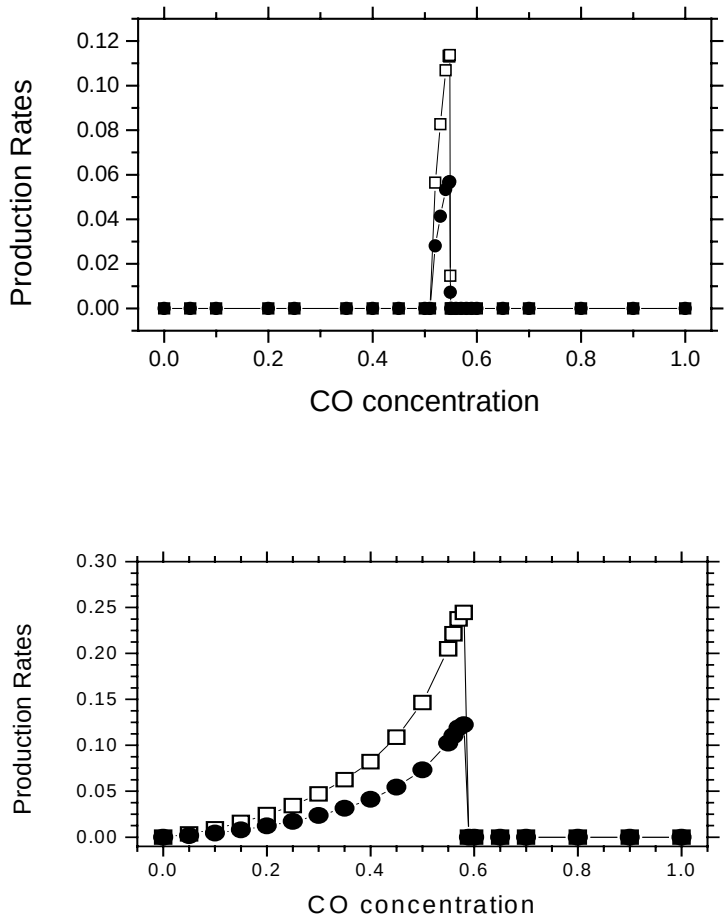

Fig. 5.8. Production rates of CO_2 (open square) and N_2 (closed circle) versus CO concentration for Model C with 20% precursor (top) and with 100% precursor (bottom).

The two transition points y_1 and y_2 for different value of precursor probability are also shown in Figure 5.9(a) and Figure 5.9(b) for second and third environment. It can be seen from Figure 5.9(a-b), that in each mode of environment, y_1 shifts backward whereas y_2 shifts forward.

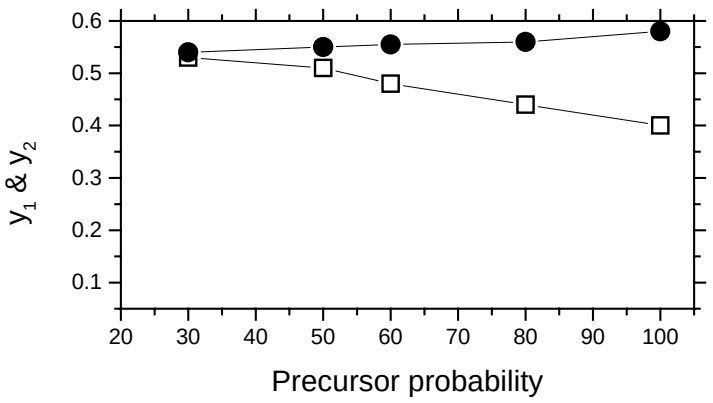

Fig.5.9(a)

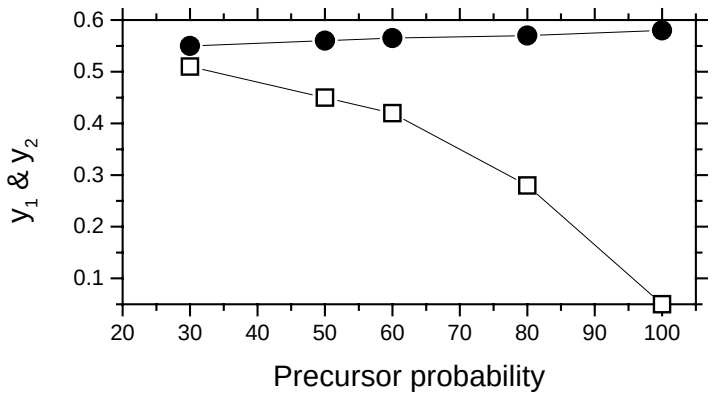

Fig.5.9(b)

Fig. 5.9(a-b):

(a) Plots of y_1 (open square) and y_2 (closed circle) versus precursor probability for Model B.

(b) Plots of y_1 (open square) and y_2 (closed circle) versus precursor probability for Model C.

The effect precursor probability for each environment on maximum production rate (MPR) is also studied and is plotted in Figure 5.10. It is observed that in each environment, MPR increases with the increase of probability of precursor.

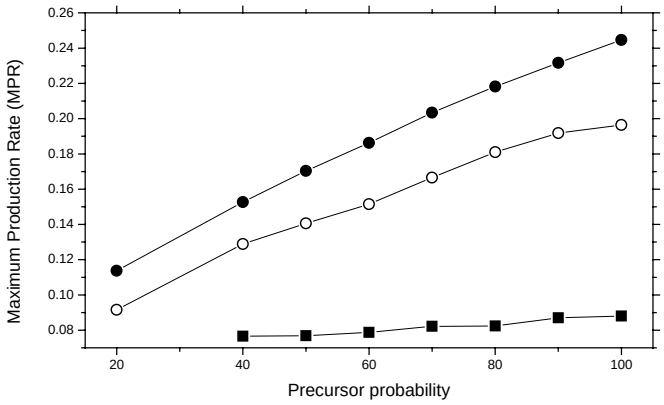

Fig. 5.10. Maximum production rates (MPR) versus environment first (closed square), environment second (open circle) and third (closed circle).

5.3 Simulation on Square Surface with Precursor and Diffusion-Mechanism

The first problem that appears in the study of catalytic reaction is related to the mechanism that controls the reaction scheme. Here the effect of transient non-thermal mobility of monomer (CO) based on the precursor mechanism, diffusion of adsorbed nitrogen and oxygen atoms is investigated. Here, we have considered the square lattice for which the first four nearest neighbours (nn) on the surface are at a distance of one atomic spacing from the site of impact.

5.3.1 Model and Simulation

The modelling follows the following steps:

$$CO^p + O^S \rightarrow CO_2 + S, \qquad (5.7)$$

$$CO^P + S \rightarrow CO^S, \qquad (5.8)$$

$$CO^S + O^S \rightarrow CO_2(g) + 2S, \qquad (5.9)$$

$$NO(g) + 2S \rightarrow N^S + O^S, \qquad (5.10)$$

$$N^S + N^S \rightarrow N_2(g) + 2S. \qquad (5.11)$$

Here (g), and S indicate gas phase and active surface sites respectively; while X^S, and X^p represent X adatom on the surface and the molecule executing precursor mechanism respectively.

Model A

In Model A (steps 5.7- 5.11) the simulation proceeds as follows: a surface site is chosen randomly and for this chosen site there are two possibilities, i.e, this site is either (i) occupied or (ii) empty. If the selected site happens to be occupied, then the trial ends. If the selected site is empty and CO happens to be the incoming molecule then precursor motion in the first environment (first four nn from the site of impact) is made via reaction step (5.7). If this reaction step succeeds then CO_2(g) is produced, leaving behind one vacancy on the surface and precursor ends its life. If CO^P does not find any oxygen in the nearest neighbourhood then it gets adsorbed on any of the one site from five sites (one site of impact and four first nn) via reaction step (5.8). After adsorption it scans randomly in its first nearest neighbourhood for the presence of oxygen atoms. The presence of O^S leads to the formation of CO_2 (g) which desorbs from the surface leaving behind two vacant sites (reaction step 5.9). If the initial selection is that of NO, then the neighbouring site of the empty site is picked up randomly. If the site is occupied, then trial ends; otherwise NO is adsorbed onto these two empty sites via reaction step (5.10). The choice for adsorption on these two sites for N and O is made randomly. Once N and O are adsorbed, the nearest neighbours of each are scanned for the presence of N^S or CO^S via reaction step (5.11) and (5.9) respectively. In the first case N_2(g) is formed and in the second case CO_2(g) is formed and librated.

Model B

For model B the simulation procedure remains the same as mentioned for model A with the introduction of diffusion of adsorbed nitrogen and oxygen atoms. For diffusion mechanism if the random selection of a surface site results in the identification of an occupied site (N^S or O^S), a nearest neighbour of this site is selected randomly. If the site is empty, N^S (O^S) is moved to this location. After diffusion the nearest neighbour of the new position is scanned for the presence of N^S (CO^S) via reaction step 5.11 (5.9). The output of this step is production of N_2(g) or CO_2(g) and two vacancies are created on the surface.

5.3.2 Results and Discussion

In the simple LH mechanism, when NO adsorbs on the surface, it is equally possible that one site is occupied by a nitrogen atom and the other by an oxygen atom. This simple fact leads to the poisoning on the square lattice by the process of ‘‘chequer boarding’’ of N

atoms [16]. The chequer boarding of N atoms cannot take place geometrically on the hexagonal lattice. This is why SRS is obtained for hexagonal lattice [10].

```
+*+++*+*+*++++*+++++++++++*+*++*+*++++
*++*++*+*++++++++*+*++++*+*++*++*+*++++*+
+*+++*++++*+*++*++++*+*+*+*+++*+*++++*++
++*+++++*++*+*+++*++*+++*+*+*+++*+*+++
+*+*+*+*+*++*++*+++*++*++*++++*++*++++*
*+*+*+*+*+*+++*+*++++++*+++*+*+*++*+++
+*+*+*+++*+++++++*+*+*+++*++++*++*+*++
++*+*+*++++*+*++*+*+++*+++++*+++++*+*+
+*+++*+*++*+*++++++*+*++*++*+*+*+*+*+*
+++++++++*+*+++*++*+*+*+++++++*+*+*+*+
+*++*+*+*+*+*+*++*+++++*++++*++*+*+*
*+*++++*+++++*++*++*+*+++*+*+*+*++++*+*+
+*+*++++*+++*++*++*++++++*+*+*+*++++*+*
*+*+*++*++*+++*++++*++*+++++++++*+*++*+
+*+*+*++++++*+++*+++*++*+++++*++*+*++*
*+++*+*+*+*++*+*+*+*+++++*++*+*++*++*+
++*++++++*++*+*+*+*+*+*+*+*++++*++++++*+*
+*++++*+*+*++++*+*+*+++*+*+*+++*+*++++
```

Fig.5.11. Snap shot on y_{co} = 0.14 (+ for oxygen, and * for N) for Model A.

Figure 5.11 shows the snap shot for y_{CO}=0.14 for model A to depict the above said situation for low CO (high NO) partial pressure. The surface contains the clusters of oxygen with N atoms trapped in these clusters. Due to the establishment of clusters of oxygen atoms around nitrogen atoms, the earlier attempts made to obtain SRS for the CO - NO reaction on the square lattice failed [10]. In this study we try to overcome this difficulty by performing the precursor motion of the CO molecule, diffusion of the adsorbed nitrogen and oxygen atoms on the surface. The diffusion of CO^S is not considered in this study as it was pointed out by Khan *et al*. [17] that it has no effect on the phase diagram.

In the following figures 5.12 and 5.13, a situation is presented when the precursor mechanism is introduced to the first environment i.e. up to the first nearest neighbours model A.

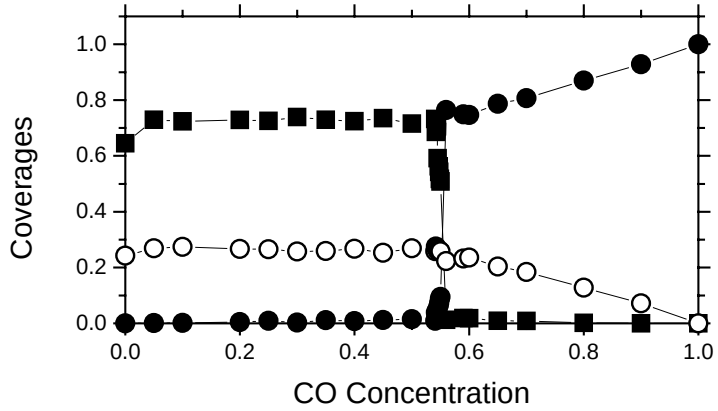

Fig. 5.12. Coverages of surface O (closed squares), CO (closed circles), and N (open circles) for Model A.

Fig. 5.12 and 5.13 show the coverage of reacting species and the production rates as a function of y_{CO}, respectively. The second order phase transition (SPOT) takes place at $y_1 = 0.544$ and the first order phase transition (FOPT) at $y_2 = 0.555$.

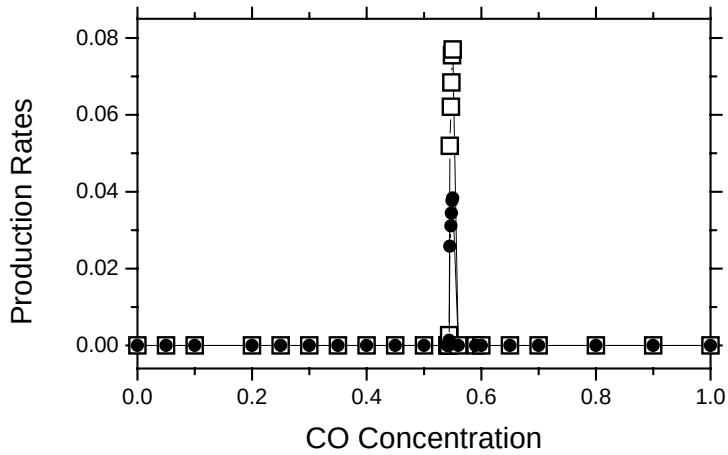

Fig.5.13. Production rate N_2(g) (closed circle)) and CO_2(g) (open square) for Model A.

It is observed from the results of simulation in this mechanism that for $y_{CO} < y_1$, the surface is totally covered with combination of nitrogen and oxygen atoms, while for $y_{CO} > y_2$; the surface is fully covered with nitrogen and carbon monoxide (Figure 5.12). The

reacting rate of oxygen is very high and at y_{CO} =0.555, where CO reacts all the oxygen of the surface. This observation is in contrast to previous observation [10].

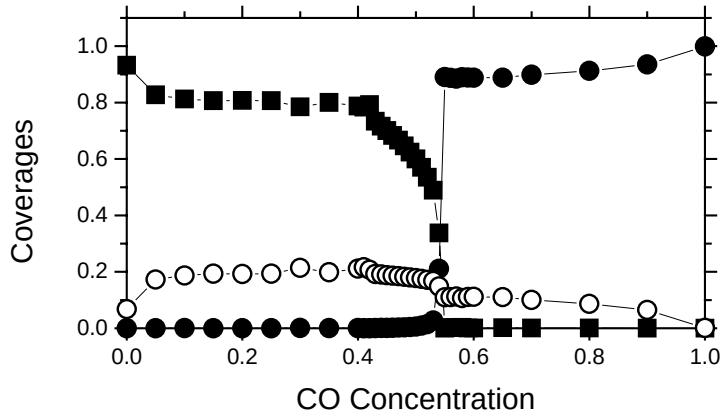

Fig. 5.14. Coverages of surface O (closed squares), CO (closed circles), and N (circle open) for Model B.

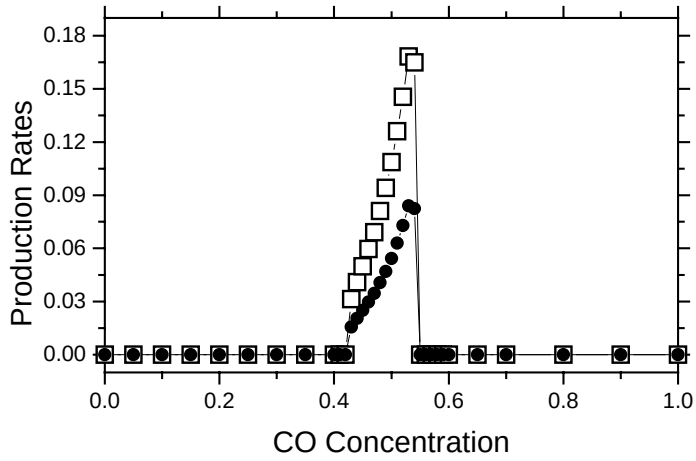

Fig. 5.15. Production rate of N_2(g) (closed circle)) and CO_2(g) (open square) for Model B.

In Figs. 5.14 and 5.15, the situation is presented when the precursor mechanism, diffusion of adsorbed nitrogen and oxygen atom is introduced to the first environment i.e. up to the first four nearest neighbours (model B). Figures 5.14 and 5.15 show the coverages of reacting species and the production rates, respectively, as a function y_{CO}. For this model the situation improves and SRS of the order 0.125 is established (Fig. 5.15). It is observed that SRS is enhanced from 0.01 (model A) to 0.125 (model B). The values of y_1 and y_2 are found to be 0.43 ± 0.005 and 0.555 ± 0.005, respectively. It must be noted that

enhancement in SRS occurs in the region of rather high concentration of NO. The reason for the establishment of SRS is the precursor motion of CO molecule. The oxygen starts reacting and isolated vacancies are created due to the precursor motion. The generation of these isolated vacancies and occupation of N atoms results in the decrease in pairs of vacancies. This reduces the chance of NO adsorption as NO requires two vacancies to be adsorbed. The reduction in NO adsorption increases the chances of CO precursor and diffusion of nitrogen/oxygen atom. This in turn ends in production of CO_2(g) and N_2(g). It is worth mentioning here that in rather low concentration of NO, the precursor mechanism becomes the main cause for creation of vacancies by reacting the adsorbed oxygen. These vacancies in turn activate the process of diffusion of nitrogen and oxygen and hence traps break apart. In this region the fabrication of CO_2(g) and N_2(g) starts and hence SRS gets enhanced.

5.4 Simulation On BCC for CO-NO with Precursor Mechanism

To know, how the precursor mechanism for CO-NO reaction on BCC lattice affects the phase diagram is the key subject of this section. In the structure of BCC, each surface site has four nearest neighbours (nn) sites in the subsurface (lower layer) and four second nn on the surface itself.

5.4.1 Model and Simulation

According to LH mechanism, it is assumed that the CO-NO reaction occurs according to the following steps:

$$CO(g) + S \rightarrow CO^S \qquad (5.12)$$

$$NO(g) + 2S \rightarrow N^S + O^S \qquad (5.13)$$

$$NO(g) + S + SS \rightarrow N^S + O^{SS} \qquad (5.14)$$

$$N^S + N^S \rightarrow N_2(g) + 2S \qquad (5.15)$$

$$CO^S + O^S \rightarrow CO_2(g) + 2S \qquad (5.16)$$

The inclusion of the subsurface will add the following extra step:

$$CO^S + O^{SS} \rightarrow CO_2(g) + S + SS \qquad (5.17)$$

Whenever precursor mechanism is taken into consideration, the following steps are simulated;

$$CO\ (g) + S \rightarrow CO^p + S \qquad (5.18)$$

$$CO^p + O^S \rightarrow CO_2 + S \qquad (5.19)$$

$$CO^P + S \rightarrow CO^S \qquad (5.20)$$

As stated previously the symbols used here are obvious. Three different ranges of the surface environment have been considered here. For example in the first environment, the range of mobility of CO molecules (precursors) on the surface is limited to maximum distance d, called the lattice constant, while the range R of CO precursors for second and third environments are limited to maximum distance having values $\sqrt{2}$ d and 2d respectively. The simulation of these three environments is carried out separately. The simulation starts with clean surface and subsurface. The following four models: A, B, C and D are considered:

Model A

In model A, steps 5.12- 5.17 are considered. A surface site is chosen randomly and for this chosen site there are two possibilities, i.e. this site is either (i) occupied or (ii) empty. If the selected site happens to be occupied, then the trial ends. If the selected site is empty and CO happens to be the incoming molecule, then the adsorption is made via reaction step (5.12) with probability y_{CO}. Soon after the adsorption, CO goes through reaction step (5.16), with the production of CO_2(g) and leaving behind two vacant sites on the surface. If this reaction step does not succeed then the reaction step (5.17) takes it turn. The success of reaction step (5.17) results in the production of CO_2(g) with leaving one vacancy on the surface and other on the sub-surface. While for adsorption of NO there is equal probability for step (5.13) and (5.14). For step (5.13), adsorption of NO is taken in such a way that N atom is adsorbed on the surface, whereas O atom is adsorbed on the second nearest neighbour on the surface. After the adsorption N atom goes for reaction step (5.15) and adsorbed oxygen atom goes for reaction step (5.16). If step (5.14) happens to be selected, the Nitrogen atom gets adsorbed on the surface and oxygen atom gets adsorbed in the sub-surface. The nitrogen atom, after adsorption, goes through usual reaction step (5.15) for production of N_2(g), while oxygen atom adsorbed in the sub-surface (O^{SS}) does not go for reaction. The subsurface is taken as an oxygen storage reservoir.

Model B

In model B, (steps 5.12- 5.20) are considered. The additional steps (5.18- 5.20) are for the Precursor mechanism. For such a mechanism, if the selected site is empty and CO

happens to be the incoming molecule then precursor motion in the first environment is made via reaction step (5.19) with some probability P_P. If this reaction step succeeds then CO_2(g) is produced, leaving behind one vacancy on the surface and precursor ends its life. If CO^P does not find any oxygen in the nearest neighbourhood then it gets adsorbed on any of the one site from five sites (one site of impact and four second NN on the surface) via reaction step (5.20). After adsorption, the four second NN surface sites of each CO^S molecule are scanned randomly for the presence of oxygen atom (O^S). The presence of O^S leads to the formation of CO_2 (g), which desorbs from the surface leaving behind two vacant sites (reaction step 5.16) on the surface. If this reaction step does not succeed then the reaction step (5.17) takes in turn. The reaction step (5.17) results in the production of CO_2(g) with leaving one vacancy on the surface and other on the sub-surface.

Model C

In model C, all the simulation steps remain the same as mentioned in model B, but range of CO molecule (precursor) is extended up to maximum distance $\sqrt{2}$ d on the surface.

Model D

For model D, all the simulation steps remain the same as mentioned in model B, but range of CO molecule (precursor) is extended up to maximum distance 2d. Results are presented in the following figures.

5.4.2 Results and Discussion

From the simulation on BCC it was found that with LH mechanism, the second order phase transition (SOPT) takes place at y_1= 0.15 and first order phase transition (FOPT) at y_2 = 0.35, respectively . Figure 5.16(a) shows the coverages of the species plotted as a function of y_{CO} for model A (LH mechanism) on the BCC lattice. For $y_{CO} < y_1$, the surface is totally covered with combination of nitrogen and oxygen atoms, while for $y_{CO} > y_2$; the surface is fully covered with nitrogen and carbon monoxide. On the other hand, in the simple LH mechanism, the square lattice fails to obtain the SRS for this reaction system. The trapping of N^S between O^S – O^S pairs and O^S atoms between N^S – N^S pairs, blocks the production of CO_2(g) and N_2(g) (Fig. 5.11). However, the introduction of single subsurface on simple cubic lattice generates a SRS with steady reactive window ≈ 0.105 in the CO-NO catalytic reaction [13]. When NO adsorbs on the surface of the

square lattice, it is equally possible that on site is occupied by N and the other by an oxygen (O) atom. This simple fact poisons the square lattice by the process of "chequer boarding" of N atoms [16]. However, the chequer boarding of N atoms cannot take place on the hexagonal lattice. This is why Yaldram *et al*. [10] observed the SRS for hexagonal lattice in their simulation work. Our recent work of simulation for the CO-NO reaction system on BCC lattice also breaks the usual chequer boarding of N atoms, and SRS is observed for simple LH mechanism.

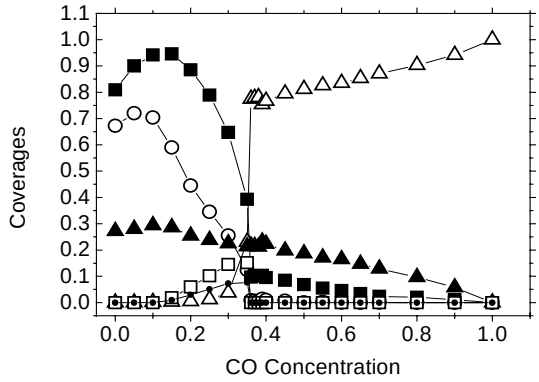

Fig. 5.16(a). A plot of surface oxygen coverage (open circles), subsurface oxygen coverage (solid squares), CO coverage (open triangles), surface nitrogen coverage (solid triangle), CO2 production rate (open squares) and N2 production rate (solid circles) versus CO concentration for model A (LH Mech.).

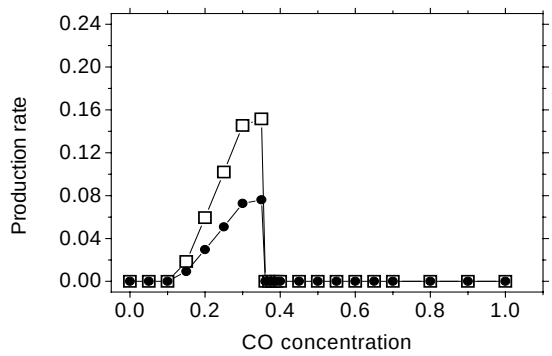

Fig. 5.16(b).

Fig. 5.16(b). shows the plot of CO_2 production rate (open squares) and N_2 production rate (solid circles) versus CO concentration for model A (LH Mech.).

It is evident from figure 5.16(b) that window width of size (0.35-0.15) = 0.2 is generated for simple LH Mechanism (Model A) for CO-NO reaction on BCC lattice. The next fig.5.17(a) shows the phase diagram for model B, when the probability of precursor mobility is taken 20 % to the first environment. The phase diagrams of figure 5.16(a) and figure 5.17(a) are almost similar with the difference that with the introduction of precursor mechanism, the production rate increases.

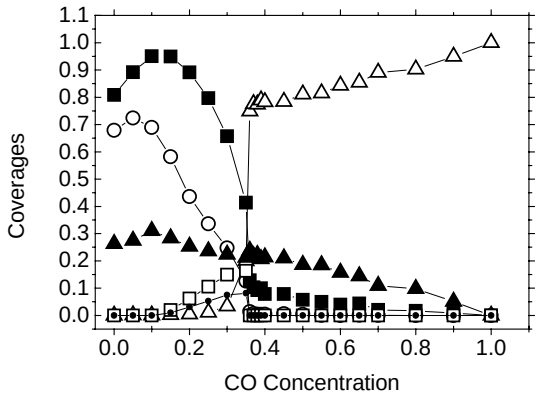

Fig. 5.17(a). Surface oxygen coverage (open circles), subsurface oxygen coverage (solid squares), CO coverage (open triangles), surface nitrogen coverage (solid triangle), CO_2 production rate (open squares) and N_2 production rate (solid circles) versus CO concentration; with 20% precursor probability for the first environment of model B.

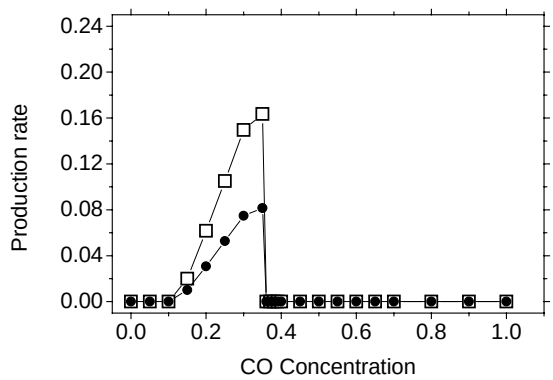

Fig. 5.17(b). CO_2 production rate (open squares) and N_2 production rate (solid circles) versus CO concentration with 20% precursor probability for the first environment of model B.

Similarly other results are presented for 60%, 80% 100% of precursor probability of CO molecules.

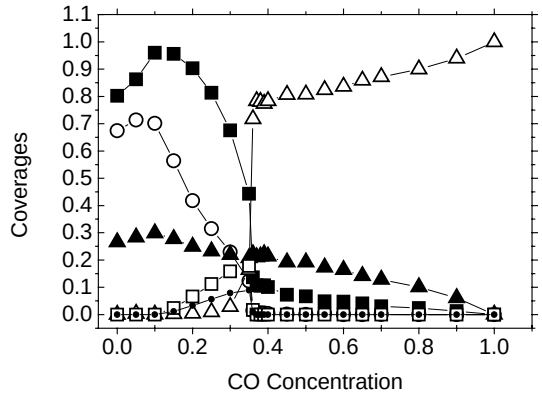

Fig. 5.18(a). The same as in Fig. 5.17(a) with 60% precursor probability for the first environment of model B.

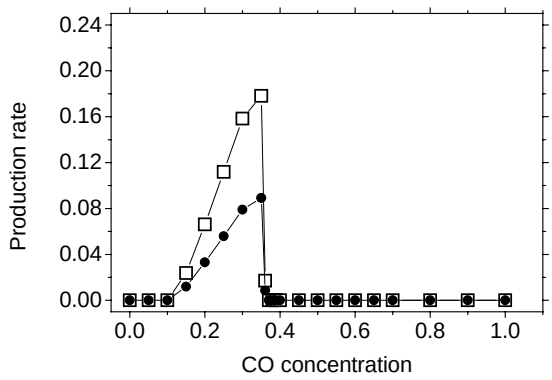

Fig. 5.18(b). CO_2 production rate (open squares) and N_2 production rate (solid circles) versus CO concentration with 60% precursor probability for the first environment of model B.

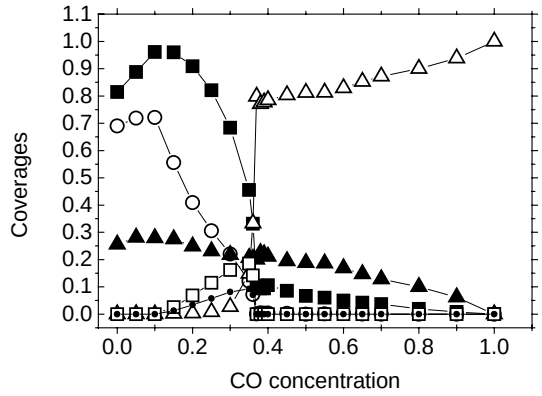

Fig. 5.19(a). Surface oxygen coverage (open circles), subsurface oxygen coverage (solid squares), CO coverage (open triangles), surface nitrogen coverage (solid triangle), CO_2 production rate (open squares) and N_2 production rate (solid circles) versus CO concentration; with 80% precursor probability for the first environment of model B.

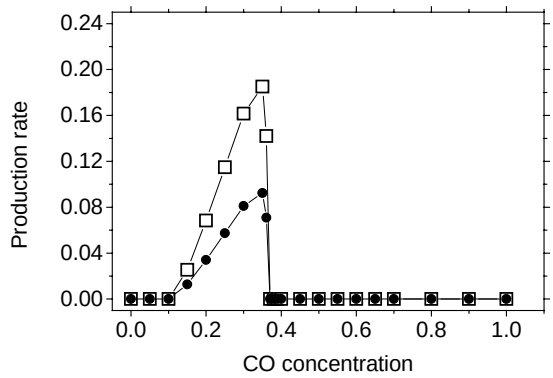

Fig. 5.19(b). CO_2 production rate (open squares) and N_2 production rate (solid circles) versus CO concentration with 80% precursor probability for the first environment of model B.

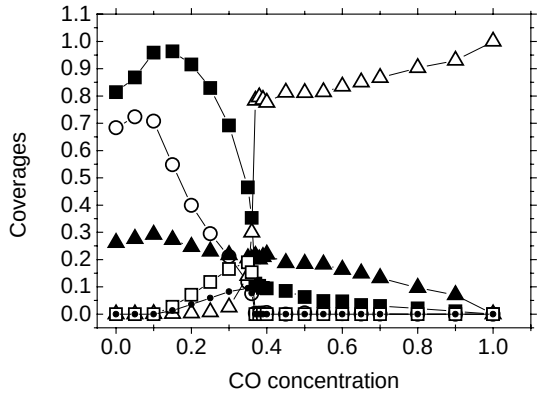

Fig. 5.20(a). Surface oxygen coverage (open circles), subsurface oxygen coverage (solid squares), CO coverage (open triangles), surface nitrogen coverage (solid triangle), CO_2 production rate (open squares) and N_2 production rate (solid circles) versus CO concentration; with 100% precursor probability for the first environment of model B.

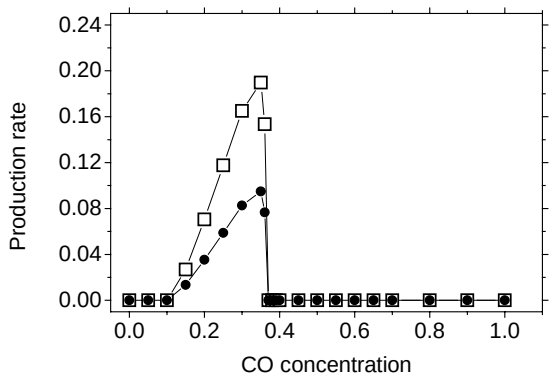

Fig. 5.20(b). CO_2 production rate (open squares) and N_2 production rate (solid circles) versus CO concentration with 100% precursor probability for the first environment for model B.

Now the overall effect of precursor mechanism on the first environment is shown in the following table (5.1).

Table 5.1. Effect of precursor on the first environment (model B) for the reaction of the CO-NO on BCC lattice.

Probabiity of Precursor of CO	**Y_1**	**Y_2**	**MPR (Maximum Production Rate)**
10%	0.15	0.35	0.1582
20%	0.15	0.35	0.1634
30%	0.15	0.35	0.1677
40%	0.15	0.35	0.1716
50%	0.15	0.36	0.1750
60%	0.15	0.36	0.1781
70%	0.15	0.36	0.1812
80%	0.15	0.36	0.1850
90%	0.15	0.36	0.1867
100%	0.15	0.36	0.1897

It is noted from the above table that the production rate increases as the probability of precursor in the first environment increases; while the transition points, y_1 and y_2 almost remains the same.

To explore that what happens when the mobility of precursor is extended to the second environment, in this case the simulation is performed for the mobility of precursor with probability 10% to 100% with step length of 10. Table 5.2 shows the effect of precursor on the second environment for the reaction of CO-NO on BCC lattice.

Table 5.2. Effect of precursor on the second environment (model C) for the reaction of the CO-NO on BCC lattice.

Probabiity of Precursor of CO	**Y_1**	**Y_2**	**MPR (Maximum Production Rate)**
10%	0.15	0.35	0.1668
20%	0.15	0.36	0.1783
30%	0.15	0.36	0.1875
40%	0.15	0.36	0.1932
50%	0.10	0.36	0.2005
60%	0.10	0.36	0.2058
70%	0.10	0.36	0.2101
80%	0.10	0.36	0.2142
90%	0.05	0.36	0.2182
100%	0.05	0.36	0.2215

The phase digrams indicating the coverages and production rates for 20%, 60%, 80% and 100% of precursor probability of CO molecules for the second environment are shown in the following figures.

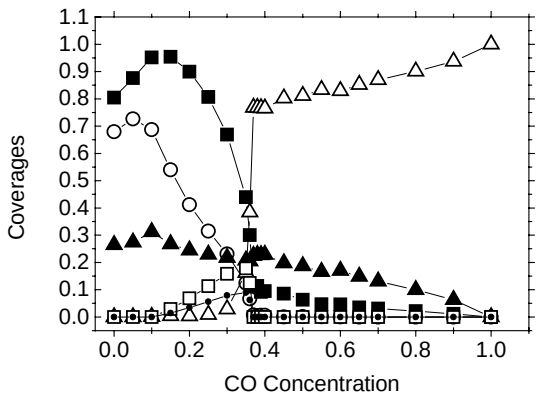

Fig. 5.21(a). Surface oxygen coverage (open circles), subsurface oxygen coverage (solid squares), CO coverage (open triangles), surface nitrogen coverage (solid triangle), CO_2 production rate (open squares) and N_2 production rate (solid circles)

versus CO concentration; with 20% precursor probability for the second environment of model C.

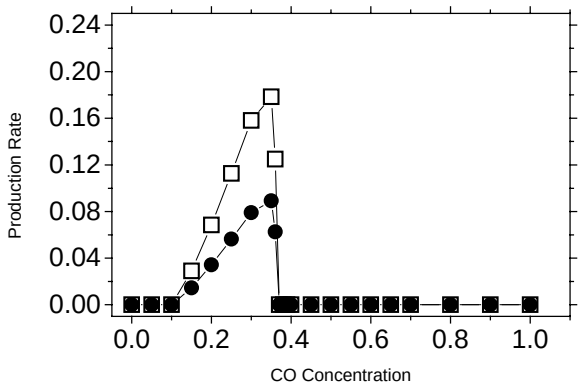

Fig. 5.21(b). CO_2 production rate (open squares) and N_2 production rate (solid circles) versus CO concentration with 20% precursor probability for the second environment of model C.

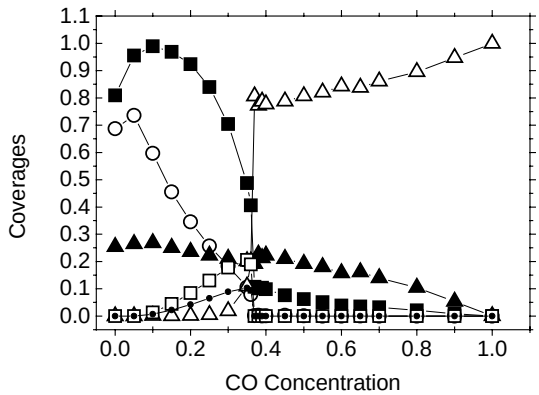

Fig. 5.22(a). Surface oxygen coverage (open circles), subsurface oxygen coverage (solid squares), CO coverage (open triangles), surface nitrogen coverage (solid triangle), CO_2 production rate (open squares) and N_2 production rate (solid circles) versus CO concentration; with 60% precursor probability for the second environment of model C.

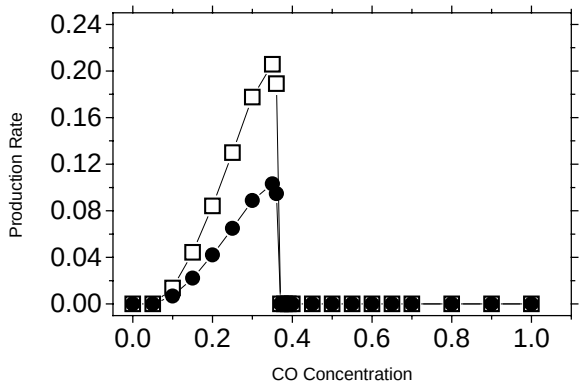

Fig. 5.22(b). CO_2 production rate (open squares) and N_2 production rate (solid circles) versus CO concentration with 60% precursor probability for the second environment of model C.

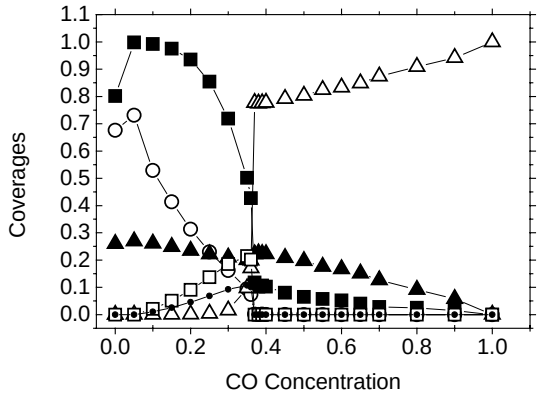

Fig.5.23(a). The same as in Fig. 5.22 (a) with 80% precursor probability for the second environment of model C.

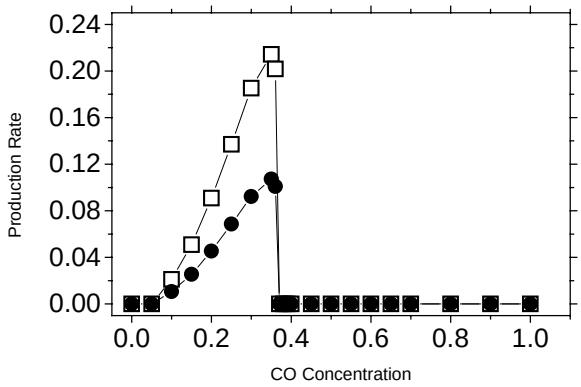

Fig. 5.23(b). CO_2 production rate (open squares) and N_2 production rate (solid circles) versus CO concentration with 80% precursor probability for the second environment of model C.

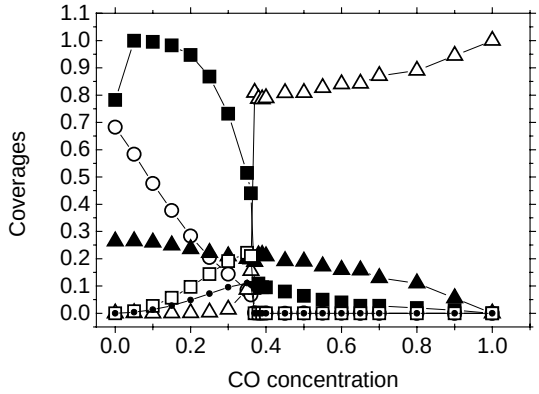

Fig. 5.24(a). Surface oxygen coverage (open circles), subsurface oxygen coverage (solid squares), CO coverage (open triangles), surface nitrogen coverage (solid triangle), CO_2 production rate (open squares) and N_2 production rate (solid circles) versus CO concentration; with 100% precursor probability for the second environment of model C.

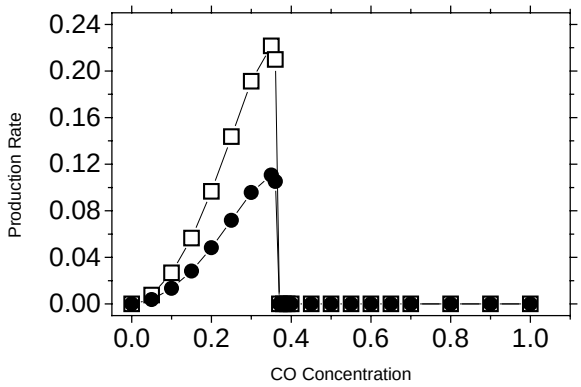

Fig. 5.24(b). CO_2 production rate (open squares) and N_2 production rate (solid circles) versus CO concentration with 100% precursor probability for the second environment of model C.

From figures 5.21(a-b) to 5.24(a-b) the results are presented when the spectrum of precursor mobility is extended up to second environment. These figure 5.21(a) and 5.24(a) are for 20% and 100% precursor probability respectively. For 20% probability of precursor, first transition occurs at $y_1 = 0.15$, while the second transition occurs at $y_2 = 0.36$, while for 100% precursor probability, we find $y_1 = 0.05$ and $y_2 = 0.36$. Therefore, if we increase the precursor probability, it is observed that y_1 is shifted toward a lower value of y_{CO}, while y_2 remains almost the same. In fact, for low concentration, the hoping of CO^P molecules into the second environment reacts more oxygen and creates more single vacant sites and hence y_1 is shifted towards lower values of y_{CO}. It is also observed from these figures that the coverage of surface oxygen drops rapidly for 100% precursor probability as compared to 20%. Moreover, it is evident from figure 5.24(a) that the continuous transition disappears and the continuous production of $CO_2(g)$, $N_2(g)$ takes place at the moment $y_{CO} \neq 0$.

In Table 5.3, we present a situation when the mechanism of precursor is included to the third environment (Model D).

Table 5.3. Effect of precursor on the third environment for the reaction of CO-NO on BCC lattice.

Probabiity of Precursor of CO	**Y_1**	**Y_2**	**MPR (Maximum Production Rate)**
10%	0.15	0.36	0.1735
20%	0.15	0.36	0.1865
30%	0.10	0.36	0.1978
40%	0.10	0.36	0.2063
50%	0.10	0.36	0.2138
60%	0.10	0.36	0.2201
70%	0.05	0.37	0.2252
80%	0.05	0.37	0.2295
90%	0.05	0.37	0.2334
100%	0.05	0.37	0.2365

From the above Table 5.3, the values of y_1 and y_2 are found to be 0.15 and 0.36, respectively when the probability of mobility of CO molecule (Precursor) is made 10% to the third environment. Our study also shows that mobility of precursor to the third environment has no significant effect on the phase diagram of the system.

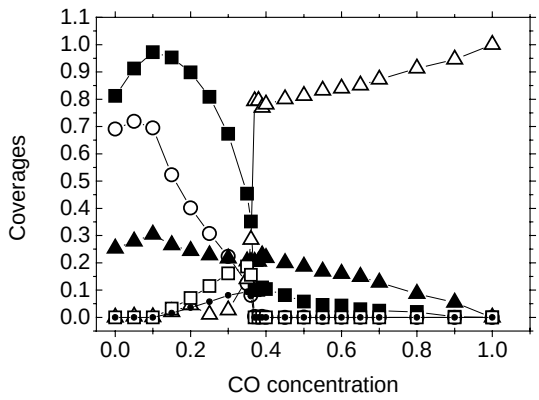

Fig. 5.25(a). Surface oxygen coverage (open circles), subsurface oxygen coverage (solid squares), CO coverage (open triangles), surface nitrogen coverage (solid triangle), CO_2 production rate (open squares) and N_2 production rate (solid circles) versus CO concentration; with 20% precursor probability for the second environment of model D.

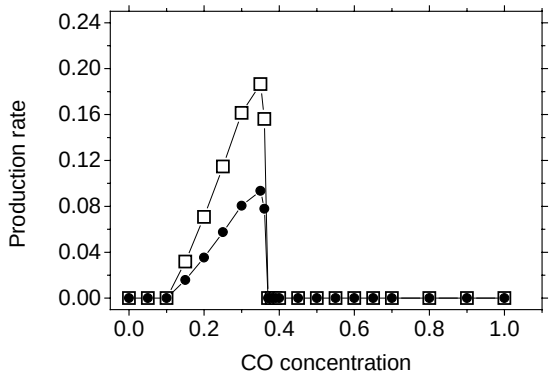

Fig. 5.25(b). CO_2 production rate (open squares) and N_2 production rate (solid circles) versus CO concentration with 20% precursor probability for the second environment of model D.

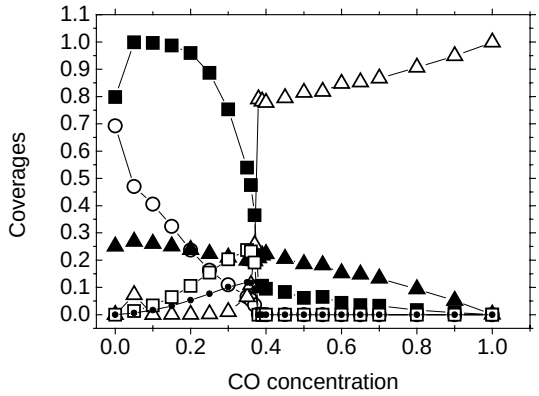

Fig. 5.26(a). Same as in Fig.5.25(a) with 100% precursor probability for the second environment of model D.

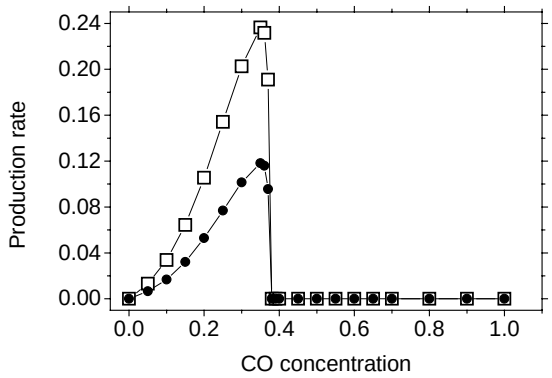

Fig. 5.26(b). CO_2 production rate (open squares) and N_2 production rate (solid circles) versus CO concentration with 100% precursor probability for the second environment of model D.

The effect of precursor probability for each mode of environment on the maximum production rate (MPR) is also studied and is plotted in figure 5.27.

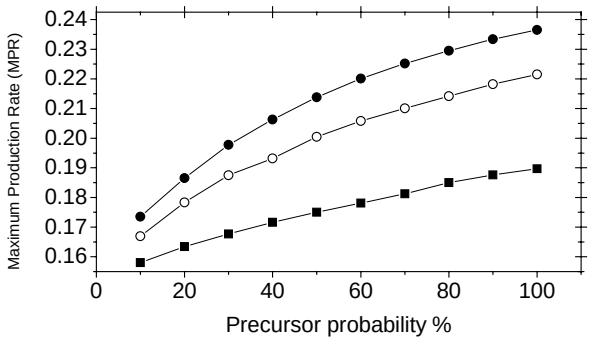

Fig. 5.27. Maximum production rate of first environment (solid squares), second environment (open circles) and third environment (solid circles) versus precursor probability.

It is observed from this figure that in each mode of environment, MPR increases as the probability of precursor increases. This is because as the mobility of precursor is increased, the probability of CO oxidation increases. The CO precursor starts reacting oxygen trapped between N^S – N^S pairs leaving behind a vacant site on the surface. This

vacant site blocks the incoming NO to be adsorbed on the surface, because a NO needs two vacant sites for adsorption.

It is concluded that in simple LH mechanism for CO-NO catalytic reaction, the SRS is established with window width ≈ 0.2 for BCC, while the same reaction system for square lattice is not capable of generating an SRS [10,12]. In the second environment, the impact of precursor mechanism is to increase the production rate as well as reactive window width which is consistent with the results of [18] for square lattice, whereas the precursor mechanism on the third environment has no significant effect on the window width.

5.5 Simulation On BCC for CO-NO with Eley Rideal and Diffusion Mechanism

It was desirable to investigate the CO-NO catalytic reaction on BCC with ER along with diffusion. The objective of this manuscript is to explore the effects of the ER process, diffusion of CO and N on the phase diagram of the LH type surface-subsurface model for MD catalytic reaction.

5.5.1 Model and Simulation

According to LH mechanism, it is assumed that the reaction occurs according to the following steps:

$$CO(g) + S \rightarrow CO^{S} \qquad (5.21)$$

$$NO(g) + 2S \rightarrow N^{S} + O^{S} \qquad (5.22)$$

$$NO(g) + S + SS \rightarrow N^{S} + O^{SS} \qquad (5.23)$$

$$N^{S} + N^{S} \rightarrow N_2(g) + 2S \qquad (5.24)$$

$$CO^{S} + O^{S} \rightarrow CO_2(g) + 2S \qquad (5.25)$$

The inclusion of the subsurface will add the following extra step:

$$CO^{S} + O^{SS} \rightarrow CO_2(g) + S + SS \qquad (5.26)$$

With the introduction of ER process, one has to add the following equation:

$$CO\ (g) + O^{S} \rightarrow CO_2\ (g) + S \qquad (5.27)$$

Here, the notations used are obvious. In this study the effect of ER, diffusion of CO and N on the surface for CO-NO is also considered. The following models are studied.

Model A

In Model A steps 5.21-5.26 are considered. The simulation proceeds as follows: A surface site is chosen randomly and for this site there are two possibilities (i) Either this site is occupied or (ii) empty. If the selected site happens to be occupied, then the trial ends. If the selected site is empty and CO happens to be the incoming molecule, then the adsorption is made via reaction step (5.21) with probability y_{CO}. Soon after the adsorption, CO goes through reaction step (5.25), with the production of CO_2 and leaving behind two vacant sites on the surface. If this reaction step does not succeed then the reaction step (5.26) takes its turn. The success of reaction step (5.26) results in the production of CO_2 with leaving one vacancy on the surface and other on the sub-surface. While for adsorption of NO there is equal probability for step (5.22) and (5.23). For step (5.22), adsorption of NO is taken in such a way that N atom is adsorbed on the surface, whereas O atom is adsorbed on the second nearest neighbour. After the adsorption N atom goes for reaction step (5.24) and adsorbed oxygen atom goes for reaction step (5.25). If step (5.23) happens to be selected, the Nitrogen atom gets adsorbed on the surface and oxygen atom gets adsorbed in the sub-surface. The nitrogen atom, after adsorption, goes through usual reaction step (5.24) for production of N_2(g), while oxygen atom adsorbed in the sub-surface does not go for reaction.

Model B

In Model B steps 5.21-5.27 are considered. In this model, the effect of ER mechanism is studied by including the step (5.27) to the already discussed six steps above. The additional step (5.27) is meant for ER mechanism. For such a mechanism, if the selected molecule is CO, and selected site is occupied by oxygen atom, then the reaction step (5.27) gets activated by producing CO_2, and leaving behind one vacant site on the surface.

Model C

In Model C the effect of ER mechanism and diffusion of CO on the phase- diagram is studied. All the other simulation steps remain the same as explained in model A and B. The additional step in this model is for diffusion of adsorbed CO, and is simulated as follows: If randomly selected site is occupied with CO, then CO diffuses to any of the randomly selected vacant site in its second nearest neighbour. After the completion of diffusion, the step (5.25) is simulated. If this step does not succeed, then the reaction step (5.26) is activated.

Model D

In Model D the effect ER mechanism, diffusion of CO and N on the phase diagram is studied. All the other simulation steps remain the same as explained in model A and B. The additional steps in this model are simulated as follows: If selected site is occupied with CO (N), then CO (N) diffuses to any of the randomly selected vacant site in its second nearest neighbour. After the completion of this step, the step (5.25), (5.26) and (5.24) is simulated.

Model E

In Model E only the impact of diffusion of CO is introduced. All the other simulation steps remain the same as given in model A and diffusion of CO is simulated as mentioned in Model C.

Model F

In Model F only the impact of diffusion of Nitrogen atom is introduced. All the other simulation steps remain the same as explained in model A and the diffusion of Nitrogen is simulated as mentioned in Model D.

5.5.2 Results and Discussion

In Figure 5.28(a-b), we present a situation when the mechanism is without ER and the probability of diffusion of CO and N on the surface is zero i.e. Model A. In this model (LH model), for low concentration of CO (high NO), the surface gets poisoned and most of the adsorbed oxygen atoms, are trapped between nitrogen atoms and adsorbed nitrogen atoms between oxygen atoms. The poisoning and trapping of atoms stops the reactive state to be established (see Figure 5.29). In this situation the first transition occurs at the lower critical point y_1 =0.15, while the second transition occurs at y_2 = 0.36. The difference $y_2 - y_1$ = 0.21, called the window width for SRS, is separated by two-phase transitions (Figure 5.28(b)). For CO oxidation, quite different results are produced by Khan *et al*. [19] as trapping of oxygen atom by CO^S- CO^S pair and CO^S trapping between O^S- O^S pair, helps in production of CO_2. In our Model the maximum production rate of CO_2 and N_2 is found at y_{CO} =0.35, after which it falls abruptly to zero. For $y_{CO} < y_1$,

surface is totally covered (poisoned) with combination of N^S and O^S, while for $y_{CO} > y_2$; the surface is poisoned with N^S and CO^S. At y_2, the coverage of CO on the surface increases suddenly and jumps to a large value (≈0.78) and the coverage of surface oxygen drops to a very small value (≈0.006). For $y_{CO}>y_1$, the coverage of N on the surface decreases slowly and drops to zero quite smoothly. For $y_{CO} < y_1$, the coverage of oxygen on the sub-surface increases as y_{CO} increases, gets maximum value (≈0.94) until $y_{CO} = y_1$(≈0.15), and then starts decreasing slowly until $y_{CO} = y_2$ (≈0.36), where it has a small value (≈0.1). Then it goes to zero quite smoothly as y_{CO} increases. The production rates of N_2 and CO_2 shows that the steady production starts at y_1 and keeps on increasing gradually until it gets a maximum, after which both (CO_2 and N_2) drop to zero abruptly. For a particular value of y_{CO}, the production of CO_2 is greater than that of N_2. Earlier attempts [10,16] on the square lattice failed to obtain the SRS (without diffusion of N) for NO-CO reaction for all values of y_{CO}. However, the introduction of single subsurface site on simple cubic lattice generates a SRS with steady reactive window ≈ 0.105 in the NO-CO catalytic reaction [13]. In the present work on BCC lattice, we find that SRS does exist with reactive window ≈ 0.21, which clearly depicts the effect of the BCC.

In Figure 5.30 (a-b), we present a situation when the ER mechanism is included (Model B) and the probability of diffusion of CO and N on the surface is to be taken zero. The ER mechanism shifts backward the transition point y_1 from 0.15 (in case of Model A) to 0.01, keeping y_2 almost at the same position. The ER model as presented in reaction step (5.27), enjoys the privilege of directly picking up the chemisorbed oxygen atom trapped between $N^S – N^S$ pairs leaving behind a vacant site on the surface. This vacant site blocks the incoming NO to be adsorbed on the surface, as NO needs two vacant sites for its adsorption. The probability of adsorption for CO on the vacant site increases and when CO is adsorbed, it triggers reaction step (5.25). In this situation, oxygen on the surface reacts quickly. Therefore in ER mechanism, the production of CO_2 starts as soon as the partial pressure (y_{CO}) departs from zero. This observation is the same as found in the experimental work [6]. It has been also found in present work that in ER model, the production rate (R) of CO_2 increases with the ER-step probability (Figure 5.30(c)), and production rate takes the mathematical form as $R = 0.16 + 2.37\times10^{-4} y_{CO} + 1.51\times10^{-5} y_{CO}^{2} – 1.1\times10^{-7} y_{CO}^{3}$ with standard deviation (SD) = 0.00134. The maximum enhancement of window width is observed on 5 % ER probability, and above this value window width becomes constant.

Figure 5.31 (a-b) shows the effect of ER and diffusion of CO (Model C), with 100% probability on the surface. It is seen that the diffusion of CO slightly shifts the transition point from y_2 =0.36 (Model A) to y_2 = 0.38, but does not modify the phase diagram. The shifting of these transition points increases the steady reactive phase width by 0.02. This is because with the introduction of diffusion, the adsorbed molecule of CO gets more quickly consumed as it gets opportunity of escaping from the trap of nitrogen atoms. Khan et al [10] have shown that diffusion of CO has no effect on the phase diagram of the system for square lattice. For square lattice the diffusion of CO gives exactly the same phase diagram as obtained without diffusion. It can also be seen from Figure.5.31(b), that the production of CO_2 and N_2 slightly increases as we introduce the diffusion of CO. The reactive window width increases to some extent with the increase in probability of diffusion of CO.

Figure 5.32 (a-b) shows the effect of ER, diffusion of CO and diffusion of N, each with 100% probability on the surface (Model D). In this situation transition point shifts from y_2 =0.36 (Model A) to y_2 = 0.4, with slight increase in the production of CO_2 and N_2 as compared to Model A. This is because with the introduction of diffusion of adsorbed CO and nitrogen atom, the adsorbed molecules of CO and N (atom) get more quickly consumed as diffusion process facilitates the system in breaking the traps. It is also seen from the Figure 5.32 (a) that coverage of N^S is less than the coverage of N^S as obtained in earlier case.

Model E results are shown in Figure 5.33 (a-b). In this model we have studied the effect of diffusion of CO only on the BCC lattice. The phase diagram is the same as found in Model A, except the position of critical point y_2. The diffusion of CO shifts the transition point y_2 from 0.36 to 0.39. The reason behind this shift is escaping of CO molecule from the trap of nitrogen atoms. In this case the maximum production rate of CO_2 also increases.

Figure 5.34 (a-b) shows the case when the diffusion of N only is considered (Model F). The Phase diagram is the same as for Model A, except the coverage of N^s. When we compare with Model A, we find that the transition point y_2 shifts from 0.36 (Model A) to 0.38 (Model F). An increase in the maximum production of CO_2 and minute increase in the production of N_2 is found. The reason behind this shift is escaping of nitrogen atom from the trap of adsorbed CO molecule. However the coverage of N^S decreases as compared to Model A.

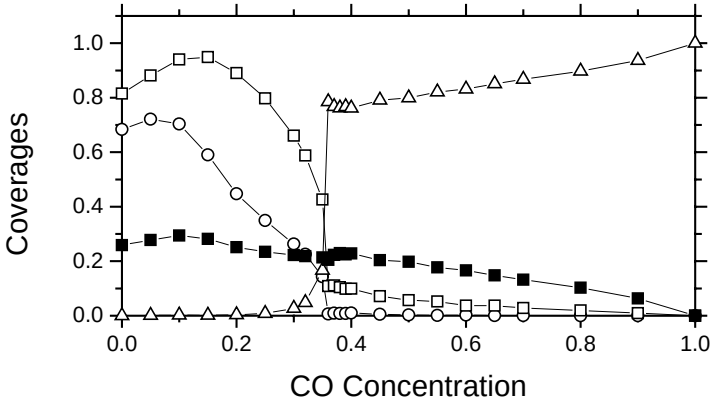

Fig. 5.28(a) Coverages of surface O (circle open), sub-surafce oxyen (square open), CO (triangle open), and N (square solid) for Model A.

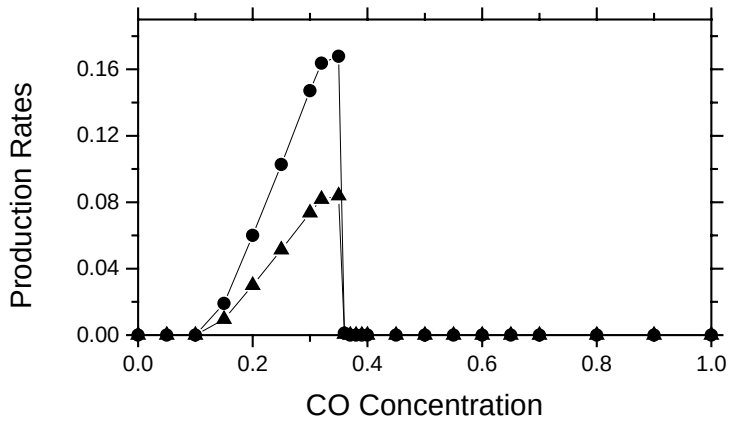

Fig. **5.28(b**) The production rate of CO_2 (circle solid) and N_2 (triangle up solid) versus CO partial pressure for Model A.

131113131311113111111111113231131311131131111131111323111111131
311311313111111131311131311311313111311311311111313111311313113 11
131111311113131131113131313111313111311311111311313131113111131131
113111113113131113113111313131113131111111313113131313131131111 3
131313131311311311131131131111311311311111311313131313113131311
313131313131113131111113111313131131111131313111131311111311131 11
131313111311111113131311131111311313113113131311313131131111131
113131311113131131311131111131111131311111311113131313113131313113
131113131131311111131311311313131313131111113131113111131313131 1
111111111313111311313131111111313131313131131111311131311131313 1

Fig. 5.29. Snap shot on y_{co} = 0.14 (1 for oxygen, 3 for N)

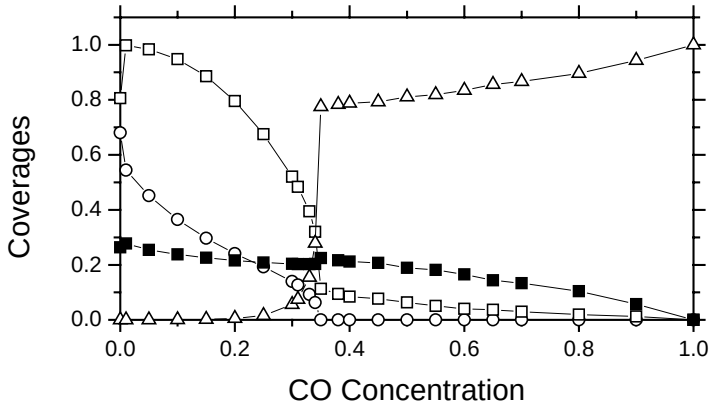

Fig. 5.30(a)

Fig. 5.30

(a) Coverages of surface O (circle open), sub-surafce oxyen (square open), CO (triangle up open), and N (square solid) (b) the production rate of CO_2 (circle solid) and N_2 (triangle solid) versus CO partial pressure (c) production rate vs ER step probability for Model B.

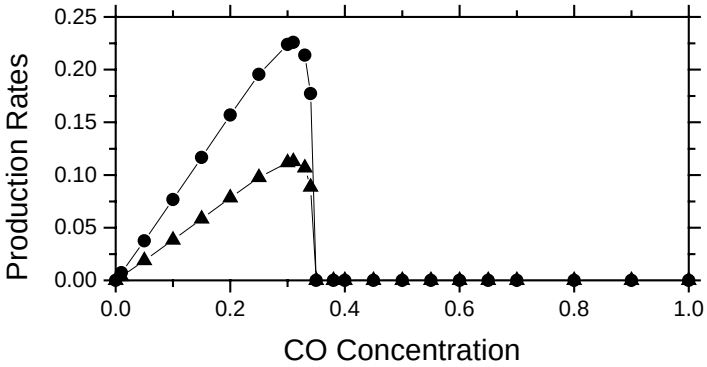

Fig. 5.30(b)

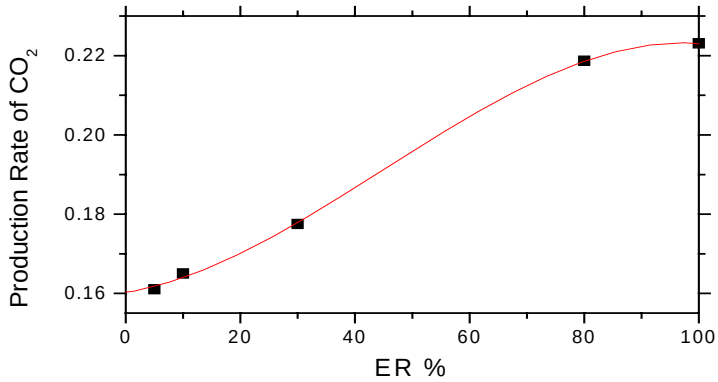

Fig. 5.30 (c)

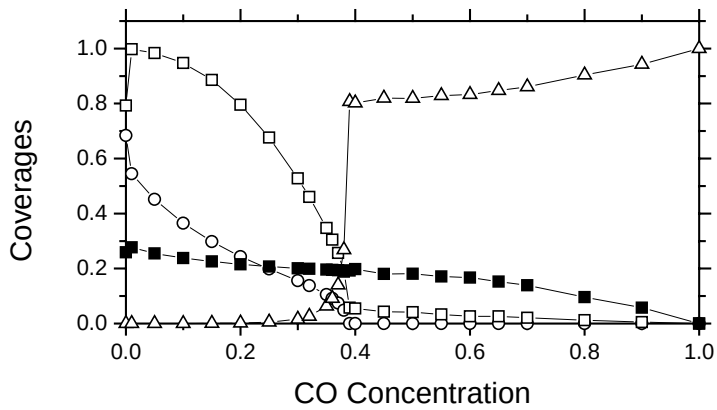

Fig. 5.31(a)

Fig. 5.31 (a) Coverages of surface O (circle open), sub-surface oxygen (square open), CO (triangle up open), and N (square solid) (b) the production rate of CO_2 (circle solid) and N_2 (triangle solid) versus CO partial pressure for Model C

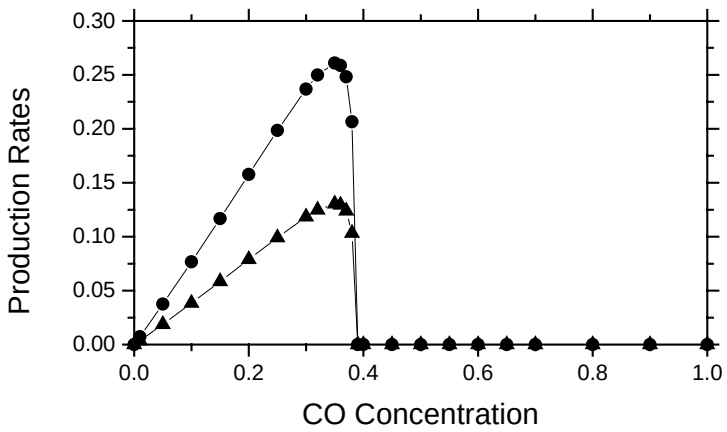

Fig. 5.31(b)

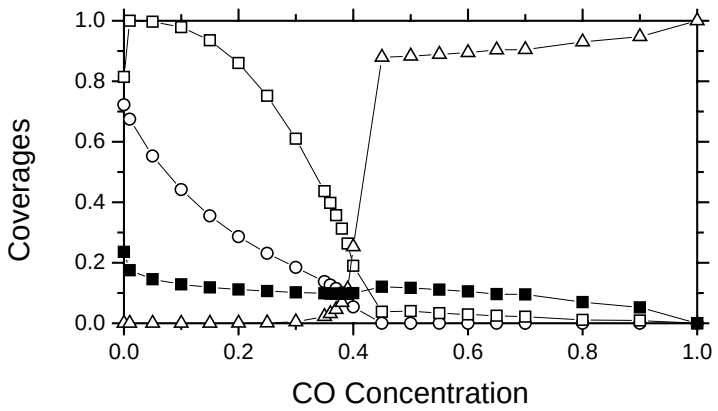

Fig. 5.32(a)

Fig. 5.32(a) Coverages of surface O (circle open), sub-surface oxygen (square open), CO (triangle up open), and N (square solid)

(b) the production rate of CO_2 (circle solid) and N_2 (triangle solid) versus CO partial pressure for Model D

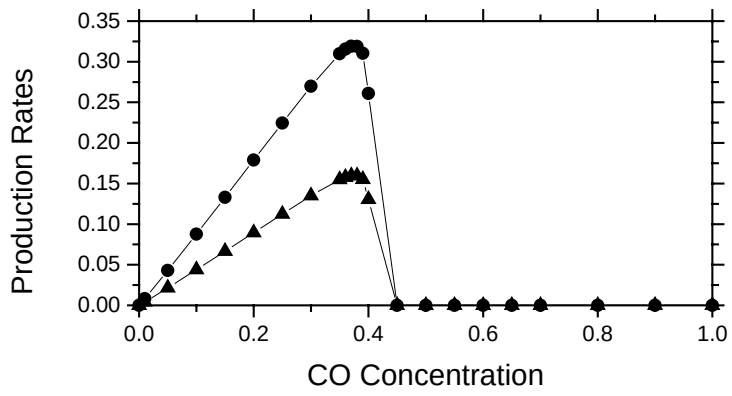

Fig. 5.32 (b)

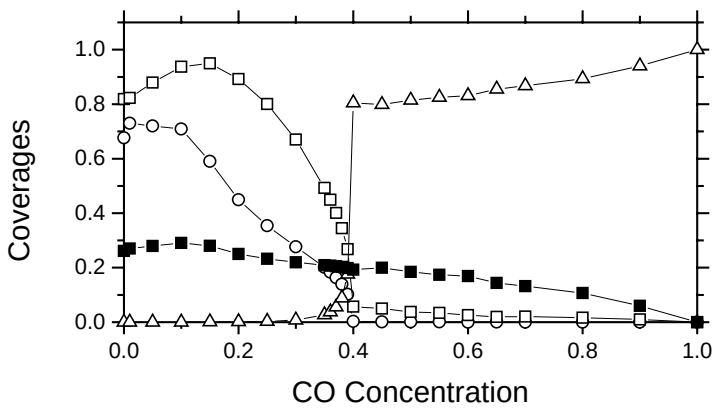

Fig. 5.33(a)

Fig. 5.33: (a) Coverages of surface O (circle open), sub-surface oxygen (square open), CO (triangle up open), and N (square solid) (b) the production rate of CO_2 (circle solid) and N_2 (triangle solid) versus CO partial pressure for Model E

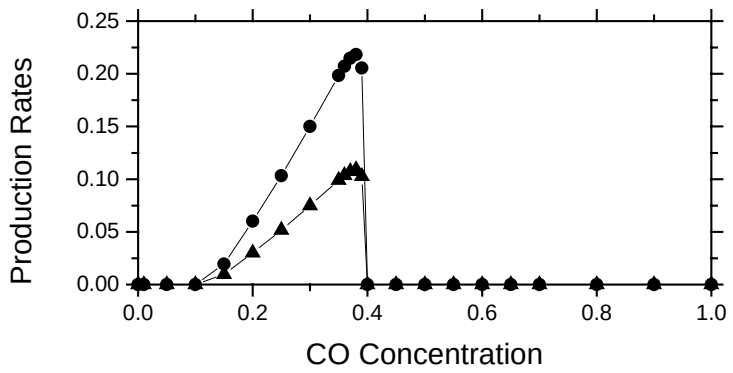

Fig. 5.33(b)

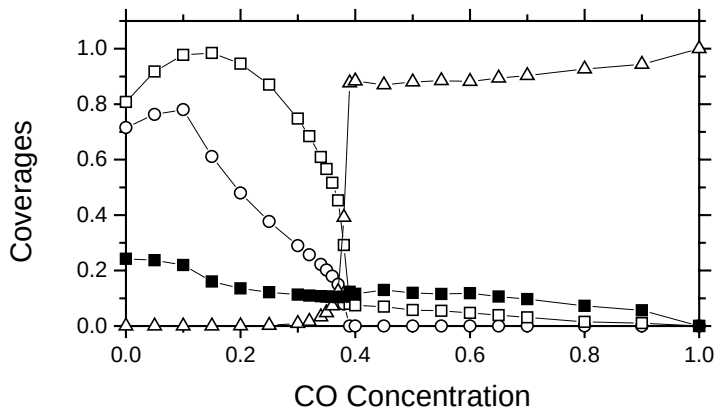

Fig. 5.34(a)

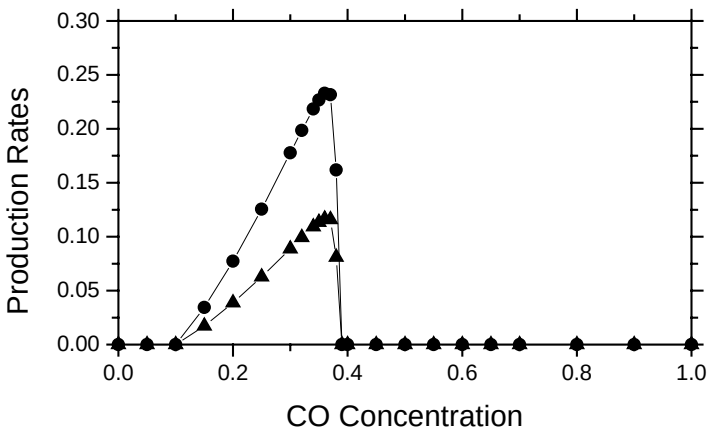

Fig. 5.34(b)

Fig. 5.34 (a).Coverages of surface O (circle open), sub-surface oxygen (square open), CO (triangle up open), and N (square solid) (b) the production rate of CO_2 (circle solid) and N_2 (triangle solid) versus CO partial pressure for Model F.

5.6 References

[1] B. A. Banse, D. T .Wickham, and B. E . Koel, J. Catal. **119** (1089) 238.

[2] L. H. Dubois and G. A. Somorjai, Surf. Sci. **91** (1980) 414

[3] R. E. Hendershot and R. S. Hansen, J. Catal. **98** (1986) 150

[4] L. H. Dubois, P.K. Hansama and G. A. Somorjai, J. Catal. **65** (1980) 318.

[5] R. E. Hendershot and R. S. Hansen, J. Catal. **98** (1986) 150.

[6] D. T. Wickham and B. E . Koel, J. Catal. **114** (1988) 207.

[7] Th. Fink, J. P. Dath, M. R. Basset, R. Imbihl and G. Ertl, Surf. Sci. **245** (1991) 96.

[8] W. F. Banholzer, Y.O. Park, K. M. Makand and R.I.Masel, Surf. Sci. **128** (1983) 176.

[9] M.F.H. von Tol and B.E. Nieuwenheys, Appl. Surf. Sci. **67** (1993) 188.

[10] K. Yaldram and M A Khan J. Catal. **131** (1991) 369.

[11] K. Yaldram and M A Khan J. Catal. **136** (1992) 279.

[12] M. A. Khan K.Yaldram, G.K. Khalil and K.M. Khan, Phys. Rev.E **50**(1994) 2156

[13] K.M Khan, Surf. Sci. **470** (2000) 155.

[14] K. M. Khan. and K. Yaldram, Surf. Sci. **445** (2000)186

[15] K.M. Khan, E.V. Albano, R.A. Monetti, Surf. Sci. **481** (2001) 78.

[16] B J Brosilow and R M Ziff J. Catal. **136** (1992) 275.

[17] K M Khan and W. Ahmed, J.Phy.A: Math.Gen. **35** (2002) 2713.

[18] M Khalid, A.U Qaisrani and W Ahmad, Chin.Phy.Lett. **22** (2005) 1533.

[19] K. M Khan. and K Yaldram. , Surf. Sci. **445 (**2000) 186.

Chapter-6

RESULTS AND CONCLUSION

6.1 Conclusions

The Transient non-thermal mobility in surface subsurface heterogeneous catalytic reactions has been investigated using the technique of Monte Carlo simulation. For such investigations, CO-O_2 and CO-NO catalytic reaction were selected. The effects of the ER process on the phase diagram of the LH type model for the monomer-dimer CO-O_2 catalytic reaction system on (001) surface and subsurface of a simple cubic structure have been investigated. Two different models have been considered. In model A, the oxygen molecule (dimer) always adsorbs in atomic form by taking one surface and one subsurface site. In model B, the oxygen molecule (dimer) is adsorbed in such a way that it takes one surface site whereas the second site may be from surface or from subsurface. The model A does not improve the LH situation of the phase diagram of the system (Fig.4.1- Fig. 4.4 & Fig.4.4(a)). However, in this model CO_2 production increases with ER step probability P_E (Fig.4.4b). On the other hand the model B shows significant effect on the LH situation of the phase diagram of the system (Figs 4.5 & 4.6). Moreover the qualitative trend of the surface oxygen coverage is consistent with the experimental situation i.e. the coverage of surface oxygen decreases slowly with increase in y_{CO}.

In the simulation of CO-O_2 catalytic reaction system on body-centred cubic structure, four different cases were studied. It was observed that in the first case (with LH mech.& priority of reaction goes to surface first), the usual second-order phase transition of ZGB model is eliminated. For the above first case, the production of CO_2 starts as soon as y_{CO} departs from zero, which is consistent with experimental observation (Fig.4.11). However, in second case (priority of reaction goes to surface first) when ER is included, CO_2 production increases with ER step-probability P_E (Fig.4.12). The third case (priority of reaction goes to subsurface first) does not improve the LH situation of the phase diagram of the system (Fig.4.14). However, in fourth case when ER is included (priority of reaction goes to subsurface first), CO_2 production also increases with ER-step probability P_E (Fig.4.16). On the other hand, the fourth case (with ER) shows significant effect on the LH situation of the phase diagram of the system (Fig.4.15). The qualitative trend of surface oxygen coverage (Fig.4.15) is consistent with the experimental situation i.e. the coverage of surface oxygen decreases slowly with increase in y_{CO}. The production of CO_2 can be predicted in the form of a mathematical relation.

The effect of the precursor mechanism on the phase diagram of CO-NO catalytic surface reaction on the square lattice is also investigated. The introduction of precursor mechanism adds some interesting features in the phase diagram of monomer-dimer catalytic surface reaction system, which were not seen by considering Langmuir-Hinshelwood mechanism. Three different cases were studied. The steady reactive state (SRS) gets established and increases with increasing the range of precursor molecule (Figs 5.5(a) & 5.5(b)). The width of the reactive window depends on the mobility of the precursors. An interesting situation is observed when the range of precursor molecule is extended to third nearest neighbours and the probability CO precursor is made 100% (Figs 5.8(a) & 5.8(b)). The moment y_{CO} is non-zero, a continuous production of CO_2 and N_2 starts (Fig. 5.8(b).

The study of CO-NO catalytic reaction through Monte Carlo Simulation was extended to explore the effects of transient non-thermal mobility of CO molecule based on precursor mechanism, and diffusion of adsorbed nitrogen and oxygen atoms on the phase diagram of square lattice. The introduction of non-thermal mechanism and diffusion adds some interesting features in the phase diagram of monomer dimmer catalytic surface reactions. It is concluded that the precursor mechanism clearly demonstrates its impact on the phase diagram with the establishment of steady reactive state (SRS). The SRS region increases whenever diffusion of nitrogen and oxygen atoms accompanies the precursor mechanism (Figs 5.13 & 5.15).

The work of simulation was also extended to study the effect of precursor mechanism for CO-NO on BCC lattice. It is concluded that in simple LH mechanism for CO-NO catalytic reaction, the SRS is established with window width ≈ 0.2 for BCC, while the same reaction system for square lattice is not capable of generating an SRS (Figs. 5.16(a) & 5.16(b)). In the second environment (Table 5.2), the impact of precursor mechanism is to increase the production rate as well as reactive window width, which is consistent with the results of square lattice, whereas the precursor mechanism on the third environment has no significant effect on the window width (it is almost the same as that of the second environment, Table 5.2 & 5.3).

In the last, we have investigated the effect of ER mechanism, diffusion of adsorbed CO molecule and diffusion of nitrogen atoms on the phase diagram of dimmer-monomer catalytic reaction system on BCC lattice. It is concluded that in simple LH mechanism, the production of CO_2 and N_2 is found very small (Fig.5.28(a-b), as most of nitrogen atoms get trapped between adsorbed pair of oxygen atoms and adsorbed oxygen

atoms get stuck between pair of adsorbed nitrogen atoms (Fig.5.29). The window width in the body centred lattice increases as compared to simple cubic results. The impact of ER mechanism on the phase diagram is not only to increase the production rate but also to enhance significantly the window width as this mechanism is capable of picking the trapped oxygen between nitrogen atoms (comparison of Figs 5.28(b) & 5.30(b)). The effect of diffusion of CO and N on the production rates is found in the high concentration region of CO. These mechanisms are found to be responsible for slight increase in the window width where the concentration of CO is high (comparison of Figs 5,28(b), 5.33(b) & 5.34(b)).

6.2 Future Research Work

The ZGB model can be extended to study the catalytic formation of CO_2 , ammonia and methanol on different lattices. Some suggestions are given for further research work and I hope these suggestions would be invaluable for future students. These suggestions are:

1) Using Monte Carlo Simulation technique, to develop surface-subsurface models for simple cubic and body centered cubic structure based on Eley-Rideal and Precursor mechanism and hot atom mechanism. These models could be applied to study catalytic reduction of NO by ammonia (NH_3).
   Comparison of the results obtained by the above-mentioned models with the result of models based on LH mechanism and experimental results.

2) To study the non-thermal effect of catalytic formation of ammonia (NH_3) through a novel approach of Monte Carlo Simulation technique.

3) To study the effect of Precursor mechanism, diffusion mechanism for the catalytic reaction of CO-O_2 on BCC lattice.

4) To study the effect of diffusion mechanism for the catalytic reaction of CO-O_2 on square lattice, simple cubic lattice and BCC lattice

5) To study the effect of Precursor mechanism for CO-NO reaction on simple cubic lattice and hexagonal lattice.

6) To study the effect of diffusion mechanism for CO-NO reaction on BCC lattice.

7) To study the catalytic formation of methanol and phase shift reactions.

THERE IS NO END OF RESEARCH WORK! IT IS ALWAYS INCOMPLETE!